RECONSTRUCTING THE *S. CEREVISIAE* GROWTH CONTROL NETWORK IN STRESS CONDITIONS

by

Jeremy Worley

A Dissertation Submitted to the Faculty of the

DEPARTMENT OF MOLECULAR AND CELLULAR BIOLOGY

In Partial Fulfillment of the Requirements

For the Degree of

DOCTOR OF PHILOSOPHY

In the Graduate College

THE UNIVERSITY OF ARIZONA

2015

THE UNIVERSITY OF ARIZONA
GRADUATE COLLEGE

As members of the Dissertation Committee, we certify that we have read the dissertation prepared by Jeremy Worley, titled Reconstructing the *S. Cerevisiae* Growth Control Network in Stress Conditions and recommend that it be accepted as fulfilling the dissertation requirement for the Degree of Doctor of Philosophy.

_____ Date: 8/4/2015
Andrew Capaldi

_____ Date: 8/4/2015
Ted Weinert

_____ Date: 8/4/2015
Carol Dieckmann

_____ Date: 8/4/2015
Frans Tax

_____ Date: 8/4/2015

Final approval and acceptance of this dissertation is contingent upon the candidate's submission of the final copies of the dissertation to the Graduate College.

I hereby certify that I have read this dissertation prepared under my direction and recommend that it be accepted as fulfilling the dissertation requirement.

_____ Date: 8/4/2015
Dissertation Director: Andrew Capaldi

STATEMENT BY AUTHOR

This dissertation has been submitted in partial fulfillment of the requirements for an advanced degree at the University of Arizona and is deposited in the University Library to be made available to borrowers under rules of the Library.

Brief quotations from this dissertation are allowable without special permission, provided that an accurate acknowledgement of the source is made. Requests for permission for extended quotation from or reproduction of this manuscript in whole or in part may be granted by the head of the major department or the Dean of the Graduate College when in his or her judgment the proposed use of the material is in the interests of scholarship. In all other instances, however, permission must be obtained from the author.

SIGNED: Jeremy Worley

ACKNOWLEDGEMENTS

Thanks to Andrew Capaldi for being an exceptional mentor and friend. Thanks to Xiangxia Luo for teaching me many lab techniques, for expert troubleshooting and data analysis, and for her immaculate lab work. Thanks to Arron Sullivan and Matt Kaplan for their partnership in designing and running the yeast growth regulator screen. Thanks to Jim Hughes Hallett for advice, moral support, and late night conversations. Thanks to Steven Fan for setting up our lab's microarray database. And thanks to my committee for their support and advice.

TABLE OF CONTENTS

LIST OF FIGURES

CHAPTER II: GENOME-WIDE ANALYSIS OF THE TORC1 AND OSMOTIC-STRESS SIGNALING NETWORK IN S. CEREVISIAE

CHAPTER III: INOSITOL PYROPHOSPHATES REGULATE CELL GROWTH AND THE ENVIRONMENTAL STRESS RESPONSE BY ACTIVATING THE HDAC RPD3L

LIST OF TABLES

ABSTRACT

To thrive when conditions are favorable and survive when they are stressful, cells must carefully regulate their growth rate and stress response programs. This requires rapid, coordinated regulation of many genes in response to information about the levels of numerous nutrients and stress conditions. We are beginning to understand how, in eukaryotes, the TORC1 and PKA pathways regulate growth in nutrient rich conditions. However, how cells tune growth and stress responses in suboptimal conditions is largely unknown. To address this, we ran screens to begin reconstructing the growth regulation network in stress conditions. We found many novel regulators, including signaling proteins, components of the vacuolar ATPase, transcription factors, and components of the endomembrane system. In order to place these regulators in the TORC1 pathway, we performed follow up experiments on over 300 of these regulators using the TORC1 inhibitor rapamycin. We were able to place many new components in the TORC1 pathway, including 59 genes that act downstream of TORC1. We were particularly interested in the discovery that Vip1, a conserved inositol pyrophosphate kinase, was necessary for the shutdown of hundreds of growth genes in stress and starvation conditions. In subsequent experiments, we learned that the inositol pyrophosphate second messengers (including 1-PP-IP5, 5-PP-IP4, and 5-PP-IP5) are critical regulators of cell growth and the general stress response, acting in parallel to the TORC1 pathway to control the activity of the class I HDAC Rpd3L. Taken together, this work reveals many new regulators of cell growth and shows how delineation of one such regulator uncovered a global role for a little known family of second messengers.

CHAPTER I: GENERAL INTRODUCTION—THE GROWTH CONTROL AND GENERAL STRESS RESPONSE NETWORK IN *S. CEREVISIAE*

1.1 How do cells set their growth rate and stress response programs in a dynamic environment?

In order to be successful in a dynamic environment, cells must carefully tune their growth rate and stress response programs.[1-3] To do this, a cell must monitor the level of numerous nutrients (such as carbon sources, amino acids, and phosphate) and stressors (including oxidative damage, heat shock, and osmotic stress). It must then integrate this information and decide how fast to grow and whether to enact a stress response.[1-3] A cell that fails to make this decision correctly may be outcompeted, starved, or irreparably damaged.[1-3] In addition, misregulation of growth in a multicellular organism can lead to cancer and other diseases.[1-3]

Cell growth control is so fundamental that the core pathways that make up the growth control network are conserved from yeast to humans and are known to play roles in cancer, diabetes, and other diseases.[2,3] The Target of Rapamycin Complex 1 (TORC1) pathway senses nutrient, hormone, and stress levels, and based on this information controls translation, ribosome production, metabolism, and autophagy[1-3]. The Ras/Protein Kinase A (PKA) pathway monitors glucose or insulin levels and, when active, promotes growth.[4] In addition, information about nutrients and stress from multiple pathways including TORC1, PKA, and the inositol pyrophosphates (discussed in Chapter III) is integrated at the transcriptional level by the class I HDAC complex Rpd3L, which regulates the transcription of hundreds of growth, metabolism, and stress response genes.[5-7,a]

---

[a] Optimizing growth rate and stress responses to fit changing conditions is also accomplished through regulation of mRNA. This may occur through mechanisms such as regulation of mRNA decay and

1.2 The TORC1 pathway: A growth control hub in eukaryotic cells.

In 1975, a small molecule was isolated from a streptomycete that had been discovered living on one of the most remote inhabited islands on earth—Rapa Nui (Easter Island). The molecule, named rapamycin, was found to strongly inhibit the growth of the pathogenic fungus C. albicans and was later found to act as an immunosuppressant.[8,9] It wasn't until 1991, however, that the Target of Rapamycin (TOR) kinase was discovered and a central growth pathway in eukaryotic cells began to be investigated.[10] In little more than a decade, TOR would be recognized as a nutrient- and stress-sensitive master regulator of cell growth and aging[11].

1.2.1 Composition of the TORC1 complex in S. cerevisiae

TOR kinase is the catalytic subunit of TOR Complex I (TORC1), and both the kinase and complex are conserved across eukaryotes.[10,12] In *S. cerevisiae*, TORC1 is made up of Kog1, Lst8, Tco89, and either Tor1 or Tor2.[12,13] Kog1 (Raptor in humans) contains both HEAT and WD-40 repeats and may act to present substrates to Tor1/2.[14,15] Lst8 also contains WD-40 repeats and may stabilize the kinase domain. Tco89 contains no obvious domains and may act to receive signals from EGO complex.[1,16] Tor1 and Tor2 are PI3K related kinases, and either may act in the TORC1 complex.[b] TORC1 is 1.2 MDa and likely exists as an obligate heterodimer.[17] In growth conditions the complex is localized to the vacuolar membrane.[18]

1.2.2 Upstream regulation of TORC1

TORC1 is rapidly inactivated in response to starvation (including carbon, nitrogen, amino acids, and phosphate starvation), and the presence of stressors (including oxidative stress, osmotic stress, heat

[b] In *S. cerevisiae*, as in higher eukaryotes, there are two TORC complexes, known as TORC1 and TORC2. TORC1 regulates ribosome biogenesis, metabolism, and stress response genes. TORC2 regulates actin cytoskeleton polarity and cell wall integrity. In *S. cerevisiae*, either Tor1 or Tor2 may act in TORC1, but only Tor2 acts in TORC2. To make things even more confusing, Tor2 is a product of the *S. cerevisiae* whole genome duplication and does not exist in other eukaryotes. (http://www.yeastgenome.org/go/GO:0031932/overview)

shock, caffeine[c], and DNA damage).[1,19] Despite knowledge of the many signals that TORC1 responds to, very little is known about how TORC1 is regulated. Work by several labs has revealed how TORC1 is regulated in response to amino acid and glucose/ATP levels (as described in detail below), but little is known about how TORC1 is regulated by other nutrients or stressors. To date, almost everything that is known about TORC1 regulation involves one of three mechanisms: 1) interaction with the EGO complex, 2) interaction with Rheb (which is regulated by Tsc1/2, or TSC Complex), or 3) phosphorylation by AMPK/Snf1.[20]

1.2.2.1 Upstream regulation of TORC1 mediated by EGO and the v-ATPase

The EGO (Exit from rapamycin-induced GrOwth arrest) complex was discovered using a screen designed to find genes required for the exit from quiescence in *S. cerevisiae*.[21] The complex is composed of Ego1/2 (Ragulator in humans) and the Ras GTPases Gtr1/2 (the Rags in humans). It resides on the vacuolar membrane and activates or inactivates TORC1 in response to high or low amino acid levels, respectively.[22,23] The mechanism by which Gtr1/2 regulate TORC1 activity is unknown.

The EGO complex was first found to respond to leucine levels, but recent discoveries in human cells suggest that it monitors the levels of other amino acids as well.[24,25] Two recent papers show that in the presence of sufficient arginine, the lysosomal amino acid transporter SLC38A9, acting in concert with the v-ATPase, induces the Rags to activate mTORC1. In their report, Wang et al. write that additional nutrient sensors are almost certain to exist.[24] Whether they exist in *S. cerevisiae* is an open question, but the conservation of EGO, the v-ATPase, and SLC38A9 suggest that they do.

In addition to responding to leucine and arginine levels through interactions with amino acid sensors, the EGO complex is negatively regulated in nitrogen (glutamine) starvation by the SEA complex (GATOR in humans).[22,26] The SEA complex also regulates EGO in response to methionine, which may represent sulfur levels and possibly other nutrients.[26]

---

[c] Caffeine is an active-site inhibitor of PI3K-like kinases.

As was discussed above, the v-ATPase plays a role in TORC1 regulation in response to amino acid levels. In response to arginine and leucine, the v-ATPase acts with EGO to activate TORC1, but EGO is not required in nitrogen/glutamine sensing.[27,28] When glutamine levels are low, the v-ATPase instead acts with another GTPase, Arf1, to activate TORC1. Interestingly, it has also recently been shown that the addition of a carbon source (glucose) causes a change in pH that, in turn, causes the v-ATPase to activate both TORC1 and PKA.[29] This activation, the authors argue, occurs through both Gtr1 (for TORC1) and Arf1 (for PKA).

1.2.2.2 Upstream regulation of mTORC1 mediated by the TSC complex

From studies focusing on the roles of the EGO, SEA, and v-ATPase complexes, a model emerges in which information about nutrient levels are funneled to TORC1 through interactions between the v-ATPase and various GTPases on the vacuole. In humans and many higher eukaryotes, however, there is another point through which information about nutrients and stress is funneled to TORC1—the TSC complex.[30-32] In these organisms, TORC1 is activated through the Rheb GTPase, which is inhibited in many adverse conditions by the GAP activity of the TSC complex.[31] The TSC complex has been found to be inhibited (activating mTORC1) in growth conditions by signals from the Tumor Necrosis Factor alpha (TNFα) and Insulin Growth Factor (IGF) pathways.[33] It is activated (inhibiting mTORC1) in low energy conditions by AMPK and in DNA damage by p53 pathway signaling (acting through AMPK).[33,34]

1.2.2.3 Upstream regulation of TORC1 mediated by the AMPK/Snf1

In humans, AMPK activates the TSC complex (inhibiting mTORC1) when the AMP:ATP ratio in the cell is high, indicating low energy. In addition, in response to DNA damage, AMPK activates TSC complex through Sestrin.[35] In *S. cerevisiae*, where there is no TSC complex, it was recently published that the AMPK orthologue Snf1 inactivates TORC1 in the absence of glucose.[36] This occurs through phosphorylation of Kog1, although it is unknown whether Snf1 phosphorylates Kog1 directly.

1.2.2.4 Upstream regulation of TORC1 in stress conditions

Virtually everything known about TORC1 regulation relates to how it is activated in nutrient rich conditions and inactivated in starvation. In humans, AMPK causes the inactivation of mTORC1 in response to DNA damage and hypoxia, but in *S. cerevisiae* Snf1/ AMPK1 has only been shown to regulate TORC1 in response to low glucose. In *S. cerevisiae*, virtually nothing is known about how TORC1 is regulated in response to stress.

The only known regulator of TORC1 in stress is MAPK Hog1, eponymous member of the High Osmolarity Glyerol (HOG) pathway[37]. In Hog1 null mutants, TORC1 is not fully inactivated and, consequently, growth genes are not fully repressed. However, the effect of Hog1 is only partial, accounting for about one-quarter of the total growth gene shutdown in osmotic stress. In addition, Hog1 regulation of TORC1 in osmotic stress only occurs in certain media (SD but not YEPD).

1.2.3 The downstream TORC1 pathway

TORC1 uses an extensive list of inputs to sense environmental flux. It then tightly regulates growth by setting the appropriate balance between anabolic processes, like macromolecular synthesis, and catabolic processes, such as autophagy and gluconeogenesis.[23,38] Additionally, it can activate stress response programs, such as the osmotic stress response, when stressors threaten to damage the cell. To regulate growth and stress responses, TORC1 uses a relatively well-studied group of effectors. In *S.* cerevisiae, most of these downstream components of the TORC1 pathway can be placed into two branches: the Sch9 kinase branch, which regulates growth genes, and the PP2A phosphatase branch, which regulates autophagy and metabolism genes.

1.2.3.1 The Sch9 branch activates growth genes in nutrient rich conditions

The best characterized TORC1 effector is Sch9, an AGC family kinase that is analogous to the human S6 kinase. In nutrient rich conditions TORC1 is active and phosphorylates Sch9 at six sites.[39] Sch9, in turn, phosphorylates the inhibitory transcription factors Stb3, Dot6, and Tod6, which keeps them inactive in the

cytosol.[5] In parallel, TORC1 phosphorylates the transcriptional activator Sfp1, which binds to both ribosome biogenesis and RP gene promoters and stimulates transcription.[40-42]

In stress and starvation conditions TORC1, and consequently Sch9, is inactivated. In turn, Stb3, Dot6, and Tod6 are dephosphorylated (by unknown means) and enter the nucleus where they recruit the Rpd3L deacetylase complex to ribosome biogenesis and RP gene promoters.[5] Deacetylation by Rpd3L leads to a rapid shutoff of transcription at these genes.[6]

Although the Sch9 branch of the TORC1 pathway is critical in stress and starvation, microarray analysis in strains that contain an ATP-analogue sensitive Sch9 allele indicate that inhibition of Sch9 kinase activity is not equivalent to inhibition of TORC1 with rapamycin. Furthermore, deletion of Dot6 and Tod6 only affects ribosome biogenesis genes but not the hundreds of genes that are turned on in stress or starvation. Thus, it is likely there are unknown TORC1 effectors that are acting in stress and starvation.

1.1.1.1 The PP2A branch inhibits autophagy and stress response genes in nutrient rich conditions.

In addition to phosphorylating Sch9, in nutrient rich conditions TORC1 phosphorylates Tap42, which binds to and inhibits five type 2A and 2A-related phosphatases (Pph3/21/22, Sit4, and Ppg1).[43,44] Investigation of the PP2A phosphatases, which are both redundant and pleotropic, has been extremely difficult.[1] However, what is known is that under certain stress and starvation conditions inactive TORC1 leads to Tap42 being dephosphorylated and releasing the phosphatases.[45] The active phosphatases then trigger a number of downstream factors, including Atg1 (a regulator of autophagy), Msn2 (transcriptional activator of about 200 general stress response genes), and Gat1 (transcriptional activator of nitrogen catabolite repression genes).[43,46] These downstream factors initiate autophagy and nutrient scavenging as well as the general stress response.

1.3 The PKA pathway

As would be expected of a microbe that evolved to grow on fruit, *S. cerevisiae* excels at two things: waiting and growing. It can survive long periods of desiccation and starvation and then transform itself into a ribosome factory when it is presented with glucose or fructose, which it prefers to all other carbon sources. Within minutes of being transferred into glucose rich media, over 40% of *S. cerevisiae* genes change transcription by 2-fold or more. Almost all of this glucose-induced signaling proceeds through the PKA/Ras pathway, which is both necessary and sufficient for most of the response to glucose.[47]

In *S. cerevisiae*, PKA is a heterotetramer comprising two identical Bcy1 regulatory subunits and two closely related catalytic subunits. The two catalytic subunits can be any two of three kinases: Tpk1, Tpk2, and Tpk3. The Tpks appear largely redundant and a deletion of any two causes only a small defect in the transcriptional response to glucose reintroduction. Deletion of all three, however, is lethal.

Unlike TORC1, the upstream regulation of PKA is well defined. The proximate activator of PKA is cyclic AMP (cAMP), which binds to Bcy1 and eliminates its inhibition of the TPKs.[48-50] cAMP is made from ATP by the adenylate cyclase Cyr1 and is degraded to AMP by the phosphodiesterase Pde1.[51] There are two upstream inputs that activate Cyr1, and thus increase cAMP levels. The first is the plasma membrane G protein alpha subunit Gpa2.[49,52] The second are the paralogues Ras1 and Ras2 (homologues of the human oncogene of the same name).[49,52] Despite much work, it is unclear how the Ras GTPases sense glucose, but it is believed that they respond to glucose-dependent acidification of the cytoplasm.[47]

The downstream effectors of PKA have also been well studied. In response to glucose, PKA inhibits Dot6 and Tod6 at the same phosphorylation motif as Sch9.[5] This phosphorylation keeps Dot6/Tod6 inactive in the cytosol, preventing them from inactivating ribosome biogenesis genes. In addition to ensuring that growth genes are not inhibited, PKA phosphorylates Msn2, preventing it from activating the general stress response and catabolism.[53] Thus, PKA both stimulates growth genes and inhibits processes that are antithetical to rapid mass accumulation.

Like the TORC1 pathway, the PKA pathway represses catabolism and stress responses in the presence of glucose. Unlike Torc1, however, PKA appears to respond only to glucose. In stress conditions, growth and stress response genes are regulated by TORC1 and other, unknown, pathways.

1.4 The Rpd3L HDAC complex

The Rpd3 histone deacetylase is the founding member of the class I HDAC family, whose catalytic domain is conserved from bacteria to humans.[54] Rpd3 is part of at least two different complexes in *S. cerevisiae*, the best characterized of which are Rpd3L and Rpd3S.[55,56] All Rpd3 complexes share a core comprising Rpd3, Sin3, and Ume1, and this core is conserved in humans.[d] [54]

In addition to the three core proteins, Rpd3L contains nine subunits: Pho23, Sap30, Sds3, Cti6, Rxt2, Rxt3, Dep1, Ume6 and Ash1.[55,56] Pho23 is known to bind methylated H3K4, causing Rpd3L to be recruited to methylated histones.[57] Ume6 binds the URS1 motif of early meiotic genes and recruits Rpd3L, leading to their repression.[58] The paralogous transcription factors Dot6 and Tod6 were not detected when Rpd3L was first defined, but they are essential for the recruitment of the complex to ribosome biogenesis gene promoters, where they recognize the PAC motif.[59] Other than the roles of these few subunits, what the remaining nine components of Rpd3L do in any condition is a mystery.

The Rpd3L complex is a global regulator of transcription, and is known to be critical to stress responses, Sir2-mediated silencing, and replication origin firing.[60-62] Interestingly, Rpd3L has recently been found to act not only through the traditional role of a deacetylation, which is to inhibit transcription by causing DNA to be bound more tightly to histones, but also as a transcriptional activator. How and why this activation occurs is not clear. Another important discovery is that in addition to histone tails, Rpd3 deacetylates proteins in the cytosol. These newly found Rpd3 activities indicate a broad and complex role in the regulation of many cellular processes.

---

[d] In human cells, the closest homologues to Rpd3 are HDAC1 and HDAC2, which are nearly identical, but HDAC3 is also a close relative.

In log growth conditions, Rpd3L is recruited to catabolism, autophagy, and stress response genes through an unknown mechanism. Consequently, transcription of these genes is repressed while Sfp1 (and possibly other TORC1 effectors) activates ribosome biogenesis and anabolism genes. In stress or starvation conditions, inactive TORC1 leads to inactive Sch9, which in turn leads to dephosphorylation and activation of Stb3 and Dot6/Tod6, which enter the nucleus and bind ribosome biogenesis and RP promoters at PAC and RRPE motifs. From these promoters, Stb3 and Dot6/Tod6 recruit Rpd3L, which rapidly inactivates over 600 ribosome biogenesis, RP, and anabolism genes.[5]

1.5 Aims

As discussed above, TORC1 and PKA are the core known growth control pathways in *S. cerevisiae*, and the PKA pathway appears to respond only to glucose. Although we have gained some understanding of how the TORC1 pathway functions in log growth and amino acid starvation, many fundamental questions remain unanswered: First, we know very little about how the cell senses stress and starvation and transmits that information to TORC1 (i.e., how is TORC1 regulated in these conditions). Second, microarray evidence suggests we are unaware of important components of the downstream TORC1 pathway in stress and starvation. And third, we have almost no knowledge of the pathways that cooperate with TORC1 to control growth in stress and starvation.

Chapter II discusses an automated screen for growth control regulators in stress and subsequent experiments to place those regulators in the known growth control pathway.

Chapter III discusses the delineation of one such growth regulator, the inositol kinase Vip1, and the discovery that inositol pyrophosphates are critical regulators of cell growth in stress and starvation.

Chapter IV discusses unanswered questions, new questions, and goals for future work.

CHAPTER II: GENOME-WIDE ANALYSIS OF THE TORC1 AND OSMOTIC-STRESS SIGNALING NETWORK IN S. CEREVISIAE

Jeremy Worley[*], Arron Sullivan[*], Xiangxia Luo, Matthew E Kaplan, and Andrew P. Capaldi

Department of Molecular and Cellular Biology and the Functional Genomics Core facility, University of Arizona, Tucson, AZ, 85721-0206

[*] Co-first authors

1.1 ABSTRACT

The Target of Rapmycin kinase Complex I (TORC1) is a key regulator cell growth and metabolism in eukaryotes--driving protein and ribosome synthesis in nutrient replete conditions, and activating catabolic metabolism in stress and starvation conditions. Studies in yeast and human cells have shown that nitrogen/amino acid starvation signals act through Npr2/3 and the small GTPases Gtr1/2 (Rags in humans) to inhibit TORC1. However, it is unclear how other stress and starvation stimuli inhibit TORC1 signaling, and/or act in parallel with the TORC1 pathway, to control cell growth. To help answer these questions, we developed a novel automated pipeline and used it to measure the expression of a TORC1 dependent ribosome biogenesis gene (NSR1) during osmotic stress in 4700 *Saccharomyces cerevisiae* strains from the yeast knock out collection. This led to the identification of 440 strains with highly significant ($p<0.001$) and reproducible defects in NSR1 repression. The cell growth control and stress response proteins deleted in these strains form a highly interconnected network, including; 56 proteins involved in vesicle trafficking and vacuolar function; 53 proteins that act downstream of TORC1 according to a rapamycin assay, including components of the HDAC Rpd3L, Elongator and the INO80, CAF-1 and SWI/SNF chromatin remodeling complexes; over 100 proteins involved in signaling and metabolism; and 17 proteins that directly interact with TORC1. These data serve as an important resource for labs studying cell growth control and stress signaling, and demonstrate the utility of our new, and easily adaptable, method for mapping gene regulatory networks.

2.1 INTRODUCTION

The Target of Rapamycin (TOR) kinases are conserved across eukaryotes, where they act as master regulators of cell growth and metabolism [1,2]. In line with their central role in cell signaling, TOR kinases respond to an enormous array of stimuli and control the activity of hundreds of proteins--functions that are supported in part by their recruitment into two distinct complexes, TOR Complex 1 (TORC1) and TOR Complex 2 (TORC2) [12,15,39,63-66]. TORC1, unlike TORC2, is rapamycin sensitive and in *S. cerevisiae* is made up of the TOR kinase Tor1 (and in its absence the homolog Tor2), the key regulator Kog1, and two poorly characterized proteins, Lst8 and Tco89 [10,12,13].

In the presence of adequate nutrients, TORC1 drives growth by activating multiple steps in protein and ribosome synthesis. First, TORC1 directly phosphorylates and activates the transcription factor Sfp1 and the AGC kinase Sch9 [39,40]. Sch9, in turn, then phosphorylates and blocks the activity of the transcriptional repressors Dot6, Tod6 and Stb3, leaving Sfp1 to promote the high level expression of 400 genes involved in ribosome biogenesis (Ribi) and translation [5,41,42,59,67]. Second, TORC1 acts in cooperation with Yak1 and the cAMP dependent protein kinase (PKA) pathway, to promote the activity of Fhl1 and up-regulate expression of the ribosome protein (RP) genes [68-70]. Third, TORC1-Sch9 phosphorylates and regulates the kinase Maf1, and other factors, to activate Pol I and Pol III and thus rRNA and tRNA synthesis [63,71,72]. Finally, TORC1 promotes translation, in part by blocking phosphorylation of eIF2 [1,66].

In contrast, when cells are starved for energy, amino acids, or nitrogen, or exposed to noxious stress, TORC1 signaling is inhibited, leading to down-regulation of Ribi and RP gene expression, rRNA and tRNA synthesis, and thus cell growth [39,73-75]. In particular, dephosphosphorylation of Dot6, Tod6 and Stb3 triggers recruitment of the Class I histone deacetylase Rpd3L to the Ribi and RP genes, leading to a rapid decrease in gene expression levels [5,6,59].

The mechanisms underlying TORC1 inhibition in nitrogen and amino acid starvation conditions are starting to come into focus. Specifically, it is now clear that nitrogen and amino acid starvation trigger

activation of the GAP Npr2/3, and this in turn alters the GTP binding state of the small GTPases, Gtr1/2 [76-79]. Gtr1/2 then bind TORC1 on the vacuolar membrane and inhibit TORC1 dependent phosphorylation of Sfp1 and Sch9 [39,40,76,79]. At the same time an interaction between Gtr1/2, the small GTPase Rho1, and TORC1 promotes release of Tap42 from the TOR complex, triggering Tap42-PP2A dependent reprogramming of nitrogen and amino acid metabolism [43,45,80,81]. At least in humans, Gtr1/2 signaling also depends on interactions with the vacuolar ATPase (V-ATPase) and amino acid transporters on the vacuolar membrane [82,83].

Outside of nitrogen and amino acid starvation conditions, however, very little is known about TORC1, and TORC1 pathway, regulation. Npr2/3, Gtr1/2, and Rho1 all play little-to-no role in transmitting glucose starvation, osmotic stress, heat stress and oxidative stress signals to TORC1-Sch9 [37,76]. Instead, the AMP activated protein kinase Snf1 partially inhibits TORC1 and/or TORC1-Sch9 signaling in glucose/energy starvation, while the MAPK Hog1 plays a small role in regulating TORC1 and/or the TORC1-Sch9 signaling in osmotic stress [37]. It is also known that TORC1 binds to stress granules during heat shock, but this interaction is not required for the initial stages of TORC1 inhibition [84]. Thus, most of the proteins and pathways that regulate TORC1 and/or TORC1-Sch9 signaling in noxious stress and energy starvation remain to be identified.

It is also unclear how the TORC1 pathway cooperates with other signaling pathways to regulate cell growth. Numerous studies have shown that the ras/PKA pathway regulates expression of the cell growth genes in glucose, primarily by acting in parallel with Sch9 to phosphorylate and regulate Sfp1 and Dot6/Tod6 [41,42,59,68,85,86]. It is also known that the inositol kinases Vip1 and Kcs1, and the inositol pyrophosphates they produce, act in parallel with TORC1 to regulate Rpd3L, and thus the Ribi and RP genes, during stress [87]. However, it is unclear how Kcs1 and Vip1 are regulated and if/how other pathways cooperate with TORC1 to control cell growth.

Therefore, to push our understanding of TORC1 signaling and cell growth control forward, we carried out a screen to identify proteins that are required for the down-regulation of Ribi gene expression in osmotic stress. Similar screens have been carried out previously to identify proteins involved in the Unfolded Protein Response (UPR) and Heat shock factor 1 (Hsf1) response pathways (in log growth conditions)--in both cases using a GFP reporter placed under a relevant promoter [88,89]. However, a GFP reporter cannot easily be used to study cell growth control since Ribi and RP genes are only transiently down regulated during stress, leading to relatively small (2-fold) changes in Ribi and ribosome protein levels [74,90]. To get around this problem, we developed a novel automated pipeline that directly measures mRNA levels at the peak of the osmotic stress response (20 min), and used it to measure Ribi gene expression in 4700 strains from the yeast knockout (YKO) collection [91]. This led to the identification of 440 strains with a reproducible and highly significant ($p<0.0001$) defect in Ribi gene repression during stress. We then went on to show that 56 of these strains also have a significant defect in the response to rapamycin, and are therefore missing proteins that act downstream of TORC1.

Among the genes that act downstream of TORC1, we find numerous factors involved in transcription and chromatin remodeling including 6 subunits of Rpd3L, 3 subunits of the Elongator complex, 3 histone proteins, 2 histone demethylases and components of the SWI/SNF, INO80 and CAF-1 chromatin remodeling complexes. We also identified 21 ribosome proteins and translation factors in the screen, 9 of which act downstream of TORC1. Other genes in the growth control network have a wide variety of functions, but include 56 proteins involved in vacuolar function and vesicle transport, including 10 components of the V-ATPase, as well as 5 kinases, 5 methyltransferases, and 9 membrane transporters. Finally, 17 genes in the network physically interact with TORC1, suggesting that we have identified numerous direct regulators and effectors of TORC1 signaling.

Overall, the data presented here serve as a valuable resource for those studying TORC1 signaling, cell growth control and/or the environmental stress response, and demonstrates the utility of our novel and easily adaptable method for mapping gene regulatory networks in yeast and other organisms

2.2 METHODS

2.2.1 Automated Pipeline

Inoculation, growth, treatment, and RNA isolation steps were performed on a Biomek FX liquid handling robot (Beckman Coulter) equipped an integrated plate hotel (Cytomat) and shaking incubator (Liconic). All 96 wells plates were labeled with barcodes, and loaded onto the Biomek using a barcode scanner, to ensure that the plates did not get inverted or mixed up. OD_{600} measurements were taken with a plate reader (BioTek Synergy 2) in sterile 96-well plates (Greiner Bio-One) at 30°C.

2.2.2 Cell Growth and Stress Treatment

YKO collection strains were pinned onto YEPD agar plates using a Singer ROTOR robot and grown for two days at 30°C. The yeast were then pinned from the agar plates into 96-well plates containing 100μl of YEPD per well and grown for 18-22 hours at 30°C. Finally, the overnight cultures were used to inoculate 2.2ml deep-well plates (VWR), containing 550μl of YEPD and one sterile 3.2mm stainless steel mixing bead per well, to an OD_{600} of 0.05 and loaded into the Liconic Incubator (shaking at 1200rpm and 30°C). Once the median OD_{600} of a plate reached 0.60 (no wells reached an OD_{600} of >0.8), 150μl of each culture was transferred to a 2.2ml 96-well plate containing 850μl of RNAse Inactivation Buffer per well (RI Buffer; 4M Ammonium Sulfate, 100mM MES buffer, and 20mM EDTA, pH 4.6) and mixed thoroughly by pipetting. 100μl of 1.875M KCl or 1μg/ml rapamycin in 30°C YEPD was then added to each remaining culture (yielding final concentration of 0.375M KCl or 200ng/ml rapamycin) and the plate returned to the Incubator for 19min (shaking at 1200rpm and 30°C). The plate was then moved back to the deck of the robot and 150μl of culture removed from each well and added to RI Buffer as described above. The plates containing RI Buffer and yeast were then stored at -20°C.

2.2.3 RNA Purification

Plates containing cells in RI Buffer were defrosted by centrifugation (25min at 3000rpm at room temperature) and the supernatant removed from each well. The pelleted cells were then resuspended in

400μl lysis buffer (4M Guanidine Thiocyanate, 25mM NaCitrate, 0.5% N-lauryl Sarcosine) and transferred to a 700μl 96-well plate (Griener) containing 300μl of zirconia/silica beads per well. The plates were then sealed with sterile foil and shaken for 5min on a mini-Beadbeater-96 (Biospec). After a second round of centrifugation (25min at 3000rpm at 4°C) the plates were loaded into the robot where 100μl of lysate was transferred to a sterile 96-well PCR plate (Thermo Scientific). At this point, 70μl of isopropanol was added to each lysate and mixed for 1min before adding 20μl of MagMax binding beads (50% slurry in binding buffer; Ambion) to each well. The isopropanol, lysate and bead mix was then mixed for 7min to ensure all of the RNA in the sample bound to the beads, the plate moved to a magnetic stand-96 (Ambion) for 5min, and the liquid removed from each well. The beads were then washed with 150μl of Wash Buffer 1 for 5min (1.7M Guanidine Thiocyanate, 0.17% N-lauryl Sarcosine, 33% isopropanol, 33mM NaCitrate, pH 7.0) followed by 150μl of Wash Buffer 2 for 5min (2M KCl, 80% Ethanol, 2mM Tris, PH 7.0). The DNA in each sample was then cleaved by treatment with Turbo DNAse (0.25μl of 2 U/μL stock in 50μl DNAse buffer from Life Technologies) for 25 minutes at room temperature. The RNA was then bound to the magnetic beads again by adding 100μl of 1.5x Wash Buffer 1 and incubating for 5min, the beads washed two more times with Wash Buffer 2 (5min each), and dried for 10min at room temperature. Finally, the purified RNA was eluted by mixing the beads with 40μl of 55°C elution buffer (1mM sterile-filtered RNAse-free Tris pH 8.0) for 5min, the plate was then returned to magnetic stand (to remove the beads), and the eluate transferred to a sterile PCR plate and stored at -80°C.

2.2.4 qPCR

1-step qRT-PCR reactions were performed using 5μl RNA, TaqMan probes/primers from Lifetech (used at the recommended concentrations; probe and primer sequences not provided by company) and 5μl PerfeCTa qPCR ToughMix, Low ROX (Quanta) in a 96-well PCR plate using an Agilent Stratagene Mx3005p cycler. One TaqMan probe bound to the reporter gene Nsr1 (labeled with FAM dye) and the other bound to a control gene, Pex6 or Ntf2 (labeled with JOE dye). The ROX normalized data from each plate was then analyzed using the Stratagene MxPro software and fluorescence thresholds (dRn) of 0.120 for FAM (Nsr1) and 0.60 for JOE (Pex6). Samples that passed the FAM or JOE threshold after >28

cycles were discarded. This filtering caused us to drop data from about 200 strains in the YKO library; most of these strains grew very poorly in the 96 well plates leading to a low RNA yield.

2.2.5 qPCR Normalization

To calculate the normalized NSR1/PEX6 and NSR1/NTF2 ratios, the FAM minus JOE (F-J) value was calculated for every well. The machine learning module, scikit-learn, in Python was then used to calculate the average F-J value for two populations on each plate--strains with expression defects, and strains without expression defects. This was done using Gaussian Mixture Models in the 'scikit.mixture' package with a covariance class of type 'full' for 2-component analysis (http://scikit-learn.org/stable/modules/mixture.html#selecting-the-number-of-components-in-a-classical-gmm). The average F-J value for the strains without an expression defect was then subtracted from the F-J value of the entire plate, setting the mean of the plate (minus the outliers) to 0.0. All values were then multiplied by -1 so that higher RNA concentrations give higher NSR1/PEX6 ratios. This normalization had little impact on the list of strains that we identified as outliers in the screen but adjusts for the 0.3-0.6 cycle variation in the average NSR1/PEX6 ratio that we observe in separate runs on the qPCR machine (even when we use the exact same samples).

2.2.6 Network Reconstruction

Interactions between the top 440 genes/proteins in our screen were mapped using the protein-protein interaction data from BioGRID (version 3.4.125). TORC1 (Tor1, Kog1, Lst8, Tco89) was also added to our model as one merged node for reference. 275 proteins, including TORC1, form the major network, while 160 genes have no connection to any other of the 440 proteins identified in the screen. Note that the HSP70 family chaperones Ssa1 and Ssb1 and the RNA binding protein Slf1 were removed from the set (along with any proteins that only interact with them) in Fig. 6 to eliminate non-specific interactions (leaving 236 genes).

2.2.7 DNA Microarrays of Rpd3L mutants

Rpd3L and Rpd3S mutants were constructed using standard methods in an EYO690 (W303) background, as described in detail previously [87]. Overnight cultures of the EY0690 or Rpd3L mutant strains were then used to inoculate 0.75L of YEPD to an OD_{600} of 0.1 in a 2.8 L conical flask, and grown shaking at 200 rpm and 30°C. Once the cultures reached an OD_{600} of 0.6, 250 ml of cells were collected by vacuum filtration and frozen in liquid nitrogen. The remaining cells were then subjected to 0.375 M KCl stress for 20min, harvested by vacuum filtration, and frozen in liquid nitrogen. Finally, the mRNA was purified from the frozen cells, converted into cDNA using reverse transcription, labeled with Cy3 or Cy5, and examined using an Agilent microarray, as described previously [87,92]

2.3 RESULTS

2.3.1 Automated Analysis of Gene Expression in Yeast

We developed an automated pipeline and used it to measure the expression of a ribosome biogenesis gene (NSR1) in 4709 a-type strains from the yeast knockout (YKO) collection [91]. This pipeline included three major steps (Fig. 1a):

First, strains were grown to an OD_{600} of 0.6 in 96-well plates and exposed to 0.4M KCl, 200nM rapamycin, or mock stress. Then, at the peak of the stress response (20 min), 4M Ammonium sulfate (pH 4.6) was then added to the cultures to promote protein precipitation and block any further RNA synthesis or degradation.

Next, the 96-well plates were centrifuged to pellet the cells and the ammonium Sulfate solution was replaced with lysis buffer and glass beads. The cells were then lysed by bead-beating and the plates centrifuged a second time to remove insoluble debris.

Finally, the RNA was purified from the lysates in each plate using silicon coated magnetic beads and loaded into a 96-well PCR plate. The gene expression levels in each strain were then measured using quantitative PCR--generally following expression of NSR1 and the housekeeping gene PEX6 (Fig. 1b and c).

All of the steps in the pipeline, with the exception of bead-beating and centrifugation, were performed on a Biomek FX liquid handling workstation with an integrated Liconic incubator. This ensured that all wells and plates were treated in an identical way, making it possible to compare data across strains and days (Methods).

2.3.2 Testing the Pipeline

To test our pipeline, we grew a 96-well plate with wild-type yeast in every well and measured NSR1 and PEX6 expression. The NSR1 and PEX6 mRNA levels were consistent across the plate, with a $\log_2$ standard deviation of 0.86 and 0.90, respectively (<2-fold average variation). Moreover, when we normalized the NSR1 data using the PEX6 data--to account for well-to-well variation in total RNA levels--we found that the standard deviation from the mean was only 0.37 on a $\log_2$ scale (~30% average variation; Fig. S1).

We then grew another plate of wild-type yeast, but this time treated half of the plate with mock stress (YEPD alone) and the other half of the plate with 0.4M KCl. The experiment showed that osmotic stress triggers a $\log_2$=2.3 fold average decrease in NSR1 expression (Fig. 2). While this expression change is compressed compared to the $\log_2$=4 fold decrease we observe using microarray methods, the standard deviation from the mean in stress was only 0.26 on a $\log_2$ scale (0.36 for mock stress samples). Thus, the expression change in osmotic stress is approximately ten times greater than the noise in our assay, indicating that our screen should be accurate enough to identify strains with moderate changes in NSR1 expression.

2.3.3 Analysis of the Yeast Knock Out Collection

After we built and tested the automated pipeline, we used it to measure the osmotic stress response in strains from the YKO library (see Methods); collecting two sets of data for 6 of the 96-well plates in the library and one set of data for the other 48 plates in the library. We then normalized the NSR1/PEX6 values to set the average expression level of the library, excluding outlier strains, to $\log_2$ =0.0 (see Methods).

Inspecting the data from the screen revealed that most of the strains in the YKO collection have a similar NSR1/PEX6 ratio, with $\log_2$ values ranging from -1.0 to +1.0 (Fig. 3a). However, there were also over 400 outlier strains, with NSR1/PEX6 ratios ranging from $\log_2$ = 1.5 to 4.5 (Fig. 4a).

To estimate the significance of these results, we analyzed the data from the six plates (570 strains) that were run through the pipeline twice (on separate days; Fig. 3b). Overall, we found a good correlation between replicates, with a Pearson's r of 0.90 and an average difference between measurements of $\log_2$= 0.29. Taking this latter value as good estimate of the average error, we then modeled the log data for the complete screen using a normal distribution with a mean of 0.0 and a standard deviation of 0.3 (Fig. 3a). This model fit the data for strains with NSR1/PEX6 ratios between -1.0 and ~0.5 very well, indicating that the variation in this range is simply due to the error in our assay. By corollary, we could then estimate the probability that a strain has a $\log_2$ NSR1/PEX6 ratio larger than 1.0 by chance at less than 0.1% (3.3 Z-score; Fig. 3a).

Our statistical analysis suggested that there are 734 strains with a significant defect in stress dependent repression of NSR1 ($\log_2$>1.0; p<0.001). However, there were two potential problems with this interpretation of the data. First, our error model is based on data from 6 out of 54 plates in the library--if the errors vary from plate to plate we could be overestimating the number of strains with real defects in NSR1 repression. Second, our analysis assumes that the expression level of the housekeeping gene PEX6 is constant across all YKO collection strains, but some strains may have a higher NSR1/PEX6 ratio than expected due to a decrease in PEX6 expression.

To address these issues we took all of the strains with a normalized NSR1/PEX6 ratio $\log_2$>1.3 (rearrayed onto 6 plates containing 494 strains plus 72 center peak [$\log_2$=0] controls) and ran them through our pipeline again. However, this time we measured the stress dependent changes in the expression level of NSR1 and a different housekeeping gene, NTF2. Just over 85% of the 494 strains had $\log_2$>1.0-fold more NSR1/NTF2 than the control strains, leaving 440 strains that have significantly more NSR1 expression (p<0.001) than the average strain in the YKO library in two separate assays (Table S1).

2.3.4 Identification of Known Components in the Cell Growth Control Circuit

To estimate the false negative rate in our screen, we examined the screen data for strains missing known components in the Ribi gene control circuit. As described in the introduction, TORC1, Sch9, Kcs1, Vip1, Hog1, and Rpd3L are all known to play a role in down-regulating Ribi gene expression during osmotic stress. However, strains missing the TORC1 components Tor1, Kog1, Lst8 and Tco89, and the kinase Sch9 should not (and do not) show up as hits in our screen since; Tor1 acts redundantly with Tor2; Tco89 has a very limited impact on TORC1 signaling; and Kog1, Lst8 and Sch9 are essential genes and thus not in the YKO library [12,91].

We did find a $\log_2$= 3.1, 1.1, and 0.6 increase in NSR1 expression in the *kcs1Δ*, *vip1Δ* and *hog1Δ* strains from the YKO collection. These numbers align reasonably well with those from our previous work, where we found that deletion of Kcs1, Vip1 and Hog1 in the W303 background all caused an approximately 2-fold increase in Ribi gene expression in osmotic stress [37,87]. The one outlier was the *kcs1Δ* strain from the YKO library (which has a larger increase in NSR1 expression than expected), but previous work has shown that this strain behaves abnormally and is likely carrying multiple mutations [93].

We also found expression changes in YKO collection strains missing some, but not all, of the Rpd3L subunits. Previous studies have shown that Rpd3 and Pho23 are required for Ribi gene repression in stress, but little is known about the role that the other subunits in Rpd3L play in stress conditions [6]. Therefore, to build a more complete picture of Rpd3L function--and calibrate our screen--we made 14 strains, each missing one subunit of Rpd3L (Rpd3, Sin3, Ume1, Pho23, Sap30, Sds3, Cti6, Rxt2, Rxt3, Dep1, Ume6 and Ash1), or as a control Rpd3S (Eaf3, Rco1), and measured their response to 0.4M KCl using DNA microarrays [55,56].

Our microarray analysis revealed that the 14 strains missing Rpd3L or Rpd3S subunits fall into three groups (Fig. 4a). The first group of strains (*rpd3Δ*, *sin3Δ*, *pho23Δ*, *dep1Δ*, *sds3Δ*, *sap30Δ*, and *rxt2Δ*) has a large defect in Ribi and RP gene repression; the second group (*ume1Δ*, *cti6Δ*, *rxt3Δ*, *ash1Δ*) has a weak

to moderate defect in Ribi and RP gene repression; while the third group (*ume6Δ*, *rco1Δ*, *eaf3Δ*) has no defect in Ribi or RP gene repression.

Comparing the microarray and screen data revealed a clear trend; the screen picked up strains with large defects in NSR1 repression but not strains with small to moderate defects in NSR1 repression (Fig. 4b). In fact, 6/7 gene deletions that caused a strong defect in NSR1 down-regulation were identified as hits (log_2>1.0) in the screen (Fig. 4b). The one outlier was *sds3D*, but in further testing we found that the conflict was caused by additional mutations in the strain from the YKO collection (Fig. S2). In contrast, 0/4 gene deletions that caused a small to moderate defect in NSR1 down-regulation in the microarray experiments were identified as hits (Fig. 4b). It is therefore likely that the 440 strains with log_2>1.0 more NSR1 expression during stress than the control strains includes most, if not all, of the strains in the YKO library with a strong defect in Ribi gene (NSR1) repression, but few strains with small to moderate defects in Ribi gene repression.

2.3.5 Complexity of Yeast Stress and Cell Growth Control Network

To begin to make sense of the screen data, we set out to organize the strains with high NSR1 expression into groups. As a first step, we ran the 331 strains with NSR1 expression log_2>1.4 in KCl (4 plates with center peak controls; the maximum that can be processed in parallel) through our pipeline, treating them with mock stress. This experiment revealed that most of the strains with high levels of NSR1 expression in stress (top panel, Fig. 5) have normal, or near normal, NSR1 expression levels during log phase growth (middle panel, Fig. 5). In fact, the average NSR1/PEX6 ratio of the 331 strains in mock stress was log_2=0.33, just 26% above that of the center peak control strains. Moreover, there were only five strains with log_2>1.0 more NSR1 expression than the controls: *mch5D* (log_2=2.6), *rpl16bD* (log_2=1.8) *puf4D* (log_2=1.7), *rpl7aD* (log_2=1.2), and *rps7bD* (log_2=1.1).

We then ran the 331 strains through our pipeline again, but this time treated them with the potent TORC1 inhibitor rapamycin. This experiment showed that 59 out of the 331 strains only partially down-regulate NSR1 in rapamycin (normalized NSR/PEX6 of log_2>1.0) and are therefore missing genes that act

downstream of TORC1 (bottom panel Fig. 5, Table S1). Many of these 59 genes are involved in gene regulation, including 30 genes that regulate transcription ($p<0.001$ by GO analysis) and 16 genes involved in chromatin organization and biogenesis ($p=2e^{-4}$). In contrast, the 272 genes that act upstream of TORC1, or in parallel with the TORC1 pathway ($\log_2<1.0$ normalized NSR1 expression), tend to be involved in vacuolar function (30 genes, $p=4e^{-7}$) or cation homeostasis (15 genes, $p=5e^{-4}$), but not transcription ($p=3e^{-4}$ under-representation).

Next, to organize the hits from our screen into functional modules, we constructed a model of the Ribi gene control circuit using the physical interaction data from BioGRID [94]. Overall, we found 1076 connections between the 440 genes/proteins with $\log_2>1.0$ NSR1 expression in salt (not including self-self interactions; see Methods). To test if this number of connections is significant we also constructed 10,000 random networks, each containing 440 out of the 4709 genes studied in the screen. These networks all had less than 980 interactions (492 interactions on average), suggesting that the probability of finding 1076 connections by chance is less than 0.01%.

Clustering the physical interaction data using Cytoscape [95] revealed a network made up of two parts (Fig. 6). The upper half includes 118 proteins connected primarily via weak and/or transient interactions (orange lines representing yeast two-hybrid and other weak interactions, but not IP data; Fig. 6). These proteins are primarily localized to the vacuole and endomembrane system (56 blue encircled nodes; Fig. 7, Table 1) and form three distinct groups. The first group includes the A, B, C and D subunits of the V_1 portion of the vacuolar ATPase (Vma1, Vma2, Vma5 and Vma8), the c, c', c" and d subunits of the Vo portion of the vacuolar ATPase (Vma3, Vma11, Vma16, and Vma6) and three associated proteins (Vma21, Vma22, and Pkr1). The second group includes two components of the EGO complex (a known regulator of autophagy and TORC1 [76]; Slm4 and Meh1), two components of the vacuolar transporter chaperone (VTC) complex, and the transporter Gap1 (EGO and VTC; Fig. 6). The third group includes endosomal and vacuolar SNARE proteins (Syn8, Vam3 and Vam7), the vacuolar Rab family GTPase, Ypt7 (involved in vacuole and endosome fusion; [96]), and a component of the CORVET membrane-

tethering complex on the vacuole, Pep5. Twenty-two other genes, distributed throughout the upper portion of the network, are also involved in vesicle trafficking (bottom, Table 1), including numerous steps in transporting cargo from the ER through the Golgi and to the Vacuole (Gyp5, Yip5, Emp70, Vfa1, Vab2 and Rcr1) and from the Cytoplasm to Vacuole (Snx4, Pfa3 and Vac8).

Interestingly, almost all of the proteins in the upper portion of the Ribi gene control network, act upstream of TORC1 or in parallel with the TORC1 pathway (grey nodes; Fig. 6). Consistent with this, TORC1 itself (green node; Fig. 6) interacts with several proteins in this portion of the network (Table 2), including Vac8, a part of the CVT pathway and Gyp5 (a GTPase-activating protein involved in ER to Golgi transport), and the kinases Nnk1, Fmp48 and Kdx1; forming a total of 17 interactions with proteins in the upper and lower parts of the network (Table 2).

In the lower half of the network (also 118 genes) we find two highly connected nodes, the histone H3 proteins, Hht1/2 (merged into one node for simplicity and shown in yellow in Fig. 6). Hht1/2 in turn form strong interactions with three major complexes (black lines showing IP data, Fig. 6). The first includes the six core subunits of Rpd3L (Rpd3, Sin3, Pho23, Sap30, Dep1 and Rxt2) as well another Class I HDAC Hos1 and the Sin3 associated transcription factor Stb4 (Table 3). The second includes three components of the Elongator complex (part of the Pol II holoenzyme responsible for transcriptional elongation; Elp3, Elp6 and Iki3) as well as an associated kinase, Vhs1 (Table 3). The third includes 13 ribosomal proteins and 4 ribosome-associated proteins (Table 3).

Hht1/2 also interact with numerous other nuclear proteins involved in NSR1 regulation (54 maroon encircled nodes, Fig. 6), including histone 2a, components of the ISW2, INO80 and SWI/SNF chromatin remodeling complexes, as well as numerous factors involved in translation and RNA decay (bottom, Table 3). Interestingly, many of the proteins in the lower half of the network, particularly those involved in chromatin remodeling and transcription, act downstream of TORC1 (34 red nodes, Fig. 6).

Outside of the portion of the Ribi gene control network connected by known physical interactions, there are many important proteins/genes (Table S1). The only enriched group includes 21 genes involved in nitrogen metabolism ($p=9e^{-5}$). However, there are also 56 enzymes in the unconnected portion of the network (including 5 kinases; Adk1, Bud17, Dgk1, Lsb6, and Yfh7, and 5 methyltrasferases; Mtq2, Sam4, Trm12, Trm44, and Ymr310c), along with 9 transmembrane transporters (Dip5, Hxt14, Mep1, Mup3, Pdr10, Sit1, Tom7, Ydr387c, and Yfl040w) and 8 DNA binding proteins (Dal82, Hal9, Hcm1, Hop1, Sip4, Sok2, Su2 and Znf1). These proteins may interact with components in the cell growth control network during osmotic stress—a stimulus rarely applied during large-scale studies of protein interactions and thus missing from the physical interaction network—or alter network activity by affecting the level of key metabolites in the cell.

2.4 DISCUSSION

We have identified 440 strains from the yeast knockout collection that have a strong defect in Ribi gene (NSR1) repression during osmotic stress. The proteins/genes knocked out in these strains fall into three major groups.

(1) The NSR1 regulation network contains 37 proteins involved in vesicle trafficking, 11 components of the vacuolar ATPase, and 50 other proteins that act as part of the endomembrane system (Table 1 and Table S1). These proteins probably influence NSR1 expression in a variety of ways.

Some of these proteins may directly, or indirectly, inhibit TORC1 signaling in stress. In line with this hypothesis, we found that strains missing components of the EGO complex (Meh1 and Slm4) and vacuolar ATPase--known regulators of TORC1 signaling in other conditions [76,82]--have large defects in NSR1 down-regulation.

Other vacuole or endomembrane proteins may be important for the transport of proteins that interact with, or support the function of, TORC1 and EGO on the vacuolar membrane.

Yet other proteins in this group may be required nutrient transport and storage, and thus deleting them could lead to changes in TORC1 and cell growth signaling. In fact, Cardenas and coworkers have already shown that disruption of the CORVET and HOPS complexes--complexes also identified in our study--cause partial inactivation of TORC1 signaling during log phase growth by inhibiting the activation of the EGO complex members Gtr1/2 [97]. This constitutive TORC1 repression may then desensitize the TORC1 pathway to inhibition by osmotic stress.

(2) The NSR1 regulation network contains at least 24 proteins involved in chromatin silencing, 6 proteins involved in general transcription, and 9 other DNA binding proteins (Table 3). Six of these proteins are subunits of the Class I HDAC Rpd3L--a complex that deacetylates the nucleosomes in Ribi gene

promoters whenever TORC1 is inactivated [5,7]. However, the other proteins identified in this group have not been linked to Ribi gene regulation previously. Some of these proteins probably cooperate with Rpd3L to inactivate NSR1 in stress--this is almost certainly the case for the histone H3 and H2A proteins--but others may simply regulate the transcription of critical proteins in the stress response network.

(3) The NSR1 regulation network also contains 17 ribosomal and ribosome associated proteins, and four translation factors (Table 3). Although it is unclear how these proteins interact with the Ribi gene control network, it is well established that blocking translation using the drug cyclohexamide triggers hyperactivation of TORC1 [98,99]. It therefore seems likely that deletion of at least some of the proteins found in this group will have a similar indirect effect on TORC1 activity by inhibiting translation.

Putting the three groups of proteins listed above together with the myriad other proteins required for NSR1 repression in stress (listed in Table S1), it is clear that the Ribi, and thus cell growth control, network is highly complex. Over seven percent of the genome (440/5820 genes) is required for proper signaling in osmotic stress conditions alone. Therefore, numerous follow up experiments will be needed to determine how such a large array of proteins contributes to the stress response. In this respect, we hope that our screen will serve as a resource that helps guide the community towards key proteins and pathways in cell growth control and TORC1 pathway signaling.

The data presented in this paper also demonstrate the power of our new method for mapping gene regulatory circuits in yeast (and potentially other organisms). It is highly quantitative, reproducible, and works well even when the resulting gene expression changes are short lived or involve a dramatic reduction in mRNA levels. Furthermore, the method can (at least in principle) be adapted to map the regulators of any gene, simply by altering the primers/probes used in the qPCR step.

2.5 ACKNOWLEDGEMENTS

This work was supported by the National Institutes of Health (NIH) grants 1R01GM097329 and 5T32GM008659.

2.6 FIGURES

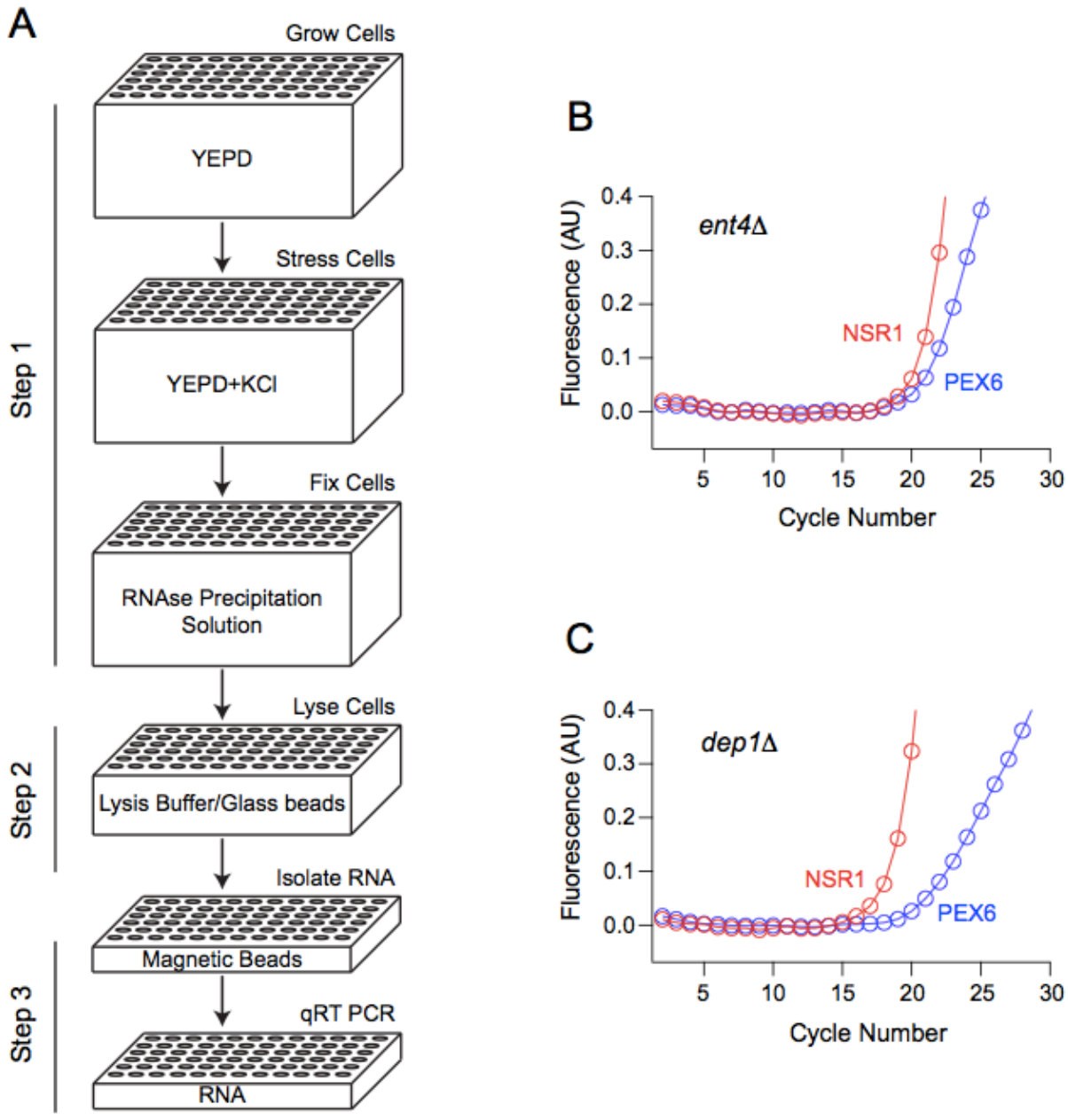

Figure 1. Automated analysis of gene expression in yeast.

(A) Strains from the Yeast Knock Out (YKO) collection were inoculated into a 96-well plate containing YEPD medium and grown to an OD_{600} of 0.6 in a Biomek FX robot with an integrated Liconic shaking incubator. The plates were then brought onto the deck of the robot, treated with 0.4M KCl, rapamycin, or mock stress, and returned to the incubator. After 20min the plates were retrieved again but this time

treated with 4M NH_4SO_4 (pH 4.6) to block all further RNA synthesis and degradation. Cells were then lysed by bead-beading, and the RNA purified from each well using magnetic beads and loaded into a PCR plate for analysis. (B and C) Duplex quantitative PCR was used to measure the expression of the Ribi gene NSR1 (FAM labeled probe; red) and the housekeeping gene PEX6 (JOE labeled probe; blue) in each well of the plate from the library. In most strains (such as *ent4Δ* from plate 1) NSR1 and PEX6 expression levels were similar. However, we also found numerous strains (such as *dep1Δ* from plate 1) with higher levels of NSR1 than PEX6. Quantitation of these data using standard procedures (see Methods) then led to a NSR1/PEX6 ratio for each sample ($\log_2$ = -2.8 for *dep1Δ* and -0.1 for *ent4Δ*).

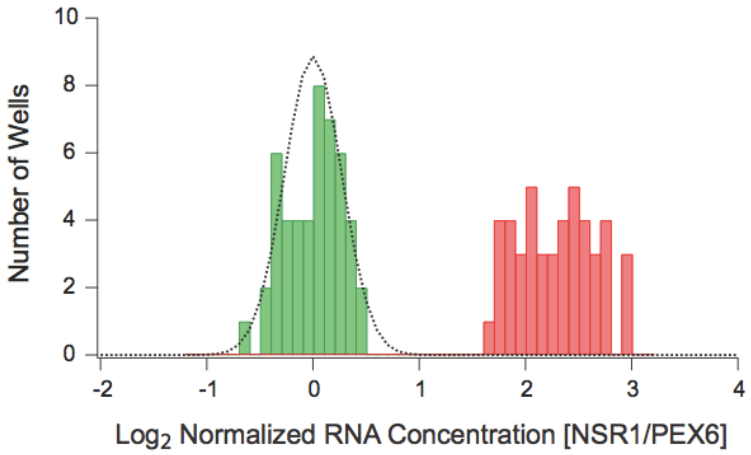

Figure 2. NSR1 expression levels during log growth and 0.4M KCl stress.

Histogram showing the distribution of NSR1/PEX6 expression ratios for wild-type cells grown on a single plate and then treated with 0.4M KCl (48 samples, green) or mock stress (48 samples, red). The data was normalized (by adding a single constant to all 96 log NSR1/PEX6 ratios) so that the average signal in stress is 0.0. The dotted line shows the fit to a normal distribution with a standard deviation of 0.26 and an average of 0.0.

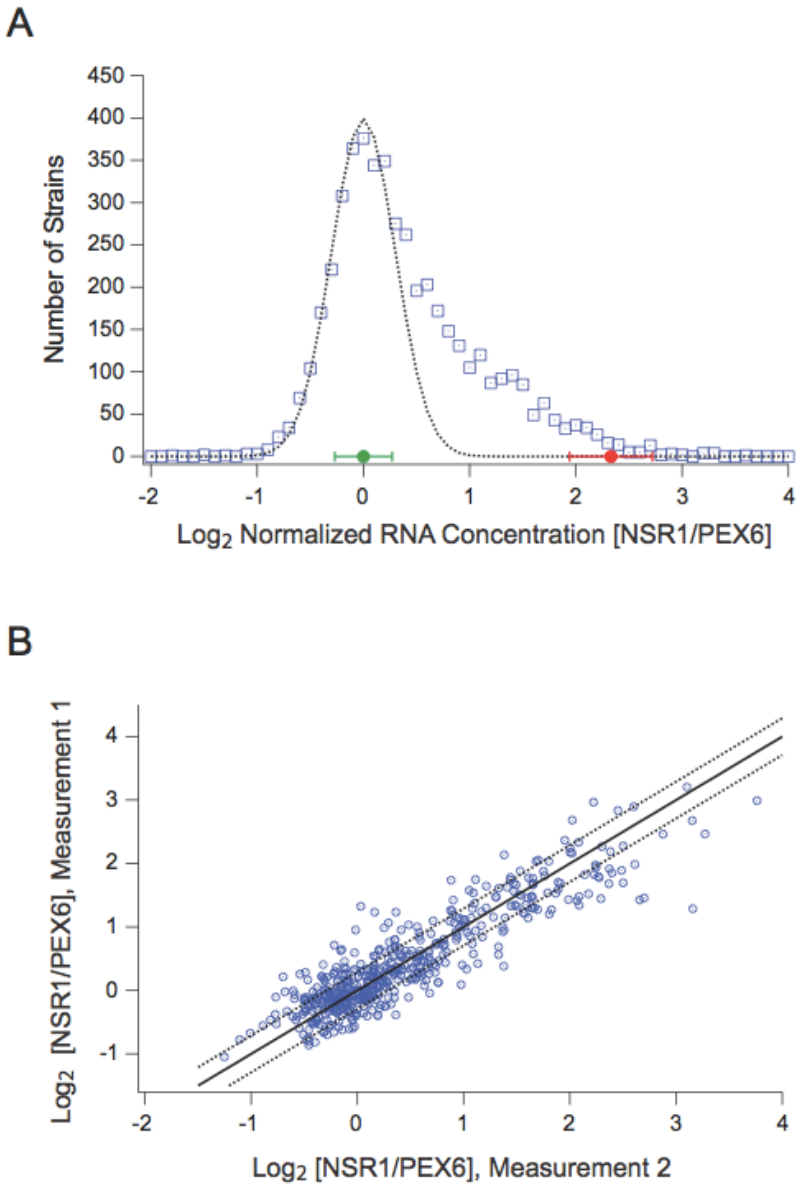

Figure 3. NSR1 expression levels for 4709 strains in the yeast knockout collection.

(A) Histogram showing the number of strains in the yeast knockout library with $\log_2$ NSR1/PEX6 expression ratios ranging from -2 to 4 in 0.1 increment bins. All data was normalized to set the average expression ratio, minus the outliers, to 0.0 (see Methods). The green point and bar show the average and standard deviation of the NSR1/PEX6 ratio for the wild-type strain in stress (from Fig. 3). The red point and bar shows the average and standard deviation of the NSR1/PEX6 ratio for the wild-type strain in mock stress (from Fig. 3). The dotted line shows the fit to a normal distribution with an average signal of 0.0 and a standard deviation of 0.30 (B) Scatter plot showing the normalized NSR1/PEX6 expression

values for 570 strains run through the automated pipeline on two separate weeks (usually more than a month apart). The solid line show the trend expected if there was a perfect correlation between datasets, the dotted line show the range expected for values that fall one standard deviation (0.3 $\log_2$ units) above or below this line.

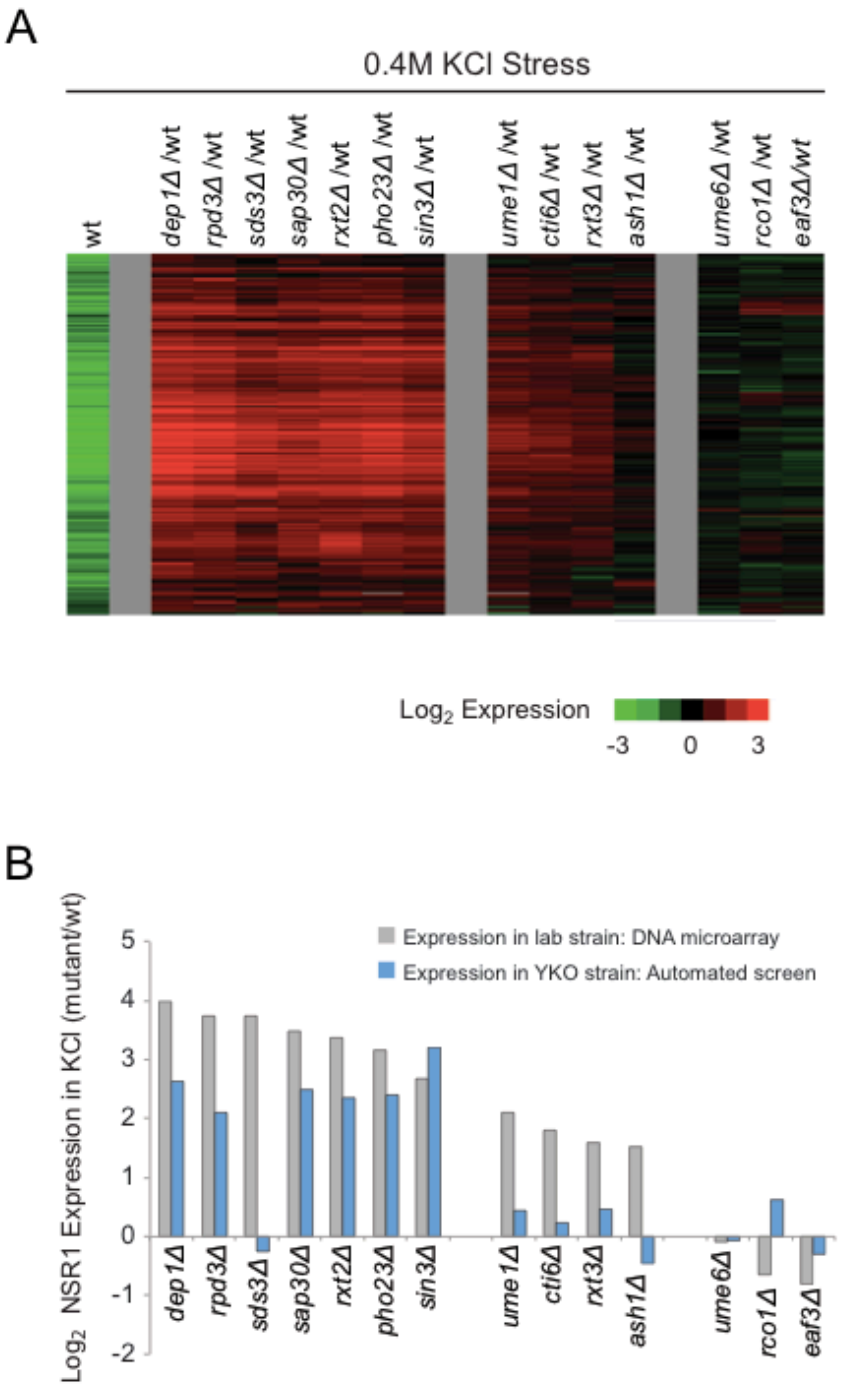

Figure 4. Rpd3L dependent gene expression in osmotic stress conditions.

(A) DNA microarrays were use to measure the expression of Ribi genes after 20 min of 0.4M KCl stress in the wild type strain (Column 1) and mutants missing all 14 subunits in the Rpd3L and Rpd3S complexes (Columns 2-15). In the experiment with the wild-type strain, we compared the cDNA from cells treated

with stress (labeled with Cy5; red) to the cDNA from cells harvested prior to stress (labeled with Cy3; green). In experiments with the mutant strains we compared cDNA from the mutant treated with stress (labeled with Cy5; red) to cDNA from the wild-type strain treated with stress (labeled with Cy3; green). Thus, the green bars in the first column show Ribi genes that are repressed in osmotic stress, while the red bars in each subsequent column show the genes that are hyper expressed in stress. (B) Graph showing the change in NSR1 expression caused by deletion of each subunit in Rpd3L/S as measured by DNA microarray analysis of strains made in the W303 background (grey bars) and the automated analysis of the YKO collection (blue bars).

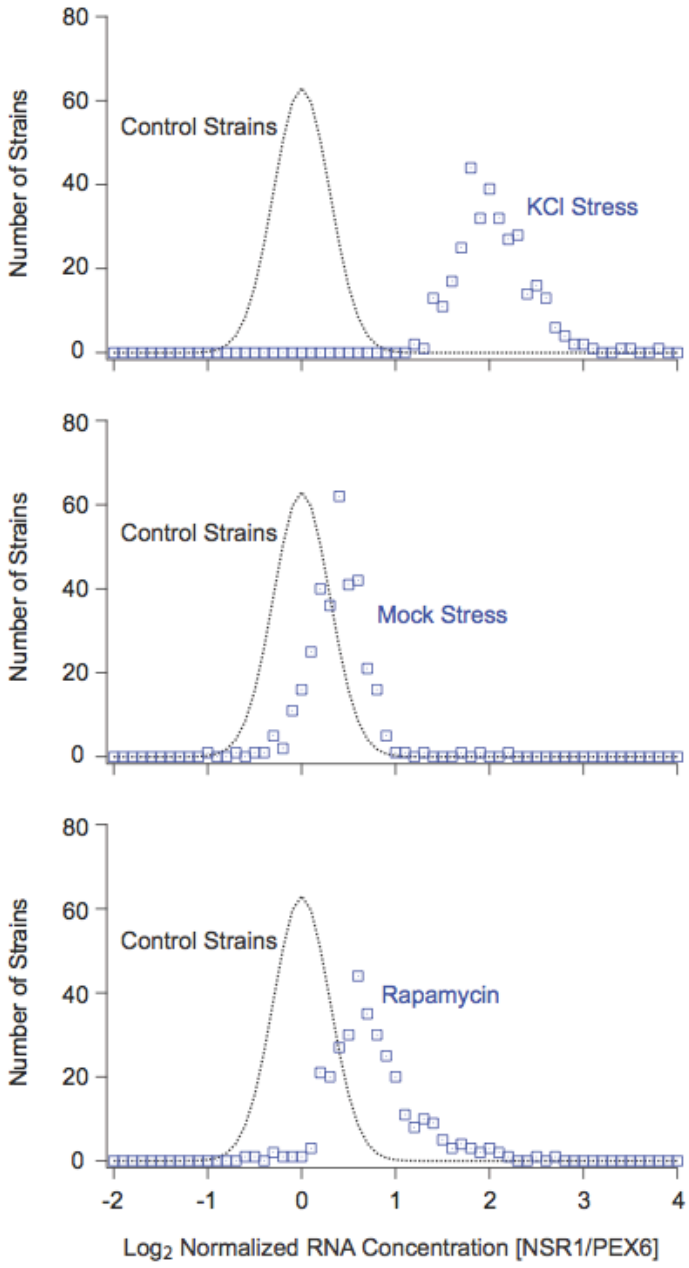

Figure 5. NSR1 expression levels in KCl, mock stress and rapamycin.

The top 331 strains in the screen were analyzed to measure the NSR1/PEX6 ratio after 20min in 0.4M KCl stress (upper panel), mock stress conditions (middle panel), or 200nM Rapamycin (lower panel). In all of these experiments the 331 strains were distributed across four 96-well plates, together with 48 strains from the center of the peak in the original screen. The average NSR1/PEX6 expression level in these control strains was set to 0.0 in each experiment. Strains with defects in repressing NSR1

expression in each condition should therefore have $\log_2$ NSR1/PEX6 expression ratios >1.0. The dotted lines show a normal distribution with an average and standard deviation of 0.0 and 0.3 for reference.

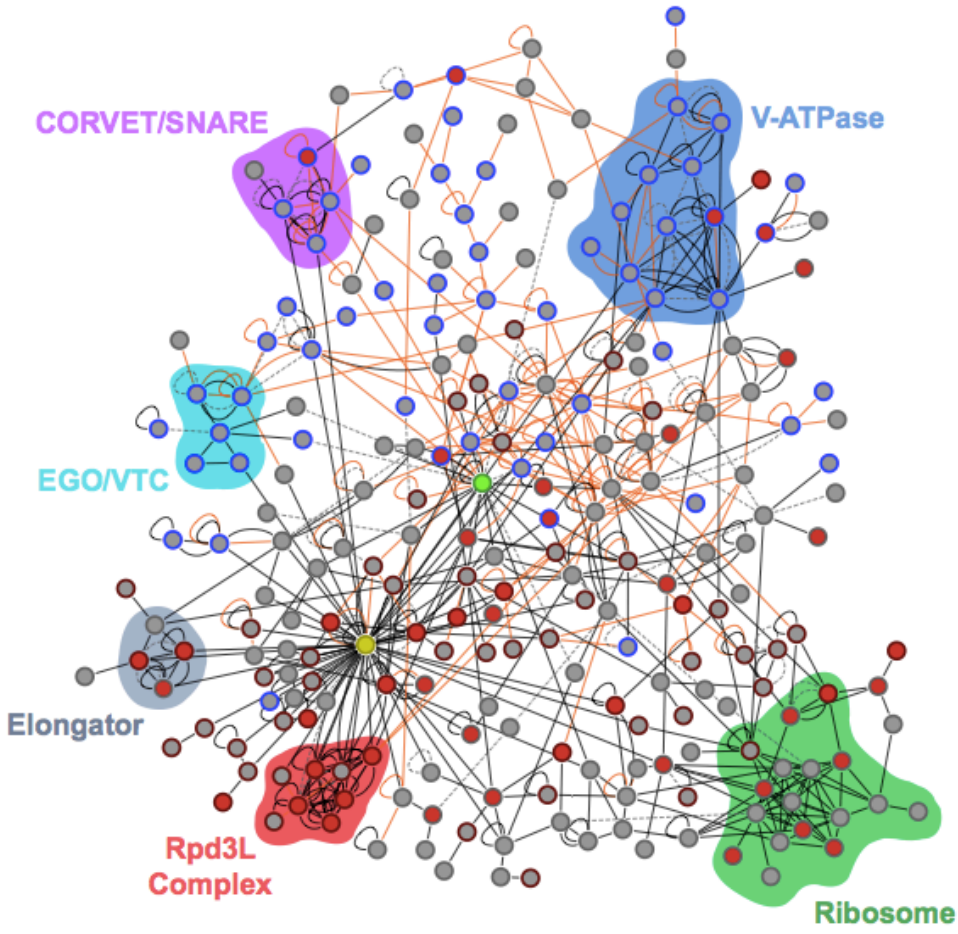

Figure 6. Physical interaction map for genes involved in stress regulated growth control.

The network map drawn using Cytoscape [95] shows physical interactions between the 440 proteins required for robust NSR1 repression in stress, along with TORC1 for reference. Each node shows a single protein, and each edge a single physical interaction from BioGRID [94]--colored black if it represents affinity capture or reconstituted complex data; orange if it represents two-hybrid or protein-fragment complementation data; and dotted grey if it represents FRET, biochemical activity, co-purification, or other types of data. The center of each node is colored red if deletion of the protein causes a defect in rapamycin dependent down-regulation of NSR1 (log_2>1)--and therefore acts downstream of TORC1--and grey if it does not. Node edges are colored maroon if the protein is the nucleus and blue if it localizes to the endomembrane system or vacuole. The green node is TORC1 and the yellow node Hht1/2. Colored regions highlight key complexes discussed in the text and listed in Tables 1-3. Only proteins with one or

more physical interaction (250 in total) are shown in this figure, and the highly connected proteins chaperones Ssa1 and Ssb1, and the RNA binding protein Slf1 are removed from the network for clarity. The Cytoscape file containing the full network, and all relevant information, is included in the supplementary materials.

2.7 TABLES

Table 1. Vacuolar, endomembrane and vesicle trafficking genes required for the down regulation of the Ribi gene NSR1 in stress.

Name	Description	Loc	[NSR1]	Down TOR	Phys Net
VMA1	Subunit A of the V1 peripheral membrane domain of V-ATPase	V	2.2	NO	YES
VMA2	Subunit B of V1 peripheral membrane domain of vacuolar H+-ATPase	V	2.3	YES	YES
VMA3	Proteolipid subunit c of the V0 domain of vacuolar H(+)-ATPase	V	1.9	NO	YES
VMA5	Subunit C of the V1 peripheral membrane domain of V-ATPase	V	2.2	NO	YES
VMA6	Subunit d of the V0 integral membrane domain of V-ATPase	V	2.1	NO	YES
VMA8	Subunit D of the V1 peripheral membrane domain of V-ATPase	V	2.1	NO	YES
VMA11	Vacuolar ATPase V0 domain subunit c'	V	1.5	NO	YES
VMA16	Subunit c'' of the vacuolar ATPase	V	1.9	NO	YES
VMA21	Integral membrane protein required for V-ATPase function	ER	1.5	NO	YES
VMA22	Protein that is required for vacuolar H+-ATPase (V-ATPase) function	ER	1.9	NO	YES
PKR1	V-ATPase assembly factor	ER	1.9	NO	YES
SLM4	Component of the EGO and GSE complexes	V	3.7	NO	YES
MEH1	Component of the EGO and GSE complexes	V	1.5	NO	YES
VTC1	Subunit of the vacuolar transporter chaperone (VTC) complex	ER/V	1.4	NO	YES
VTC4	Vacuolar membrane polyphosphate polymerase	ER/V	2.3	NO	YES
GAP1	General amino acid permease	V	1.9	NO	YES
SYN8	Endosomal SNARE related to mammalian syntaxin 8		1.8	NO	YES
VAM3	Syntaxin-like vacuolar t-SNARE	V	2.6	NO	YES
VAM7	Vacuolar SNARE protein	V	2.4	NO	YES
YPT7	Rab family GTPase	V	2.5	YES	YES
PEP5	Histone E3 ligase, component of CORVET membrane tethering complex	V	1.9	NO	YES
RCR1	Involved in chitin deposition; may function in endosomal-vacuolar trafficking	ER	2.0	NO	NO
YOP1	Membrane protein that interacts with Yip1p to mediate membrane traffic	ER	1.7	NO	YES
GYP5	GTPase-activating protein (GAP) for yeast Rab family members	G	1.8	NO	YES
RGP1	Subunit of a Golgi membrane exchange factor (Ric1p-Rgp1p)	G	1.4	NO	NO
SYS1	Integral membrane protein of the Golgi	G	1.8	NO	YES
TVP15	Integral membrane protein; localized to late Golgi vesicles	G	1.8	NO	YES
TVP38	Integral membrane protein; localized to late Golgi vesicles	G	1.9	NO	YES
VPS52	Component of the GARP (Golgi-associated retrograde protein) complex	G	1.3	NO	NO
YIP5	Protein that interacts with Rab GTPases; localized to late Golgi vesicles	G	1.6	NO	YES
EMP70	Endosome-to-vacuole sorting	V	1.6	NO	YES
SNX4	Sorting nexin; involved in the retrieval of late-Golgi SNAREs	Endo	2.0	NO	YES
SNX41	Sorting nexin; involved in the retrieval of late-Golgi SNAREs	Endo	2.0	NO	YES
VFA1	Protein that interacts with Vps4p and has a role in vacuolar sorting	Endo	1.8	NO	YES
VPS5	Nexin-1 homolog; moves proteins from endosomal compartment to Golgi	Endo	1.7	NO	YES
PFA3	Palmitoyltransferase for Vac8p	V	2.4	NO	YES
VAC8	Phosphorylated and palmitoylated vacuolar membrane protein	V	2.9	NO	YES
LST4	Protein possibly involved in a post-Golgi secretory pathway		2.7	YES	NO
EDE1	Scaffold protein involved in the formation of early endocytic sites		1.6	NO	YES
ENT2	Epsin-like protein required for endocytosis and actin patch assembly		1.8	NO	YES
KIN2	Serine/threonine protein kinase involved in regulation of exocytosis		1.7	?	YES
VAB2	Subunit of the BLOC-1 complex involved in endosomal maturation		2.4	?	YES
MDR1	Cytoplasmic GTPase-activating protein; regulation of Golgi secretory function		2.4	NO	NO
APL4	Gamma-adaptin	Endo	1.8	NO	YES
APM1	Mu1-like medium subunit of the AP-1 complex	G	1.8	NO	YES
CHC1	Clathrin heavy chain		1.5	?	YES
DYN1	Cytoplasmic heavy chain dynein		1.7	?	YES

The top three groups of genes encode proteins highlighted in the top portion of the physical interaction network shown in Fig. 7; V-ATPase, EGO/VTC and CORVET/SNARE respectively. The fourth group lists other genes found in our screen encoding vacuolar, vesicle transport of endomembrane proteins. The

third column (Loc) lists the localization of each protein; V is vacuole, ER is endoplasmic reticulum, G is Golgi, and Endo is other parts of the Endomembrane system. The fourth column [NSR1] lists the $\log_2$ NSR1/PEX6 expression ratio from the screen. The fifth column notes if the gene acts downstream of TORC1 (has $\log_2 > 1$ normalized NSR1/PEX6 ratio in rapamycin). The sixth column (Phys Net) states whether the genes is part of the physical interaction network shown in Fig. 6.

Table 2. Proteins required for the down regulation of the Ribi gene NSR1 in stress that physically interact with TORC1.

Name	Description	Loc	[NSR1}	Down TOR
VAC8	Vacuolar membrane protein; CVT pathway	C	2.9	YES
GYP5	GTPase-activating protein for Rab proteins; ER to Golgi transport	C	1.8	NO
DAL82	Positive regulator of allophanate inducible genes	N	2.6	NO
FMP48	Protein kinase	C/M	1.7	NO
KDX1	Protein kinase	M	1.5	NO
NNK1	Protein kinase	C	1.8	NO
SAP185	Protein that forms a complex with the Sit4p protein phosphatase	C/M	1.9	YES
POP2	RNase of the DEDD superfamily	C	1.4	YES
TIF1	Translation initiation factor eIF4A	C	1.6	?
MRPS17	Mitochondrial ribosomal protein of the small subunit	C	1.5	?
GAS1	Beta-1,3-glucanosyltransferase	C/M/N	1.1	?
HXT2	High-affinity glucose transporter of the major facilitator superfamily		1.9	?
ICL1	Isocitrate lyase	C	2.1	NO
SAC6	Fimbrin, actin-bundling protein	C	1.8	NO
TPO3	Polyamine transporter of the major facilitator superfamily	C	1.7	?
YKU80	Subunit of the telomeric Ku complex (Yku70p-Yku80p)	N	1.5	?
YLR108C	Protein of unknown function	N	1.8	YES

The third column (Loc) lists the localization of each protein; C is cytosol, M is membrane, N is nucleus. The fourth column [NSR1] lists the $\log_2$ NSR1/PEX6 expression ratio from the screen. The fifth column notes if the gene/protein acts downstream of TORC1 (has $\log_2$ >1 normalized NSR1/PEX6 ratio in rapamycin). A question mark means that the protein/gene was not analyzed in the rapamycin subscreen.

Table 3. Ribosomal and nuclear genes required for the down regulation of the Ribi gene NSR1 in stress.

Name	Description	Loc	[NSR1]	Down TOR	Ph Net
ELP3	Subunit of Elongator complex	N	2.8	YES	YES
ELP6	Subunit of Elongator complex		1.8	YES	YES
IKI3	Subunit of Elongator complex	N	1.8	YES	YES
VHS1	Cytoplasmic serine/threonine protein kinase		2.5	NO	YES
RPD3	Histone deacetylase, component of Rpd3S and Rpd3L	N	2.1	NO	YES
SIN3	Component of Rpd3S and Rpd3L	N	2.6	YES	YES
PHO23	Component of Rpd3L	N	2.4	YES	YES
SAP30	Component of Rpd3L	N	2.2	YES	YES
DEP1	Component of the Rpd3L	N	2.6	YES	YES
RXT2	Component of Rpd3L	N	2.4	YES	YES
HOS1	Class I histone deacetylase	N	1.9	NO	YES
STB4	Putative transcription factor	N	2.4	NO	YES
RPS6A	Protein component of the small (40S) ribosomal subunit	R	2.4	YES	YES
RPS7B	Protein component of the small (40S) ribosomal subunit	R	1.4	YES	YES
RPS9A	Protein component of the small (40S) ribosomal subunit	R	1.9	NO	YES
RPS22A	Protein component of the small (40S) ribosomal subunit	R	1.4	NO	YES
RPS17A	Protein component of the small (40S) ribosomal subunit	R	2.4	YES	YES
RPL2B	Ribosomal 60S subunit protein L2B	R	1.3	NO	YES
RPL6A	Ribosomal 60S subunit protein L6A	R	2.1	NO	YES
RPL6B	Ribosomal 60S subunit protein L6B	R	2.6	YES	YES
RPL7A	Ribosomal 60S subunit protein L7A	R	2.1	NO	YES
RPL13A	Ribosomal 60S subunit protein L13A	R	1.8	NO	YES
RPL16B	Ribosomal 60S subunit protein L16B	R	1.8	NO	YES
RPL22A	Ribosomal 60S subunit protein L22A	R	1.9	NO	YES
RPL24A	Ribosomal 60S subunit protein L24A	R	2.0	YES	YES
SSZ1	Hsp70 protein that interacts with Zuo1p (a DnaJ homolog)		2.0	YES	YES
ZUO1	Ribosome-associated chaperone	R/N	1.9	YES	YES
NOP12	Nucleolar protein involved in pre-25S rRNA processing	N	2.1	NO	YES
RQC1	Component of the ribosome quality control complex (RQC)	R	2.0	NO	YES
RPL38	Ribosomal 60S subunit protein L38	R	2.0	YES	NO
RPL43B	Ribosomal 60S subunit protein L43B	R	1.6	NO	NO
RPS27A	Protein component of the small (40S) ribosomal subunit	R	2.1	NO	NO
CLU1	Subunit of the eukaryotic translation initiation factor 3 (eIF3)		2.3	YES	YES
EFT1	Elongation factor 2 (EF-2), also encoded by EFT2	R	1.6	NO	YES
TIF1	Translation initiation factor eIF4A	R	1.6	NO	YES
YGR054W	Eukaryotic initiation factor (eIF) 2A	R	2.2	NO	YES
CAF20	Phosphoprotein of the mRNA cap-binding complex		2.0	NO	YES
ASK10	Component of RNA polymerase II holoenzyme	N	2.4	NO	YES
CAF130	Subunit of the CCR4-NOT transcriptional regulatory complex		1.6	NO	YES
ELA1	Elongin A; Required for Pol II degredation	N	2.6	NO	YES
ELC1	Elongin C; Required for Pol II degredation	N	1.5	NO	YES
PGD1	Subunit of the RNA polymerase II mediator complex	N	2.0	NO	YES
NUT1	Component of the RNA polymerase II mediator complex	N	1.7	NO	YES
GIS1	Histone demethylase and transcription factor	N	1.7	NO	YES
HIR2	Subunit of HIR nucleosome assembly complex	N	2.0	NO	YES
HIR3	Subunit of the HIR complex	N	2.5	NO	YES
HPA2	Tetrameric histone acetyltransferase		1.9	NO	YES
HTA1	Histone H2A	N	2.4	YES	YES
IES4	Component of the INO80 chromatin remodeling complex	N	1.8	YES	YES
ITC1	Subunit of Isw2p-Itc1p chromatin remodeling complex	N	1.6	NO	YES
DPB4	Subunit of ISW2 chromatin accessibility complex	N	2.0	NO	YES

The top three groups of genes encode proteins highlighted in the bottom portion of the physical interaction network shown in Fig. 7; V-ATPase, Elongator, Rpd3L and Ribosome respectively. Note that three

ribosomal proteins not connected to the others by physical interactions were included in the list. The fourth group lists other genes found in our screen involved in transcription and chromatin remodeling, all of which are part of the lower half of the physical interaction network in Fig. 7. The third column (Loc) lists the localization of each protein; R is ribosome, N is nuclear. The fourth column [NSR1] lists the $\log_2$ NSR1/PEX6 expression ratio from the screen. The fifth column notes if the gene acts downstream of TORC1 (has $\log_2$ >1 normalized NSR1/PEX6 ratio in rapamycin). The sixth column (Phys Net) states whether the genes is part of the physical interaction network shown in Fig. 6.

2.8 SUPPLEMENTAL FIGURES

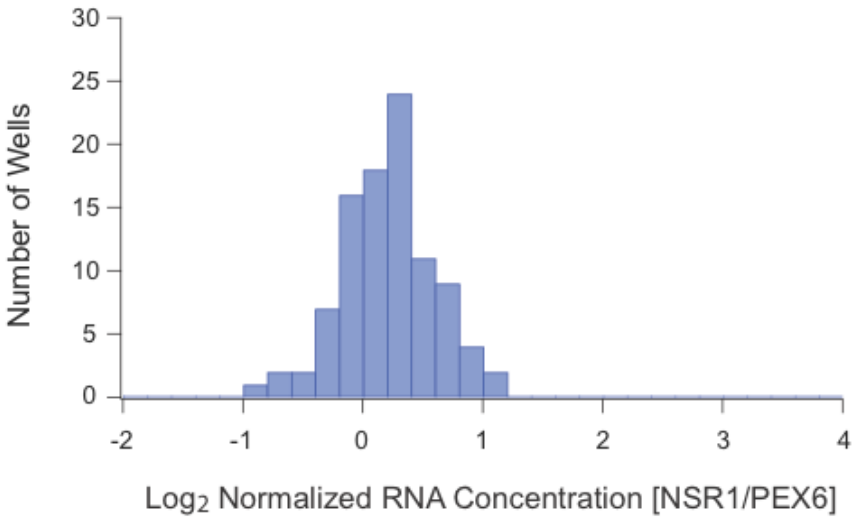

Figure S 1. NSR1 expression levels during log growth.

Histogram showing the distribution of NSR1/PEX6 expression ratios for wild-type cells grown on a single plate and then treated with mock stress (YEPD medium). The data was normalized (by adding a single constant to all 96 log NSR1/PEX6 ratios) so that the average signal in stress is 0.0. The standard deviation for the 96 measurements of NSR1/PEX6 expression is $\log_2 = 0.37$.

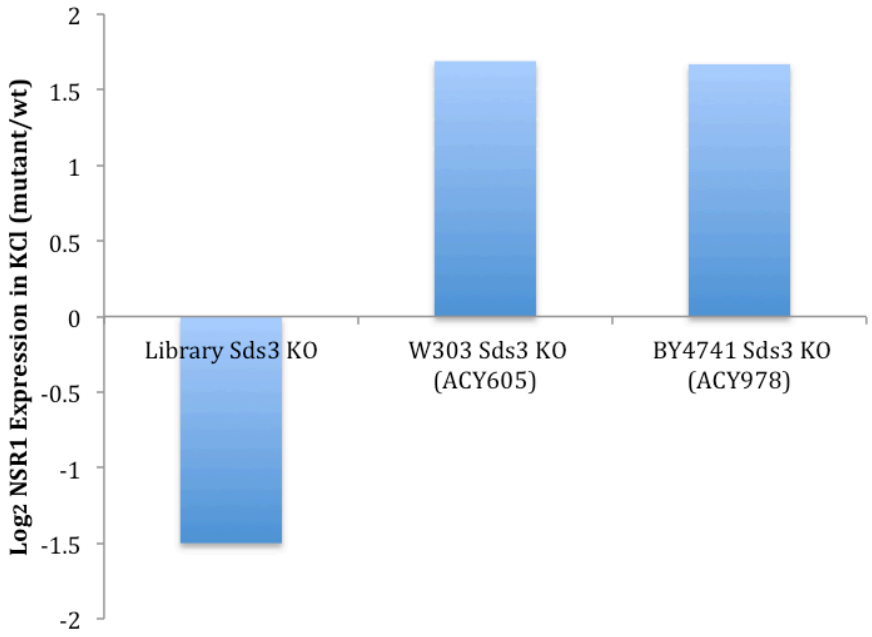

Figure S 2. Graph showing the change in NSR1/PEX6 expression caused by deletion of Sds3 in the W303 background (ACY605 strain used in microarray analysis), the BY4741 background used in the YKO collection (ACY978), and the *sds3Δ* strain from the YKO collection.

Each bar shows the expression level compared to that found in the wild-type strain (both 20min after treatment with 0.4M KCl), as measured by qPCR (Methods). In this experiment cells were grown and harvested as described for the DNA microarray experiments but the mRNA was purified using a RiboPure RNA purification kit (Ambion).

CHAPTER III: INOSITOL PYROPHOSPHATES REGULATE CELL GROWTH AND THE ENVIRONMENTAL STRESS RESPONSE BY ACTIVATING THE HDAC RPD3L

Jeremy Worley, Xiangxia Luo, and Andrew P Capaldi

Department of Molecular and Cellular Biology, University of Arizona, Tucson AZ 85721-0206

This work has been published in

Cell Reports, 2013 May 30. PMID: 23643537.

3.1 ABSTRACT

Cells respond to stress and starvation by adjusting their growth rate and enacting stress defense programs. In eukaryotes this involves inactivation of TORC1, which in turn triggers downregulation of ribosome and protein synthesis genes and upregulation of stress response genes. Here we report that the highly conserved inositol pyrophosphate second messengers (including 1-PP-IP_5, 5-PP-IP_4, and 5-PP-IP_5) are also critical regulators of cell growth and the general stress response, acting in parallel to the TORC1 pathway to control the activity of the class I HDAC Rpd3L. In fact, yeast cells that cannot synthesize any of the PP-IPs mount little to no transcriptional response in osmotic, heat, or oxidative stress. Furthermore, PP-IP dependent regulation of Rpd3L occurs independently of the role individual PP-IPs (such as 5-PP-IP_5) play in activating specialized stress/starvation response pathways. Thus, the PP-IP second messengers simultaneously activate and tune the global response to stress and starvation signals.

3.2 INTRODUCTION

To thrive when conditions are favorable and survive when they are stressful, cells must set their growth rate based on the level and combination of numerous intracellular and extracellular stimuli [100]. How this is accomplished remains unclear.

What is known is that in eukaryotes cell growth depends to a large degree on a single kinase called TOR [1,2]. When conditions are favorable, TOR drives mass accumulation by promoting all aspects of protein and ribosome synthesis. Conversely, in stress conditions or when hormone or nutrient levels fall outside of an ideal range TOR activity is repressed. This triggers inhibition of protein synthesis and activation of numerous stress and starvation response pathways.

Studies in the budding yeast *S. cerevisiae* have begun to reveal the precise mechanisms underlying TOR dependent regulation of growth. In particular it is now clear that TOR is part of a multisubunit complex called TORC1 [12], and that this complex signals through two distinct channels to regulate a global gene expression program known as the Environmental Stress Response or ESR [12,74,75,101].

In one channel, active TORC1 promotes the expression of 650 genes involved in ribosome and protein synthesis by regulating the activity of the S6 kinase Sch9 and numerous transcription factors, including Sfp1, Fhl1, Maf1, Dot6, and Tod6 [5,40,41,59,68]. When TORC1 is inactivated, dephosphorylation of the TORC1 and Sch9 dependent transcription factors triggers recruitment of the Class I histone deacetylase (HDAC) Rpd3L to ribosome and protein synthesis genes, leading to their repression [5,6].

In the other channel, active TORC1 blocks the expression of 600 stress and starvation response genes by binding and sequestering a key regulator of the PP2A phosphatases, Tap42 [5,6]. In stress and starvation conditions, Tap42 is released from TORC1 and activates PP2A [45,80]. This in turn triggers the dephosphorylation and activation of transcription factors that promote amino acid synthesis, nitrogen

metabolism, the TCA cycle, and the general stress response, including: Gln3, Gat1, Rtg1/3, and Msn2/4 [63,102]. Together, the PP2A dependent transcription factors function by converting the HDAC Rpd3L from a repressor to an activator at the stress/starvation response genes [6].

What remains to be determined, in both *S. cerevisiae* and other organisms, is how stress and starvation signals are transmitted to TORC1 and which pathways (if any) cooperate with TORC1 to regulate growth and metabolism. Answering these questions is a prerequisite to building a realistic model of the cellular growth control circuitry, and ultimately to understanding how cells decide how fast to grow in different environments, how they keep growth and metabolism balanced, and how malfunction of the growth control system leads to diseases such as cancer and diabetes [1,2].

Here, to gain insight into the structure and function of the eukaryotic growth control network, we use DNA microarray analysis to examine the influence that 17 signaling proteins, known to be (de)phosphorylated during stress in S. cerevisiae (Fig. S1, [103], have on the ESR. Surprisingly, our data reveal that only one of these factors, the inositol kinase Vip1, plays a significant role in regulating the ESR and thus cell growth.

Previous studies have shown that Vip1 is part of the inositol pyrophosphate synthesis pathway, which is conserved throughout eukaryotes (Fig. 1). In the first step of this pathway, Phosphatidylinositol 2-Phosphate (PIP_2) is cleaved by Phospholipase C (Plc1) to release the lipid diacylglycerol and the soluble inositol head group IP_3 [104]. IP_3 itself is a signaling molecule with a well-established role in calcium signaling [105,106]. More recently, however, it has been shown that IP_3 can be converted to IP_4 and IP_5 in the nucleus by the inositol polyphosphate multikinase Arg82, and then to IP_6 by the inositol polyphosphate kinase Ipk1 [104,107-109]. IP_5 and IP_6 can also be pyrophosphorylated by Kcs1 to create a diphosphate at the 5-position (5-PP-$IP_{4/5}$), while IP_6 can be pyrophosphorylated by Vip1 to create a diphosphate at the 1-position (1-PP-IP_5; [104,110,111]. The diphosphorylated inositols synthesized by Vip1 and Kcs1 are known as the inositol pyrophosphates or PP-IPs.

Identification of Vip1 as an important regulator of the ESR led us to investigate the role that inositol pyrophosphates play in regulating cell growth. To do this we measured the influence that each enzyme in the PP-IP synthesis pathway (Arg82, Ipk1, Vip1 and Kcs1) has on gene expression, in both log growth and stress conditions. Through this analysis we discovered that the three major PP-IPs cooperate to activate the ESR. In fact, a strain that is unable to synthesize any PP-IP (*kcs1Δvip1Δ*) mounts little to no transcriptional response in heat, osmotic, or oxidative stress.

To determine how the PP-IPs regulate the ESR and cell growth, we also measured signaling at each stage of the TORC1 pathway in *kcs1Δvip1Δ* and wild-type strains. These experiments revealed that the PP-IPs act in parallel with the canonical TORC1 signaling pathway to activate the HDAC Rpd3L. PP-IP activation of Rpd3L may be direct since we found that mutation of residues in an inositol binding site on the surface of Rpd3, identified when a crystal structure of human HDAC3-SMART complex was found to contain IP_4, has the same general effect on cell signaling as blocking the production of the PP-IPs themselves.

Taken together, our data show that the inositol pyrophosphates are critical regulators of the ESR and cell growth, with an overall impact similar to that of TORC1 itself. Moreover, our discovery that the PP-IPs activate the HDAC Rpd3L reveals the core function of these conserved second messengers in cell signaling. These results have important implications for understanding cell growth control in eukaryotes as well as the regulation of HDAC activity in health and disease.

3.3 RESULTS

3.3.1 Vip1 Regulates the Environmental Stress Response

To identify proteins that regulate the ESR, and thus cell growth, we performed a directed screen. In the first step, we searched a recently published phosphoproteomics dataset [103] to find proteins that are rapidly (<5 min) phosphorylated or dephosphorylated in osmotic stress (at $p<0.05$, Fig. S1). Through this analysis we generated a list of 24 signaling proteins likely to regulate the ESR, but that have not been studied in detail previously (see Supplement for details). We then created a series of strains, each missing one of the 17 non-essential genes on our list, and measured their response to osmotic stress using DNA microarrays. These data revealed that deletion of Vip1, an evolutionarily conserved inositol pyrophosphate synthase, inhibits the ESR (238 genes≥ 1.5-fold change, Fig. S2).

3.3.2 Inositol Pyrophosphates act redundantly to regulate the Environmental Stress Response

Our discovery that Vip1 regulates the ESR led us to study the role that inositol phosphates and pyrophosphates play in stress signaling.

First, we asked if Vip1 influences the ESR through 1-PP-IP_5 by measuring gene expression in a strain carrying a catalytically dead Vip1 mutant (D487A; [111]. We found that *vip1*^{D487A} and *vip1*Δ strains have similar expression patterns, both with defects in their stress response (Fig. S3 and Table S1). Thus, 1-PP-IP_5 and/or other PP-IPs synthesized by Vip1 are required for activation of the ESR.

Next, we asked if inositol phosphates besides 1-PP-IP_5 influence the ESR. To do this we measured the impact that each enzyme in the PP-IP synthesis pathway (Fig. 1) has on gene expression, in both log growth and osmotic stress conditions. Remarkably, these data show that there are 1647 genes activated/repressed (≥2-fold) by Arg82, Ipk1, Kcs1 and/or Vip1. Most of these genes (1272/1647) are part of the ESR (Fig. 2a and Fig S4), in line with our results for the *vip1*Δ and *vip1*^{D487A} strains. The remaining genes are primarily known targets of the PP-IPs, including the phosphate-signaling pathway, a target of 1-

PP-IP_5 via Pho80/85 [112,113], and the glycolysis pathway, a target of 5-PP-$IP_{4/5}$ via Gcr1 [114], as described in detail in the Supplement (Fig. S4).

The expression data for genes within the ESR were especially illuminating. First, the data show that deletion of the two inositol-pyrophosphate synthases in yeast, Kcs1 and Vip1, has a much bigger effect on the transcriptional response to stress than deletion of Vip1 alone (Fig. 2a). Specifically, the *kcs1*Δ*vip1*Δ strain has a dramatic defect in: (1) the down-regulation protein synthesis genes in stress, (2) the repression of stress genes in log growth conditions, and (3) the activation of stress genes in stress conditions. Second, the data show that the enzymes upstream of Kcs1 and Vip1 in the PP-IP synthesis pathway (Arg82 and Ipk1) regulate nearly the same expression program as Kcs1 and Vip1 (Fig. 2a, see legend for Pearson's r values). However, the influence that each enzyme in the PP-IP synthesis pathway has on the level of gene expression is roughly proportional to the number of PP-IPs it helps to synthesize (Fig. 2b, S5). Taken together, these data indicate that the PP-IPs, including 1-PP-IP_5 and 5-PP-$IP_{4/5}$, act partially redundantly to regulate the ESR (see Supplement for further discussion).

Finally, we asked if the PP-IPs activate the ESR in conditions other than osmotic stress. We found that *kcs1Δvip1Δ* cells have similar, dramatic, defects in their response to osmotic, oxidative, and heat stress (Fig. 3). In fact, *kcs1Δvip1Δ* cells fail to mount any significant response to H_2O_2 stress (Fig. 3). Thus, Kcs1, Vip1, and the PP-IPs are among the most potent regulators of the Environmental Stress Response (ESR) identified to date, with an influence similar to that of TORC1 itself (Table S1).

3.3.3 PP-IPs Regulate the ESR by activating the HDAC Rpd3L

How then do the PP-IP second messengers regulate the ESR? To answer this question we first sought to determine whether the PP-IPs act upstream or downstream of TORC1. We reasoned that if the PP-IPs act upstream of TORC1 then we should be able to rescue the stress response in a strain missing the PP-IPs (*kcs1Δvip1*Δ) by inhibiting TORC1 using the potent inhibitor rapamycin. Surprisingly, this was not the

case. In fact, rapamycin has almost no effect on signaling in *kcs1Δvip1Δ* cells (Fig. 4a), indicating that the PP-IPs act at or below the level of TORC1.

To determine how the PP-IPs act downstream of TORC1, we next examined signaling through the Sch9 channel. Previous studies have shown that in log growth conditions TORC1 phosphorylates the S6 kinase Sch9, leading to its activation (Fig. 4b; [39]). Active Sch9, in turn, phosphorylates and inactivates the transcriptional repressors Dot6 and Tod6 [59], both part of the HDAC complex Rpd3L [5,115]. When TORC1 is inactivated by stress, Sch9, Dot6, and Tod6 are all rapidly dephosphorylated and the protein synthesis genes are repressed by active Dot6/Tod6-Rpd3L. [5,7,63]. Using bandshift analysis we monitored the stress dependent phosphorylation of Dot6 and Tod6 and found that the switch from active TORC1 in log growth conditions, to inactive TORC1 in stress conditions, occurs normally in the *kcs1Δvip1Δ* strain (Fig. 4c). Therefore TORC1 is inactivated by stress, leading to dephosphorylation of Dot6/Tod6, even in a strain missing all PP-IPs.

As inactivation of TORC1 and the subsequent dephosphorylation of transcription factors, including Dot6 and Tod6, ultimately leads to activation of the ESR via the HDAC Rdp3L, we next asked whether the PP-IPs regulate Rpd3L itself. To do this we measured the acetylation of three of the most PP-IP dependent protein synthesis genes (shown previously to be deacetylated by Rpd3L during the ESR, [5,6], both before and after osmotic stress, using a chromatin immunoprecipitation (ChIP) assay. These experiments revealed a significant defect in stress dependent histone deacetylation in the *kcs1Δvip1Δ* strain at all three genes (Fig, 4d), indicating that Rpd3L does not function appropriately in stress without the PP-IPs.

To test whether the PP-IPs influence the entire Rpd3-mediated ESR, we next measured the ESR in a strain missing the catalytic subunit in the Rpd3L complex (*rpd3Δ*), and compared it with the data for *kcs1Δvip1Δ* strain. We found that the expression profiles for the *rpd3Δ* and *kcs1Δvip1Δ* strains are remarkably similar; both in pre-stress conditions, where Rpd3 acts to represses the expression of stress genes, and in stress conditions, where Rpd3 switches to an activator of stress genes and a repressor of

ribosome and protein synthesis genes (Fig. 4e). We therefore conclude that the PP-IPs are required for Rpd3L activity in both log growth and stress conditions.

3.3.4 Do PP-IPs activate Rpd3L directly?

After discovering that the inositol pyrophosphates activate Rpd3L in vivo, we wanted to determine if the PP-IPs function by binding directly to the Rpd3L complex. While this work was in progress, Watson et. al. published a crystal structure of human HDAC3 (Rpd3 in yeast) bound to the co-repressor SMRT. The structure revealed that the interaction between HDAC3 and SMRT depends on an inositol 1,4,5,6-phosphate (IP_4) molecule located at the interface between the two proteins [116]. Watson et. al. further showed that IP_4 is required for activation of HDAC3 by SMRT, in vitro. Although it is unclear if there is a corepressor that acts like SMRT in yeast (see supplement for discussion), these findings led us to ask if the PP-IPs activate Rpd3L by binding to the "IP_4" site described in the HDAC3-SMRT crystal structure. This seemed reasonable given that: (1) sequence alignment shows that the residues mediating the HDAC3-IP_4 interaction are conserved across the class I HDACs, including in Rpd3 [116], and (2) Examination of the HDAC3-SMRT structure (pdb 4A69) shows that approximately half of the IP_4 ring is exposed to solvent, suggesting that the inositol binding site on Rpd3 could also accommodate 1-PP-IP_5 or 5-PP-$IP_{4/5}$.

To test whether the PP-IPs activate the Rpd3L complex by binding to the inositol phosphate binding site on Rpd3, we created a strain missing the side chains of three solvent exposed residues that form salt bridges with IP_4 in the HDAC3 structure ($Rpd3^{K41A,R280A,R316A}$, *rpd3Δibs* for short) and studied its response to stress. We found that this *rpd3Δibs* strain has a similar expression profile to those of the *kcs1Δvip1Δ* and *rpd3Δ* strains, in both log growth and stress conditions (Fig. 4e). Thus, activation of Rpd3L to wild-type levels requires *both* the PP-IPs and an intact inositol-phosphate binding site on Rpd3. It therefore seems likely that the PP-IPs activate Rpd3L, at least in part, by binding to same pocket that is occupied by IP_4 in the IP_4-HDAC3 complex. However, further work is needed to confirm that the PP-IPs bind and

activate Rpd3L directly since the *rpd3Δibs* mutation could inhibit Rpd3L by disrupting a PP-IP independent function of Rpd3.

3.4 DISCUSSION

Over the last five years, the inositol pyrophosphates have emerged as important signaling molecules in eukaryotic cells. First, it was discovered that yeast synthesize 1-PP-IP_5 in phosphate starvation conditions and that this form of IP_7 binds to Pho80/85, triggering activation of phosphate-scavenging genes [113]. Later, 5-PP-IP_5 was shown to play a role in human insulin signaling, where it blocks activation of AKT by the lipid PIP_3 [117]. Finally, a recent study in yeast revealed that 5-PP-IP5 inhibits transcription of glycolysis genes by regulating the transcription factor Gcr1 [114]. Here we show that these specific roles of 1-PP-IP_5 and 5-PP-IP_5 are just one aspect of inositol pyrophosphate function. Significantly, the PP-IPs also act together (partially redundantly) to regulate a Class I HDAC and thus the global gene expression program. In yeast this means that 1-PP-IP_5 activates both the phosphate starvation pathway (15 genes) and the ESR (>1200 genes), while 5-PP-$IP_{4/5}$ downregulates glycolysis (50 genes) while activating the ESR.

Beyond uncovering a core function of the inositol pyrophosphates, our study provides important insight into the mechanisms underlying regulation of the ESR and cell growth in yeast. A key conclusion from the work here is that the PP-IPs act in parallel with the known master regulator of growth in eukaryotes, TORC1, to control Rpd3L. Furthermore, the influence that the PP-IPs have on gene expression is similar in both scale and impact to that of TORC1 itself (Figs. 4a and 4e).

This raises the question, why would the cell use two parallel signaling systems to control growth and the ESR, with TORC1 targeting Rpd3L to the appropriate promoters and the PP-IPs regulating Rpd3L activity? We favor two nonexclusive possibilities. First, this AND gate may filter noise in the TORC1 and PP-IP synthesis pathways, preventing unintentional and transient reprogramming of one-fifth of the genome. Second, PP-IP signaling may tune or control the dynamics of the response to TORC1 inhibition. This latter point may be especially important, as total Rpd3L activity increases dramatically in stress conditions (Fig. 4e).

Distinguishing between these and other models of PP-IP and TORC1 cooperation will require a more detailed view of the way PP-IP synthesis is regulated. Currently, no upstream regulators of Kcs1 or Vip1 have been identified in yeast, and it is only possible to measure the bulk level of inositol phosphates and pyrophosphates in the cell [104]. These bulk measurements are unlikely to provide a realistic view of PP-IP production as synthesis may occur at specific locations within the cell and the PP-IPs are known to turn over rapidly [118]. It is clear, however, that PP-IP levels increase in some stress and starvation conditions [113,119,120], in line with a model where PP-IP levels increase in stress to upregulate Rpd3L activity.

The results presented here also have important implications for cancer research. Studies in human cells have shown that IP6K2, a human homologue of Kcs1, is required for efficient induction of apoptosis in stress conditions, and is missing in some squamous cell carcinomas [119,121,122]. Cells missing the PP-IPs fail to activate apoptosis in stress because they erroneously upregulate cell cycle arrest genes when they should only activate pro-apoptotic genes [123]. In other words, the cells arrest before they can apoptose. Our discovery that the PP-IPs are required for HDAC activation sheds light on why this happens since it is known that HDAC1 (another homologue of Rpd3L) must cooperate with p53 to downregulate the cell cycle arrest genes in stress [124,125]. This suggests that small molecules that mimic PP-$IP_{4/5}$ and activate HDAC1 may help push cancer cells away from arrest and towards apoptosis in stresses such as chemotherapy.

3.5 EXPERIMENTAL PROCEDURES

Yeast were grown from OD_{600} = 0.10 to 0.60 in YEPD at 30 °C and then harvested for further analysis (log growth samples) or treated with stress (0.4M KCl, 42 °C final temperature or 0.4 mM H_2O_2) and harvested after 5/10 min to examine signaling/histone acetylation or after 20 min to examine mRNA levels. For microarrays, mRNA was extracted from the cells using hot phenol, purified using a poly A sepharose column, and converted to aa-UTP labeled cDNA using StrataScript reverse transcriptase. The cDNA was then labeled with Cy3 or Cy5, and transcript levels measured using Agilent G4813A DNA microarrays and an Axon 4000B scanner. For band-shift experiments TCA treated cells were lysed by bead-beating in urea buffer, the cell extracts run on a SDS-PAGE gel, and Dot6 and Tod6 mobility measured using Western Blotting and the Li-Cor infrared imaging system. ChIP samples were purified using standard procedures and the enrichment levels measured using real-time PCR. A more detailed description of the Methods, including all buffers and reagents used, is included in the Expanded Experimental Procedures.

3.6 ACCESSION NUMBERS

The GEO accession number for the microarray data reported in this paper is GSE45370.

3.7 ACKNOWLEDGEMENTS

We thank Jim Hughes Hallett and Tushar Chawala for help with the initial microarray based screen. We are also grateful to Roy Parker, Ted Weinert and Rod Capaldi for critical reading of the manuscript, and to the Parker lab for use of equipment and reagents. This work was supported by grants 5T32GM008659 and 1R01GM097329 from the NIGMS.

3.8 FIGURES

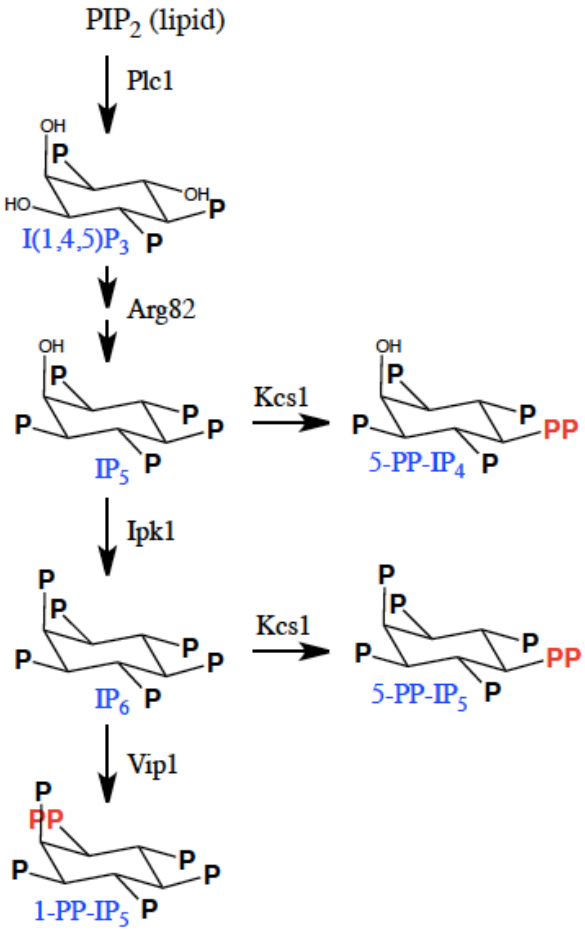

Figure 1. The PP-IP synthesis pathway.

See text for details.

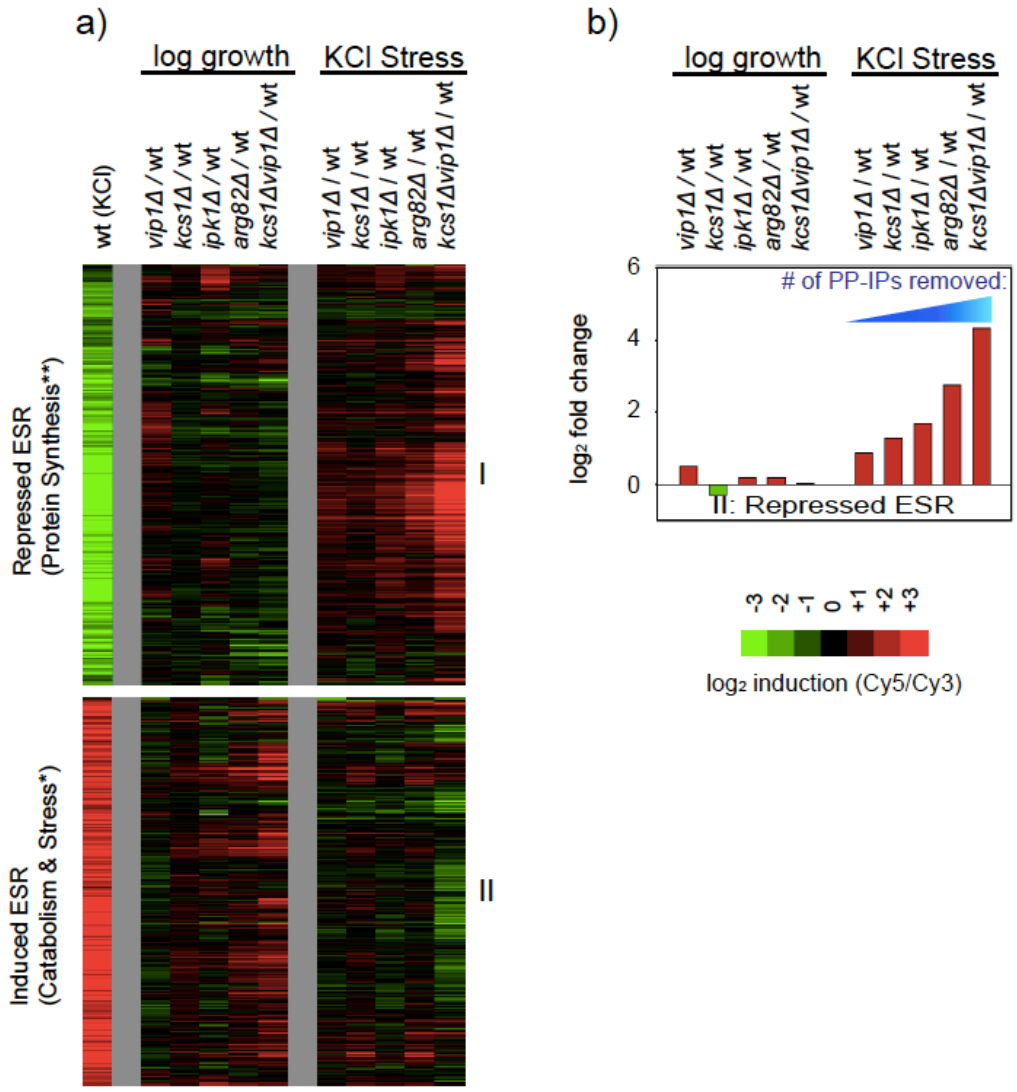

Figure 2. The role of the Inositol Phosphates and Pyrophosphates in Gene Regulation.

(a) DNA microarray data showing gene expression in log growth (YEPD, OD_{600}= 0.6) or in response to osmotic stress (0.4 M KCl, 20 minutes) in strains missing one or more of the enzymes inositol polyphosphate/pyrophosphate (IP) synthesis pathway. Each experiment compares the mRNA levels in a mutant strain to those in the wild type strain, in identical conditions. In all of these experiments cDNA from mutant strains are labeled with Cy5 while the wild type strain is labeled with Cy3. Thus, genes that are upregulated in the mutant strains appear red while genes that are downregulated are green. The wild type stress response (osmotic stress sample labeled red, log growth labeled green) is shown at far left for comparison. The heat map shows data for all of the genes in the ESR based on the average of two to

three replicate experiments per microarray (Table S1). Other genes regulated by the inositol phosphate pathway are described in the Supplement. Within the ESR, the correlation between the expression changes found in the *kcs1*D*vip1*D strain and the *arg82*D strain are very strong, with a Pearson's r of 0.70 in YEPD, 0.77 for genes repressed in stress, and 0.63 for genes activated in stress. The correlation between the expression changes found in the *kcs1*D*vip1*D and *ipk1*D strains are also strong for genes repressed in stress (r=0.69), but moderate in YEPD (r=0.45) and for genes activated in stress (r=0.49). Last, the expression changes found in the *kcs1*D and *vip1*D strains also correlate well with those found in the *arg82*D strain (r values ranging from 0.76 to 0.52, for the three gene groups listed above) except that there is little to no correlation between the influence of Vip1 and Arg82 in YEPD (r=0.12), suggesting that Vip1 is less important than Kcs1 for PP-IP synthesis in YEPD growth conditions. Overall, the strong correlation between the expression changes caused by deleting Kcs1 and Vip1, and removing their key substrates (IP_5 and IP_6) via deletion of Arg82 or Ipk1, indicates that it is the PP-IPs, and not other (unknown) molecules synthesized by Kcs1/Vip1, that regulate the ESR. (b) Bar graph showing the defect in Ribi gene repression for each mutant strain and condition in (a). Note that *arg82*D cells still produce some PP-IPs since Kcs1 phosphorylates and pyrophosphorylates IP_3 to create PP-IP_3, PP-IP_4, and other PP-IP species, when IP_5 and IP_6 are not available as substrates [126]. Accordingly, the expected concentration of PP-IPs in *kcs1*D*vip1*D < *arg82*D < *kcs1*D and *ipk1*D < *vip1*D [126].

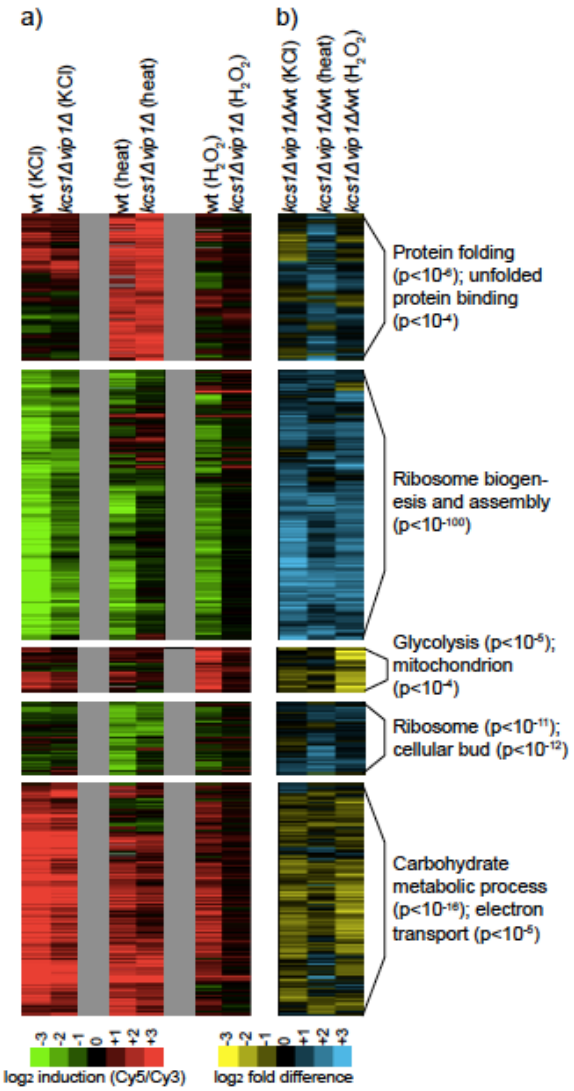

Figure 3. Inositol pyrophosphates (PP-IPs) Regulate the Environmental Stress Response.

DNA microarray data showing the gene expression programs activated in various stresses in wild type and *kcs1Δvip1Δ* strains. (a) Each column compares the mRNA levels in log growth conditions (YEPD, OD=0.6) to the mRNA levels in the same strain after 20 minutes of the indicated stress. In all of these experiments cDNA from cells collected prior to stress treatment were labeled with Cy3 (green) while cDNA from cells treated with stress stimuli were labeled with Cy5 (red). Thus, genes activated by 0.4M KCl, 42° C heat shock, or 0.4 mM H_2O_2 are red on the heat map while genes repressed in these stimuli are green. Only genes that are up or downregulated by >3-fold, in one or more experiment, are shown on the heat map. Clustering these data revealed five gene groups, each of which is labeled by its major

gene ontology groups and the probability that a GO group was found by chance. Microarrays are the average of at least two replicates. (b) Each column shows the difference between the *kcs1Δvip1Δ* and wild-type response to the stress indicated to highlight the Kcs1 and Vip1 regulated genes.

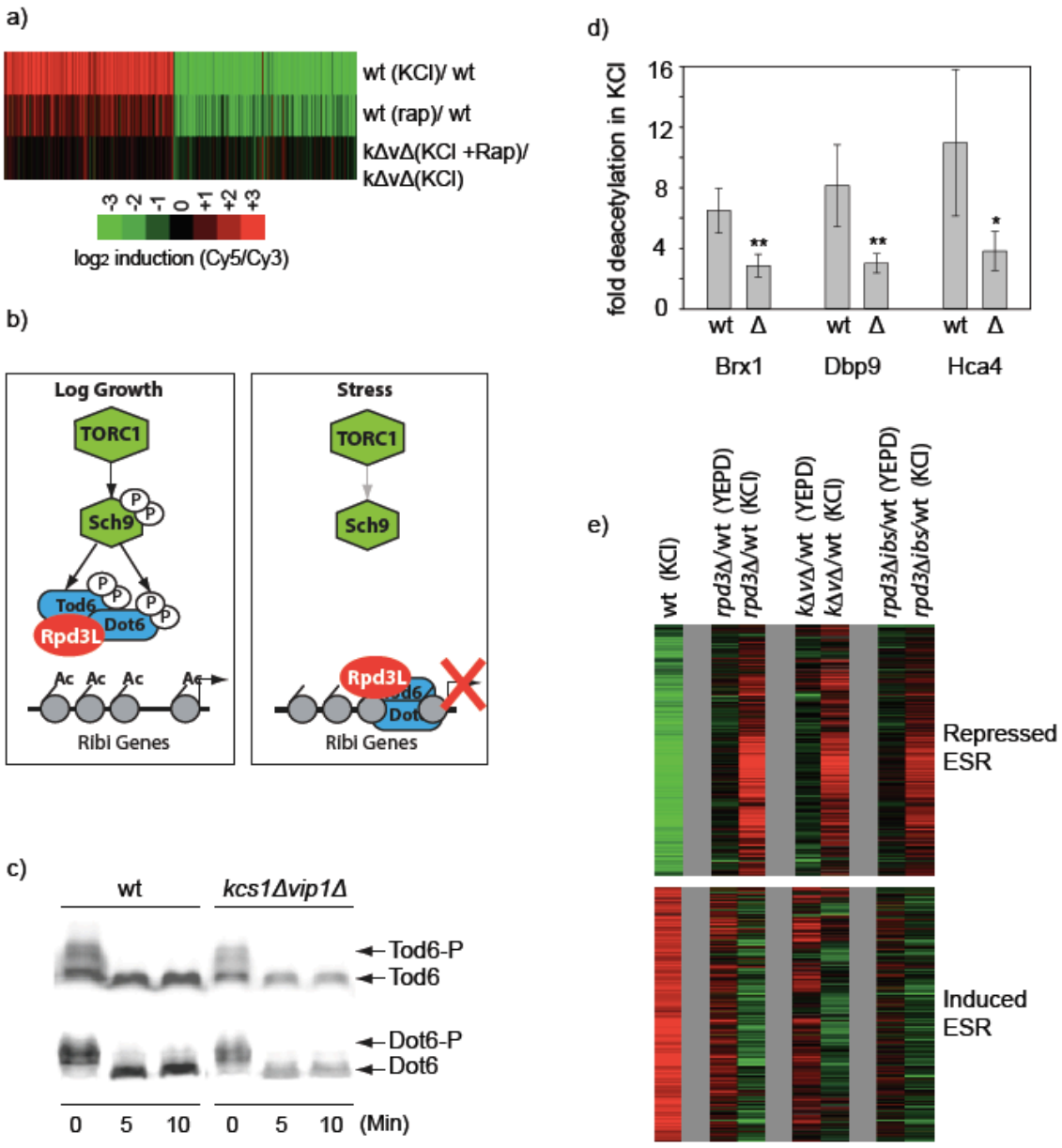

Figure 4. Inositol Pyrophosphates Regulate Rpd3L.

(a) Inositol pyrophosphates act at or below the level of TORC1. DNA microarray data showing genes up or downregulated >3-fold in response to 20 minutes of 0.4M KCl in wild type (top), or in *kcs1Δvip1Δ* strain (Cy3) compared to the same strain treated with 0.4M KCl and 300 nM rapamycin for 20 minutes (Cy5) (bottom). The gene expression changes induced by rapamycin in the wild-type strain are also shown for comparison (middle). If the PP-IPs acted upstream of TORC1 then treatment with rapmycin in stress would have rescued expression defect found in the *kcs1Δvip1Δ* strain, leading to dramatic changes in

gene expression in rapamycin. Microarrays are the average of three replicates. (b) Known mechanism of stress induced repression of Ribosome Biogenesis (Ribi) genes. Inactivation of TORC1 leads to Tod6/Dot6 activation and recruitment of the histone deacetylase Rpd3L to Ribi promoters, as described in the text. (c) Stress signaling through the TORC1 pathway still occurs in the absence of the PP-IPs. The phosphorylation of Dot6-HA and Tod6-HA was monitored using band-shift analysis, both before and after treatment with 0.4M KCl. Here cells were treated with TCA, lysed and whole cell extracts run on SDS-PAGE. Dot6 and Tod6 were identified using a western blot with an anti-HA antibody (12-CA5). The band-shifts monitored here have previously been show to be due to phosphorylation by Sch9 [63]**.** (d) PP-IPs are required for deacetylation at Ribi genes in 0.4M KCl stress. The acetylation level of three highly regulated Ribi genes was measured in the *kcs1Δvip1Δ* and wild-type strains, both before and after KCl stress, using an anti acetylated-H4 antibody and quantitative PCR. Plotted here is the ratio of the pre-stress to post-stress acetylation level. No significant changes in the pre-stress acetylation levels were found in the *kcs1Δvip1Δ* strain. However, stress triggers more deacetylation in the wild-type strain than it does in the *kcs1Δvip1Δ* strain; **($p<0.03$) and *($p<0.1$), t-test values for null hypothesis**.** (e) Rpd3, the PP-IPs, and disrupting the inositol-phosphate binding site on Rpd3L have similar effects on the ESR. The DNA microarrays show the change of gene expression caused by deleting Rpd3, Kcs1 and Vip1, or mutating the inositol binding site in Rpd3 (*rpd3Dibs*), in both log growth and 0.4M KCl stress (after 20 min). In each case cDNA from the mutant strain is labeled with Cy5, while cDNA from the wild-type strain, grown in identical conditions, is labeled with Cy3.

3.9 SUPPLEMENT

3.9.1 Extended Results

3.9.1.1 Screen for Regulators of TORC1 in Stress and Vip1 activates the ESR

A recent proteomic analysis in budding yeast found 5534 unique phosphopeptides in 3380 proteins [103]. Many of these peptides are phosphorylated or dephosphorylated 5 minutes after osmotic stress treatment (Fig. S1). To estimate the statistical significance of the changes observed, we fit the data describing the fold phosphorylation change to a normal distribution (Fig. S1). Assuming the noise in the data follows this standard probability density function, the cut-off for a p-value of 0.05 is a 5-fold change ($\log_2$=2.3). 133 proteins have one or more peptide (250-peptides total) with a change at or above this cut-off, 24 of which are involved in cell signaling by GO analysis. We were able to grow and perform null-mutant microarray analysis on the following 17 out of the 24 genes: Akc1, Bem3, Blm10, Fmp48, Inp52, Kic1, Kns1, Pem1, Pkh1, Pkh2, Pkh3, Ptk2, Rga2, Tel1, Ira2, Vip1, and Spa2. Only one of these strains (*vip1*Δ) had a significant defect in the activation of the ESR (Figs. 2 and S2). This expression defect is primarily due to loss of kinase activity since a strain carrying a kinase dead allele of Vip1 (*vip1*^{D487A}) and a strain with Vip1 deleted (*vip1*Δ) have similar expression defects (Fig. S3).

3.9.1.2 PP-IPs Regulate the ESR

Our discovery that Vip1 regulates Ribi and protein synthesis genes led us to test the role that other inositol poly and pyrophosphate synthases play in stress signaling. To do this we measured the impact that each enzyme involved in the PP-IP synthesis pathway has on gene expression in both log growth (YEPD) and osmotic stress conditions, using DNA microarrays. These data revealed that Kcs1, Vip1, Arg82 and Ipk1 regulate gene expression in a complex manner. Some genes are regulated by Vip1, others by Kcs1 and Vip1, and yet others by Kcs1, Vip1 and Arg82 (Fig. S4). Furthermore, each inositol kinase regulates a different set of genes in stress versus log growth conditions. Therefore, to make sense of the data, we looked to see if there are distinct gene groups, each regulated in a unique way by

the inositol kinases. We found that this is indeed the case as the genes regulated by the inositol kinases fall into seven statistically distinct groups (Fig. S4). Each of these gene modules, defined solely by the gene expression data, has a unique function or set of functions as defined by Gene Ontology (GO) analysis:

(1) Kcs1 and Vip1 promote the appropriate activation/repression of the 1272 genes in the osmotic stress response or ESR (Groups I and II, Fig. S4). In the case of the Ribi and protein synthesis module, Kcs1 and Vip1 simply act to inhibit gene expression in stress (Group I, Fig. S4). By contrast, at the stress defense module, Kcs1 and Vip1 act either to repress genes in log growth conditions, activate genes in stress conditions, or both (Group II, Fig. S4).

(2) Kcs1 and Vip1 also cooperate to regulate approximately 200 genes involved in metabolism, but not up or down regulated in stress. Specifically, Kcs1 and Vip1 constitutively activate genes involved in glycolysis and constitutively repress genes involved in siderophore transport (Groups III and IV, Fig. S4). The glycolysis gene module is a known target of the PP-IP signaling pathway and is thought to involve 5-PP-IP_5 dependent activation of Gcr1 [114].

(3) Kcs1 and Vip1 also regulate genes in the phosphate pathway (Group VII, Fig. S4) as described previously [112,113]. The best-characterized portion of this regulation involves Vip1 dependent synthesis of 1-PP-IP_5, which in turn binds and activates the Pho80/85 cyclin/cyclin dependent kinase complex.

(4) The inositol phosphate kinases also have mixed effects on 120 amino acid synthesis genes (Groups V and VI, Fig. S4). The mechanisms underlying this regulation are unknown, but are likely linked to the known role of Arg82 in arginine metabolism [127].

3.9.1.3 Kcs1/Vip1 Act through synthesis of the PP-IPs

Our microarray analyses (Fig. S4) show that Kcs1 and Vip1 regulate the ESR through synthesis of PP-IPs since deletion of Ipk1 and Arg82 (Fig. 1), enzymes upstream of Kcs1 and Vip1 in the PP-IP synthesis pathway, mimic deletion of Kcs1 and Vip1 themselves. This is best seen in examining the expression of the Ribi genes (Fig. 2b). Here removal of all PP-IPs, by deletion of Kcs1 and Vip1, causes the largest defect in gene repression. However, deletion of Arg82, which blocks production of 1-PP-IP_5, 5-PP-IP_4 and 5-PP-IP_5 via pyrophosphorylation of IP_5 and IP_6 (but allows some production of PP-IP_3 and PP-IP_4 by Kcs1 dependent pyrophosphorylation of IP_3 [126] also has a dramatic defect in gene repression. Finally, deletion of Ipk1 also causes a defect in Ribi gene repression, but less than that found in *kcs1*Δ*vip1*Δ or *arg82*Δ cells, as expected since *ipk1*Δ cells can still synthesize 5-PP-IP_5. Overall, therefore, the defect in Ribi gene repression in stress is proportional to the number of PP-IPs lost in a strain: *kcs1*Δ*vip1*Δ < *arg82*Δ < *ipk1*Δ and *kcs1*Δ < *vip1*Δ. This pattern of PP-IP level dependent defect is also found at many other genes in the ESR as described below.

Outside of driving repression of Ribi and protein synthesis genes in stress conditions (Group I, Fig. S4), Kcs1/Vip1 also influence the ESR by (1) repressing the stress-activated genes in log growth conditions and (2) promoting the activation of stress genes in stress conditions. As seen in Fig. S5, repression of stress genes in log growth conditions is inhibited by deletion of most enzymes in the PP-IP synthesis pathway, again roughly following the expected order: *kcs1*Δ*vip1*Δ < *arg82*Δ < *ipk1*Δ and *kcs1*Δ < *vip1*Δ (Fig. S5a and b). By contrast, examining the influence of the PP-IP pathway on the induction of stress genes reveals two behaviors. Some genes show the trend described above for PP-IP dependent gene repression, where expression is proportional to the number of PP-IPs removed (Fig. S5c). However, the majority of genes only have a significant expression defect when both Kcs1 and Vip1 are deleted (Fig. S5d). Therefore, PP-IP dependent gene activation is generally less sensitive to a decrease in PP-IP level than PP-IP dependent gene repression. This is entirely consistent with our model where PP-IPs activate Rpd3L, which then acts as both an activator and repressor (Fig. 4e), since gene

repression and gene activation by Rpd3L are likely to occur via different mechanisms and thus have different dependencies on PP-IP concentration.

3.9.1.4 Snt1 is not involved in the ESR

As discussed in the main text of the paper Watson et al found that HDAC3 is activated by IP_4. IP_4 acts by promoting the interaction between HDAC3 and the Corepressor SMRT. Although SMRT has a homolog in yeast Snt1, this protein does not play a role in the ESR as a *snt1*Δ cells have no change in gene expression in YEPD or KCl stress conditions (Table S1).

3.9.2 Extended Experimental Procedures

3.9.2.1 Strains

All strains used in this study were generated starting with an ADE2 strain in the W303 strain background (trp1 leu2 ura3 his3 can1 GAL+ psi+). The origin strain, EYO690, came from the O'Shea lab (Capaldi, 2010), and all other strains were constructed for this study. Null mutants were produced by transformation with PCR products including auxotrophic markers, flanked by the 40 bp sequence found directly up and downstream from the gene, and selection on the appropriate medium [128]. HA-tagged strains were constructed similarly but the primers directed the recombination to the sites directly upstream and directly downstream from the stop codon [129]. PCR was used to confirm the location of the marker gene or epitope tag insertion. Western blots were used to confirm the integrity of the HA tags

3.9.2.2 Gene expression microarray experiments

Overnight cultures of the desired strains were used to inoculate a 0.75 L culture to an OD_{600} of 0.1 (in YEPD media) in a 2.8 L conical flask shaking at 200 rpm at 30°C. These cultures were grown to an OD_{600} between 0.55 and 0.65, and then 250 ml of cells were collected by vacuum filtration and frozen in liquid nitrogen. Next, the remaining cells were subjected to stress (by addition of KCl in YEPD, addition of heated YEPD and incubation at 42 °C, addition of H_2O_2 in YEPD, or addition of KCl and/or 200 ng/L rapamycin in YEPD). Cells were then grown in the relevant condition for 20 min before 250-300 ml of

cells were collected by vacuum filtration and frozen in liquid nitrogen. Finally, RNA was purified from the frozen cells, converted into cDNA using reverse transcription, labeled with Cy3 (pre-stress/log growth) or Cy5 (post-stress or rapamycin) and examined using Agilent microarrays, as described previously [92,114].

All of the raw data from the microarray experiments described in this paper are included in the accompanying spreadsheet (Table S1).

3.9.2.3 Bandshifts

Yeast cultures, grown overnight, were used to inoculate 150 ml of fresh rich media to an OD_{600} of 0.1. These cultures were grown in 500 ml conical flasks shaking at 200 rpm at 30 °C until mid log phase (OD_{600} 0.5-0.6). At this point a 47 ml sample, providing the zero time point, was collected, mixed with 3 ml 100% Trichloroacetic acid (TCA), and held on ice for at least 30 mins (and up to 6 hrs). The remaining culture volume was adjusted to 100 ml before adding 10 ml of 4.125 M KCl in YEPD (final concentration 0.375 M KCl). Cultures were returned to the shaker for further growth and 47 ml samples were collected and treated with TCA, as above, at 5 and 10 minute time points. TCA treated samples were centrifuged at 4000 rpm for 5 mins at 4 °C to collect the cell pellets, which were then washed with 5 ml chilled water, centrifuged again and resuspended in 1 ml of 4 °C water. These samples were then transferred to 2 ml screw cap tubes and centrifuged at 8000 rpm for 30 s. The resulting cell pellets were washed twice in 1 ml acetone and disrupted by sonication at 15% amplitude for 5 s before centrifugation at 8000 rpm for 30 s. Cell pellets were then dried in a speedvac for 10 mins at room temperature, and frozen.

Protein extraction was performed in urea buffer (6M Urea, 50mM Tris-HCl pH 7.5, 5mM EDTA, 1mM PMSF, 5mM NaF, 5mM NaN_3, 5mM NaH_2PO_4, 5mM p-nitrophenylphosphate, 5mM β-glycerophosphate, 1% SDS) supplemented with complete protease and phosphatase inhibitor tablets (Roche #04-693-159-001 and #04-906-845-001). Specifically, the cell pellets were resuspened in 600 ml urea buffer by vortexing, and lysed using bead beating (five 1 minute cycles at maximum speed). The lysate was collected after centrifugation for 5 minute at 3000 rpm, ressuspened into a homogenous slurry by

vortexing, and heated at 65 °C for 10 minutes. Soluble proteins were separated from insoluble cell debris by centrifugation at 16,000 rpm for 5 minutes, and the lysates stored at -80 °C until required. Cell extracts were then to 95 °C in SDS sample buffer for 5 min before they were run on an SDS-PAGE gel, transferred to a nitrocellulose membrane, and then detected using 12CA5 (anti-HA).

3.9.2.4 Chromatin immunoprecipitation

The ChIP experiments, used to measure histone deacetylation by Rpd3L, were performed following the procedure that Gasch and coworkers [6] used to demonstrate that Rpd3L is a key regulator of the ESR. Specifically, an overnight culture of the desired strain was used to inoculate a 0.4 L culture to an OD_{600} of 0.1 (in YEPD media) in a 1 L conical flask shaking at 200 rpm at 30°C. These cultures were grown to an OD_{600} between 0.55 and 0.65, at which time 180 ml was removed and added to a new 1 L flask that contained 20 ml of YEPD+KCl (for a final concentration of 0.375M KCl). Both flasks shook (200 rpm, 30°C) for 7 minutes (during which time 20 ml was removed from the YEPD-only flask so both flasks contained 200 ml total). Next, 37% formaldehyde was added to a final volume of 1% and the flasks were swirled by hand every 2-3 minutes at 23 °C for 15 minutes. At that point glycine was added to a final concentration of 125 mM and the flasks were mixed by hand every minute or two for 5 minutes. Cultures were then collected by centrifugation and washed twice with 25 ml cold PBS buffer.

Cell pellets were resuspended in 800 µl lysis buffer (50mM HEPES/KOH pH 7.5, 140mM NaCl, 1mM EDTA, 1% triton X-100, 0.1% (w/v) sodium deoxycholate) with fresh protease inhibitor (Roche #04-693-159-001) and split into two 2ml screw cap tubes (~500 µl each) and lysed by bead beating 5x 1 min with 2 min on ice between intervals. The lysate was collected and the chromatin was sheared to average size of 500 bp by sonicating, 5x 15 sec, with 1 min interval on ice at a power of 15% using a Fisher Sonic Dismembrinator Model 500 fitted with a microtip. Next, the samples were centrifuged 14,000 rpm for 10 min at 4 °C and the supernatant (crude cell lysate) was collected. 2.5-5 µl anti acetyl-H4 antibody (Millipore #06-866) and 25 µl of Thermo Protein A/G UltraLink resin was then added to 500 ml of the supernatant and incubated overnight on a nutator at 4 °C. The beads were then spun down at 2000 rpm,

washed 2x with lysis buffer (5 min rotation at 23°C), followed by 1x with TE (5 min rotation at 23°C). The supernatant was removed and the beads were resuspended in 100 µl TE 1% SDS. The DNA fragments were then eluted by overnight incubation at 65 °C. The DNA was then purified using phenol-cholorform extraction, as described previously (Capaldi et al., 2008).

The concentration of DNA bound to the nucleosome just downstream of the start codon of the three Ribi genes most repressed in the ESR (Brx1, Dbp9 and Hca4), along with that from a region of the telomere (Ars503) where nucleosomes are highly acetylated in both log growth and stress conditions [6], were then quantified for each sample using real-time PCR (details below). The level of acetylation was calculated by dividing the concentration of DNA from Brx1, Dbp9 and Hca4 by the concentration of DNA from Ars503. The graphs in Fig. 4d show the change in this ratio (for example [Brx1]/[Ars503]) in log growth compared to stress conditions (i.e., a large number means more deacetylation in stress). Each bar shows the average and standard deviation for three separate experiments. At all genes, the acetylation level in the *kcs1*Δ*vip1*Δ strain matched that of the wt strain in log growth conditions (less than 1.5-fold change for all genes).

3.9.2.5 Quantitative PCR

Quantitative PCR was performed in 96-well plates using an Agilent Technologies Stratagene Mx3005P using taq polymerase and Sybr green dye. A dilution of genomic DNA was used to establish a standard curve for each primer pair on each run. In all cases this 4 point standard cure was fit to a line yielding an R value of 0.98-1.0, allowing us to accurately calculate the DNA concentration in the samples. In all cases thermal denaturation curves showed that the primer pairs produce a single PCR product (two sets of primers that did not meet this criteria were thrown out). The Thermal profile and primers are listed in Table S3.

3.10 SUPPLEMENTAL FIGURES

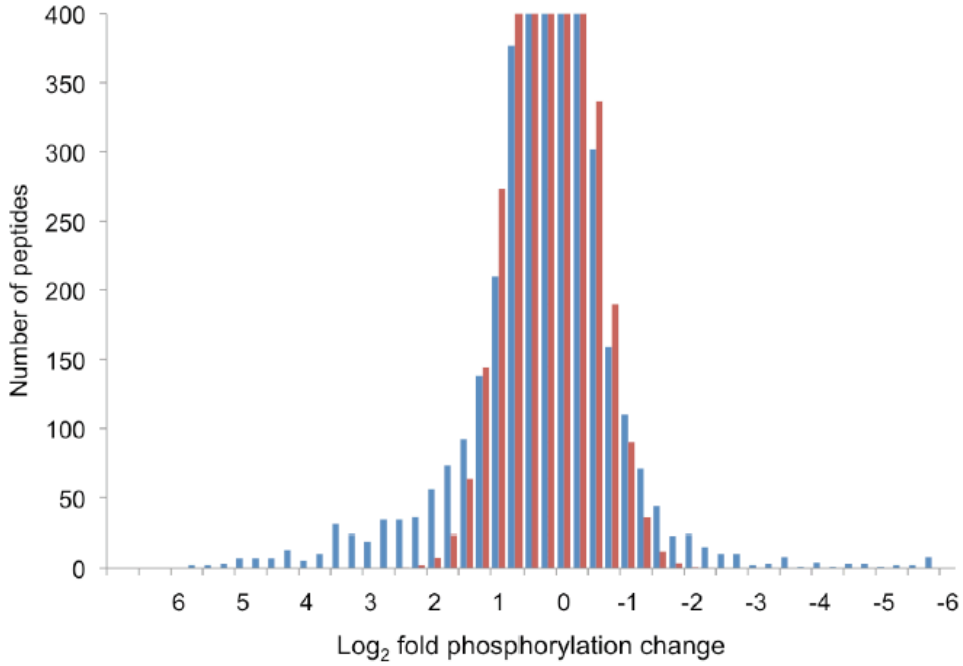

Figure S1. Phosphorylation Changes in the yeast proteome after 5min of 0.4M KCl stress.

The blue histogram shows the distribution of phosphorylation changes for the yeast genome for the data of [103], while the red bars show the best fit of these data to a normal distribution.

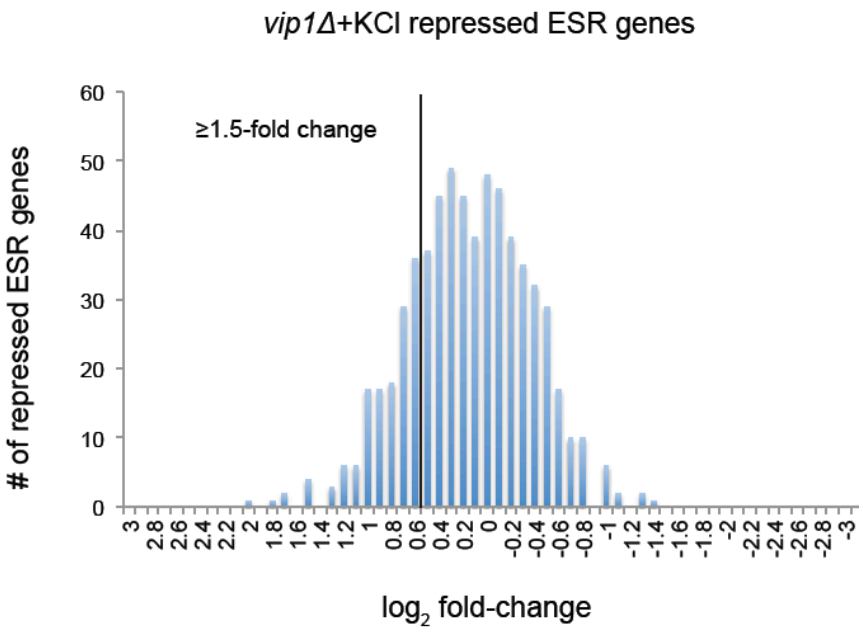

Figure S2. Vip1 is required for gene repression in the ESR.

The histogram shows the $\log_2$ ratio of mRNA levels in *vip1Δ* versus wt cells in 0.4M KCl (from the average of three replicates). Only genes repressed >2-fold during osmotic stress in the wild-type strain (Fig. 2) are included in this plot.

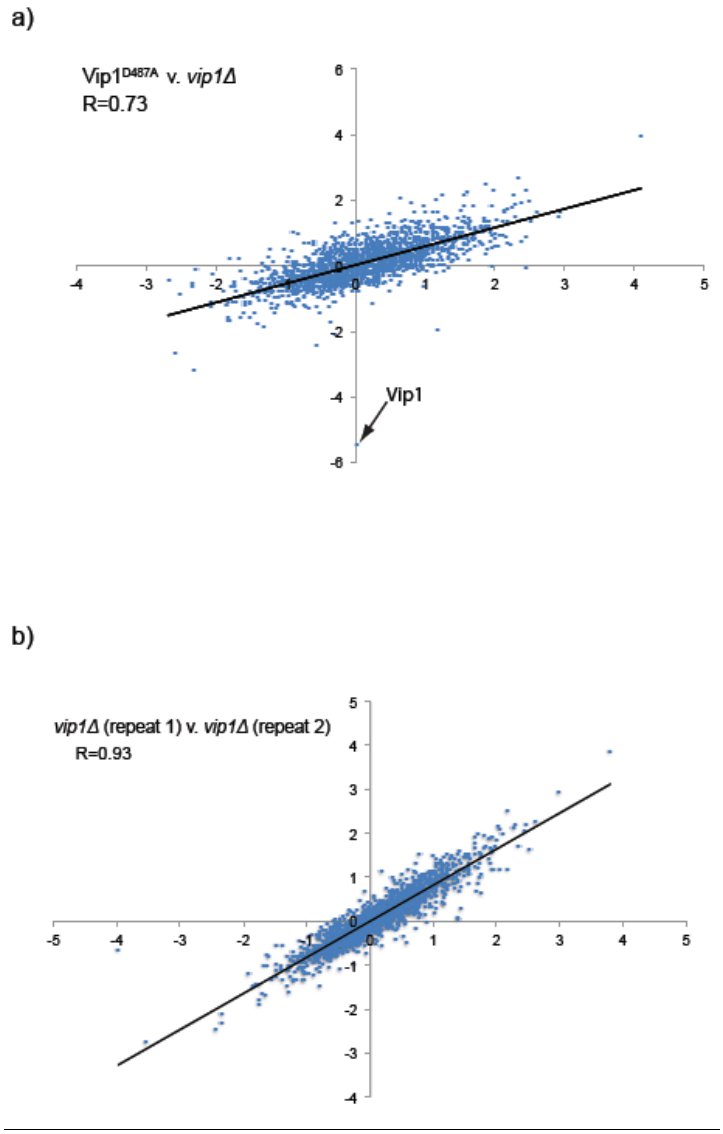

Figure S3. A kinase dead allele Vip1^{D487A} has a defect in induction of the ESR.

(a) Scatterplot comparing the stress activated expression changes in the kinase-dead Vip1 allele (*vip1*^{D487A} +KCl/wt+KCl; X-axis) to those in the Vip1 null mutant (*vip1Δ*+KCl/wt+KCl; Y-axis). For comparison, (b) shows a scatterplot of two biological replicates of the Vip1 null mutant (*vip1Δ*+KCl/wt+KCl). Axes are labeled in $\log_2$ scale. The reduced correlation in (a) is likely due to activity of the phosphatase domain [111], not eliminated in Vip1^{D487A}.

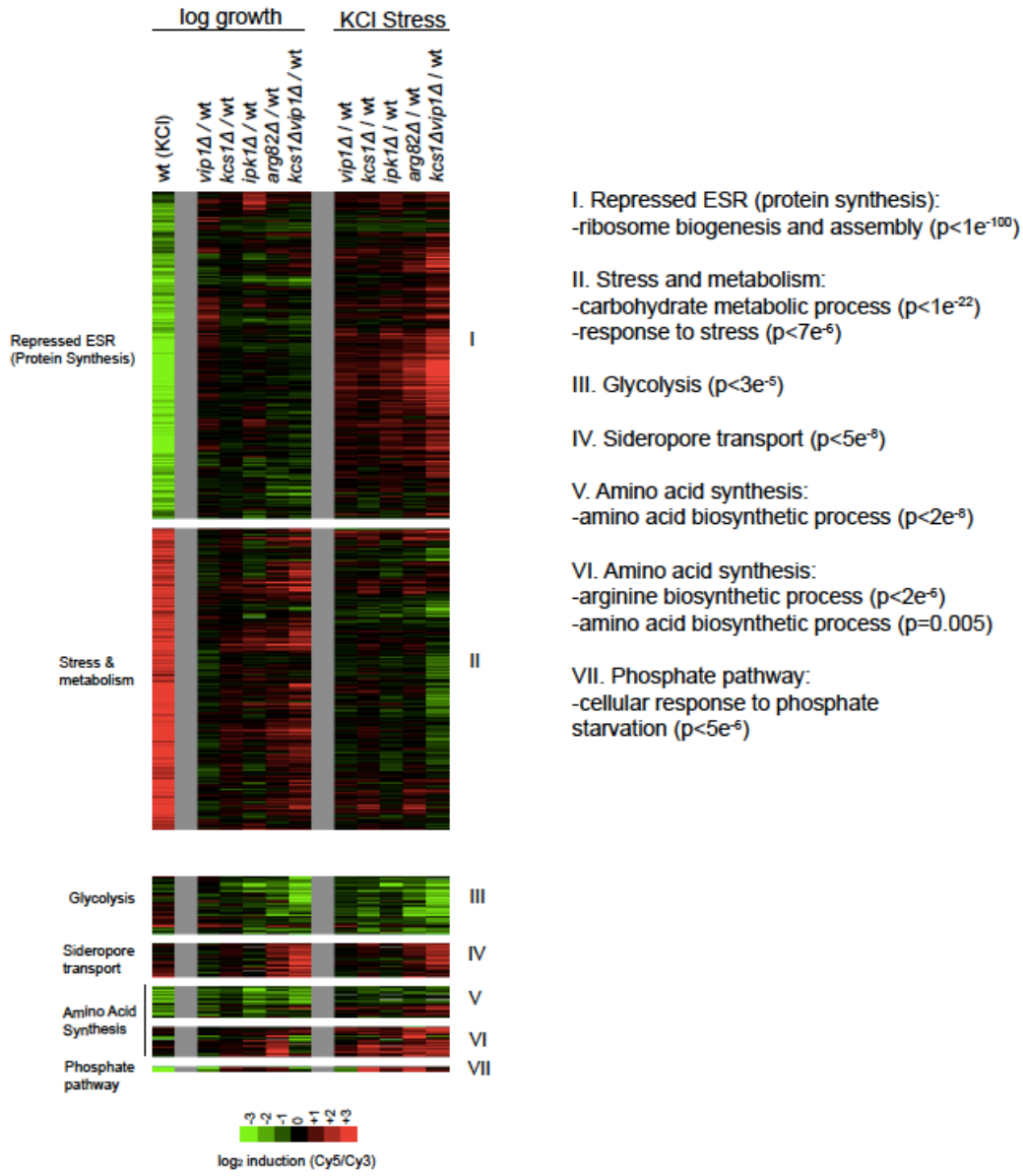

Figure S4. The role of the Inositol Phosphates and Pyrophosphates in Gene Regulation.

(a) DNA microarray data showing gene expression in log growth (YEPD, OD_{600}= 0.6) or in response to osmotic stress (0.4 M KCl, 20 minutes) in strains missing one or more of the enzymes inositol polyphosphate/pyrophosphate (IP) synthesis pathway. Each experiment compares the mRNA levels in a mutant strain to those in the wild type strain, in identical conditions. In all of these experiments cDNA from mutant strains are labeled with Cy5 while the wild type strain is labeled with Cy3. Thus, genes that are upregulated in the mutant strains appear red while genes that are downregulated are green. The wild type stress response (osmotic stress sample labeled red, log growth labeled green) is shown at far left for

comparison. All genes that change greater than 2-fold in one or more mutant or condition were included in the cluster analysis and are shown in the heat map. However, one group containing ribosomal proteins were excluded as the Cy5/Cy3 ratio was <1 due to FRET between Cy5 and Cy3 (caused by the very high expression levels of these genes) and not a change in the mRNA levels themselves, as shown by a dye swap experiment (Table S1). Microarrays are the average of two (log growth) or three (stress conditions) replicates. Labels on the right show the most significant GO terms, along with their statistical significance, as determined using GOstat [130]. The top two groups (genes involved in the ESR) are also shown in Fig. 2.

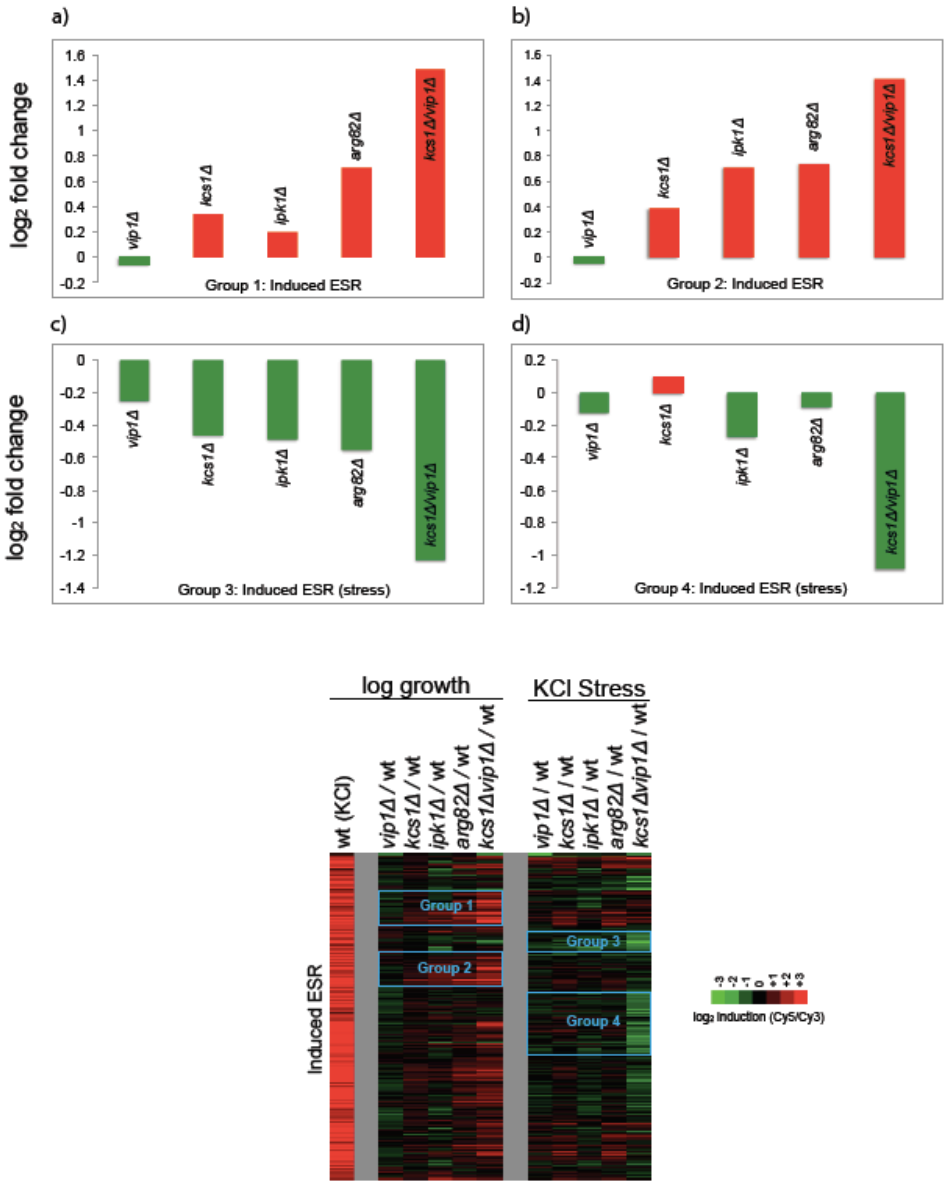

Figure S5. PP-IP Dependence of Genes induced in the ESR.

(a-d) bar graphs showing the average log_2-fold change in four induced ESR gene subgroups for null mutant strains. The four subgroups chosen are indicated in the heatmap, Group II from Fig. S4. Each Bar shows the average change for all genes in the subgroup.

3.11 SUPPLEMENTAL TABLES

Table S1.

Sample	title	raw data file	ch1: source name	ch1: characteristics: strain	ch1: label	ch2: source name	ch2: characteristics: strain	ch2: label	description
Sample 1	wt (ACY044)+Osmotic Stress 0.375MKCl: 251632210087-5	251632210087-5	KCl stress 0.375M, 20min	acy 044	cy3	mid-log, yepd	acy 044	cy5	251632210087-5 is a dye swap
Sample 2	wt (ACY044)+Osmotic Stress 0.375MKCl: 251632210246-2	251632210246-2	mid-log, yepd	acy 044	cy3	KCl stress 0.375M, 20min	acy 044	cy5	
Sample 3	ipk1: 251632210246-5	251632210246-5	mid-log, yepd	acy 044	cy3	mid-log, yepd	acy 237	cy5	
Sample 4	ipk1+Osmotic Stress KCl 0.375M: 251632210246-6	251632210246-6	KCl stress 0.375M, 20min	acy 044	cy3	KCl stress 0.375M, 20min	acy 237	cy5	
Sample 5	kcs1/vip1: 251632210246-7	251632210246-7	mid-log, yepd	acy 044	cy3	mid-log, yepd	acy 236	cy5	
Sample 6	kcs1/vip1+Osmotic Stress: 251632210246-8	251632210246-8	KCl stress 0.375M, 20min	acy 044	cy3	KCl stress 0.375M, 20min	acy 236	cy5	
Sample 7	arg82: 251632210249-5	251632210249-5	mid-log, yepd	acy 044	cy3	mid-log, yepd	acy 207	cy5	
Sample 8	arg82+Osmotic Stress KCl 0.375M: 251632210249-6	251632210249-6	KCl stress 0.375M, 20min	acy 044	cy3	KCl stress 0.375M, 20min	acy 207	cy5	
Sample 9	vip1: 251632210249-7	251632210249-7	mid-log, yepd	acy 044	cy3	mid-log, yepd	acy 211	cy5	
Sample 10	vip1+Osmotic Stress KCl 0.375: 251632210249-8	251632210249-8	KCl stress 0.375M, 20min	acy 044	cy3	KCl stress 0.375M, 20min	acy 211	cy5	
Sample 11	vip1: 251632210250-1	251632210250-1	mid-log, yepd	acy 044	cy3	mid-log, yepd	acy 211	cy5	
Sample 12	vip1+Osmotic Stress KCl 0.376: 251632210250-2	251632210250-2	KCl stress 0.375M, 20min	acy 044	cy3	KCl stress 0.375M, 20min	acy 211	cy5	
Sample 13	wt (ACY044)+Osmotic Stress 0.375MKCl: 251632210250-3	251632210250-3	mid-log, yepd	acy 044	cy3	KCl stress 0.375M, 20min	acy 044	cy5	
Sample 14	arg82: 251632210250-5	251632210250-5	mid-log, yepd	acy 044	cy3	mid-log, yepd	acy 207	cy5	
Sample 15	arg82+Osmotic Stress KCl 0.375M: 251632210250-6	251632210250-6	KCl stress 0.375M, 20min	acy 044	cy3	KCl stress 0.375M, 20min	acy 207	cy5	
Sample 16	kcs1: 251632210250-7	251632210250-7	mid-log, yepd	acy 044	cy3	mid-log, yepd	acy 209	cy5	
Sample 17	kcs1+Osmotic Stress KCl 0.375M: 251632210250-8	251632210250-8	KCl stress 0.375M, 20min	acy 044	cy3	KCl stress 0.375M, 20min	acy 209	cy5	
Sample 18	kcs1/vip1+ KCl + Rap v. kcs1/vip1+KCl : 251632210259-2	251632210259-2	KCl stress 0.375M, 20min	acy 236	cy3	200nM Rapamycin +KCl 0.375M, 20min	acy 236	cy5	
Sample 19	kcs1/vip1+Oxidative Stress 0.4mM H2O2: 251632210259-5	251632210259-5	H2O2 0.4mM, 20min	acy 044	cy3	H2O2 0.4mM, 20min	acy 236	cy5	
Sample 20	wt+Oxidative Stress 0.4mM H2O2: 251632210259-6	251632210259-6	mid-log, yepd	acy 044	cy3	H2O2 0.4mM, 20min	acy 044	cy5	
Sample 21	kcs1/vip1+0.375M KCl + Rapamycin 200nM: 251632210288-1	251632210288-1	KCl stress 0.375M, 20min	acy 236	cy3	200nM Rap +KCl 0.375M, 20min	acy 236	cy5	
Sample 22	kcs1/vip1+KCl v. kcs1/vip1, osmotic stress 0.375M KCl: 251632210288-2	251632210288-2	KCl stress 0.375M, 20min	acy 236	cy3	KCl stress 0.375M, 20min	acy 236	cy5	
Sample 23	ipk1: 251632210288-5	251632210288-5	mid-log, yepd	acy 044	cy3	mid-log, yepd	acy 237	cy5	
Sample 24	ipk1+Osmotic Stress KCl 0.375M: 251632210288-6	251632210288-6	KCl stress 0.375M, 20min	acy 044	cy3	KCl stress 0.375M, 20min	acy 237	cy5	
Sample 25	kcs1/vip1: 251632210288-7	251632210288-7	mid-log, yepd	acy 044	cy3	mid-log, yepd	acy 236	cy5	
Sample 26	kcs1/vip1+Osmotic Stress: 251632210288-8	251632210288-8	KCl stress 0.375M, 20min	acy 044	cy3	KCl stress 0.375M, 20min	acy 236	cy5	
Sample 27	rpd3: 251632210393-3	251632210393-3	mid-log, yepd	acy 044	cy3	mid-log, yepd	acy 433	cy5	
Sample 28	rpd3+Osmotic Stress 0.375M KCl: 251632210393-4	251632210393-4	KCl stress 0.375M, 20min	acy 044	cy3	KCl stress 0.375M, 20min	acy 433	cy5	
Sample 29	arg82+Osmotic Stress KCl 0.375M: 251632210393-5	251632210393-5	KCl stress 0.375M, 20min	acy 044	cy3	KCl stress 0.375M, 20min	acy 207	cy5	
Sample 30	kcs1+Osmotic Stress KCl 0.375M: 251632210393-6	251632210393-6	KCl stress 0.375M, 20min	acy 044	cy3	KCl stress 0.375M, 20min	acy 209	cy5	
Sample 31	kcs1/vip1+Osmotic Stress: 251632210393-7	251632210393-7	KCl stress 0.375M, 20min	acy 044	cy3	KCl stress 0.375M, 20min	acy 236	cy5	
Sample 32	ipk1+Osmotic Stress KCl 0.375M: 251632210393-8	251632210393-8	KCl stress 0.375M, 20min	acy 044	cy3	KCl stress 0.375M, 20min	acy 236	cy5	
Sample 33	vip1+osmotic stress KCl 0.375M: 251632210394-4	251632210394-4	KCl stress 0.375M, 20min	acy 044	cy3	KCl stress 0.375M, 20min	acy 211	cy5	
Sample 34	kcs1/vip1: 251632210394-5	251632210394-5	mid-log, yepd	acy 044	cy3	mid-log, yepd	acy 236	cy5	
Sample 35	kcs1/vip1+Osmotic Stress v. kcs1/vip1: 251632210462-5	251632210462-5	mid-log, yepd	acy 236	cy3	KCl stress 0.375M, 20min	acy 236	cy5	
Sample 36	kcs1/vip1+Oxidative Stress 0.4mM H2O2: 251632210462-7	251632210462-7	H2O2 0.4mM, 20min	acy 044	cy3	H2O2 0.4mM, 20min	acy 236	cy5	
Sample 37	kcs1/vip1+Heat Shock 42C: 251632210462-8	251632210462-8	heat shock 42C, 20min	acy 044	cy3	heat shock 42C, 20min	acy 236	cy5	
Sample 38	wt+Heat Shock 42C: 251632210464-5	251632210464-5	mid-log, yepd	acy 044	cy3	heat shock 42C, 20min	acy 044	cy5	
Sample 39	wt+Oxidative Stress 0.4mM H2O2: 251632210465-1	251632210465-1	mid-log, yepd	acy 044	cy3	H2O2 0.4mM, 20min	acy 044	cy5	
Sample 40	kcs1/vip1+H2O2 v. kcs1/vip1: 251632210465-2	251632210465-2	mid-log, yepd	acy 236	cy3	H2O2 0.4mM, 20min	acy 236	cy5	
Sample 41	kcs1/vip1+KCl+Rap v. kcs1/vip1+KCl: 251632210465-3	251632210465-3	KCl stress 0.375M, 20min	acy 236	cy3	200nM Rapamycin +KCl 0.375M, 20min	acy 236	cy5	
Sample 42	kcs1: 251632210465-4	251632210465-4	mid-log, yepd	acy 044	cy3	mid-log, yepd	acy 209	cy5	
Sample 43	snt1: 251632210531-5	251632210531-5	mid-log, yepd	acy 044	cy3	mid-log, yepd	acy 591	cy5	
Sample 44	snt1+Osmotic Stress KCl 0.375M: 251632210531-6	251632210531-6	KCl stress 0.375M, 20min	acy 044	cy3	KCl stress 0.375M, 20min	acy 591	cy5	
Sample 45	Vip1D487A: 251632210531-7	251632210531-7	mid-log, yepd	acy 044	cy3	mid-log, yepd	acy 584	cy5	
Sample 46	Vip1D487A+Osmotic Stress KCl 0.375: 251632210531-8	251632210531-8	KCl stress 0.375M, 20min	acy 044	cy3	KCl stress 0.375M, 20min	acy 584	cy5	
Sample 47	Rpd3ibs: 251632210532-7	251632210532-7	mid-log, yepd	acy 044	cy3	mid-log, yepd	acy 614	cy5	
Sample 48	Rpd3ibs+Osmotic Stress 0.375M KCl: 251632210532-8	251632210532-8	KCl stress 0.375M, 20min	acy 044	cy3	KCl stress 0.375M, 20min	acy 614	cy5	
Sample 49	snt1: 251632210533-1	251632210533-1	mid-log, yepd	acy 044	cy3	mid-log, yepd	acy 591	cy5	
Sample 50	snt1+Osmotic Stress KCl 0.375M: 251632210533-2	251632210533-2	KCl stress 0.375M, 20min	acy 044	cy3	KCl stress 0.375M, 20min	acy 591	cy5	
Sample 51	Rpd3ibs: 251632210533-3	251632210533-3	mid-log, yepd	acy 044	cy3	mid-log, yepd	acy 614	cy5	
Sample 52	Rpd3ibs+Osmotic Stress 0.375M KCl: 251632210533-4	251632210533-4	KCl stress 0.375M, 20min	acy 044	cy3	KCl stress 0.375M, 20min	acy 614	cy5	
Sample 53	Vip1D487A: 251632210637-7	251632210637-7	mid-log, yepd	acy 044	cy3	mid-log, yepd	acy 584	cy5	251632210637-7 is a dye swap
Sample 54	Vip1D487A+Osmotic Stress KCl 0.375: 251632210637-8	251632210637-8	KCl stress 0.375M, 20min	acy 044	cy3	KCl stress 0.375M, 20min	acy 584	cy5	251632210637-8 is a dye swap
Sample 55	wt (ACY044)+Rapamycin 200nM: 251632210103-1	251632210103-1	mid-log, yepd	acy 044	cy3	200nM rap, 20min	acy 044	cy5	

Table S2.

Strain	Genotype	Background
EY0690 (ACY 044)	w303 MATa	
ACY211	vip1::His3 MATa	EY0690
ACY209	kcs1::His3 MATa	EY0690
ACY207	arg82::His3 MATa	EY0690
ACY237	ipk1::Leu2 MATa	EY0690
ACY236	vip1::Leu2 kcs1::His3 MATa	EY0690
ACY359	Sch9-HA(Trp1) MATa	EY0690
ACY 435	Sch9-HA(Trp1) vip1::Leu2 kcs1::His3 MATa	EY0690
ACY 493	Sch9-HA(Trp1) vip1::Ura3 MATa	EY0690
ACY 519	Sch9-HA(Trp1) kcs1::Ura3 MATa	EY0690
ACY 322	Dot6-HA(Kan) MATa	EY0690
ACY 321	Dot6-HA(Kan) vip1::Leu2 kcs1::His3 MATa	EY0690
ACY 491	Dot6-HA(Kan) vip1::Ura3 MATa	EY0690
ACY 518	Dot6-HA(Kan) kcs1::Ura3 MATa	EY0690
ACY 320	Tod6-HA(Kan) MATa	EY0690
ACY 490	Tod6-HA(Kan) vip1::Ura3 MATa	EY0690
ACY 520	Tod6-HA(Kan) kcs1::Ura3 MATa	EY0690
ACY 456	Tod6-HA(Kan) vip1::Leu2 kcs1::His3 MATa	EY0690
ACY 433	*rpd3:: Ura3 MATa*	EY0690
ACY 591	*snt1:: Leu2 MATa*	EY0690
ACY 584	$Vip1^{D487A}$ MATa	EY0690
ACY 614	$Rdp3^{K41A,R280A,R316A}$ MATa	EY0690

Table S3. qPCR primers and conditions.

Cycles	Temp (degrees Celcius)	Time (minutes)
1	95	3
35	95	0.5
	55	1
	70	0.75
1	95	1
	55	0.5
	55-95	~25

Primers	Left	Right
Ars503-1	ACCAGGAATACACATAAGTGCAAA	AAGAATATTTTGTGAGTGAGCTGGT
Brx1	CGTCAGGTGTTGAAAGAGTT	TTTATTATCTTTGCTCTTTCCTG
Dbp9	AGCCAAAACTGCAACGAAAG	TAAGCGCCTTCCACAGACTT
Hca4	TTGAAAGGCTCGAGAACCTAAT	TGGCCTTGGTTATCTTAGGG

CHAPTER IV: OPEN QUESTIONS AND FUTURE RESEARCH

Our automated screening protocol for identifying growth regulators, described in Chapter II, is a powerful, quantitative tool for studying growth control in *S. cerevisiae*. It allows us to identify growth regulators in conditions that have gone relatively unstudied, and it lets us begin placing those regulators in the growth control network. Chapter III illustrates how novel growth regulators can be delineated using established techniques. But in addition to leaving many important questions unanswered, this work raises new questions of its own. Foremost amongst these questions is the need to continue adding detail to the growth regulation network. However, it will also be exciting to use the techniques we have developed to search for the first direct regulators of inositol pyrophosphate kinases in any organism.

4.1 What are the direct regulators of growth control in stress conditions?

Our screen of the yeast deletion collection uncovered over seven hundred genes that are necessary to shut down growth genes in osmotic stress. However, our screen did not distinguish between genes that are direct regulators of ribosome biogenesis mRNA and strains that affect ribosome biogenesis indirectly. In addition, the yeast deletion collection is known to contain many aneuploid strains and suppressor mutations, which could lead to false positives or negatives.

It is not currently feasible to test over seven hundred yeast deletion strains to determine which ones are acting on ribosome biogenesis mRNA through a direct mechanism. We can, however, combine our data with other published high-throughput datasets, such as phosphoproteomic, yeast two hybrid, and co-IP data (and we have already done some of this as described in Chapter II). Knowing which of our growth regulators have known physical interactions with components of the TORC1, inositol polyphosphate synthesis, or Snf1 pathways will give us a clue about which are likely to be direct. In addition, we can search our growth regulator collection for phosphorylation motifs of known growth pathway components.

One problem with using published datasets, however, is that almost all high-throughput physical interaction data has been collected in log growth conditions, and it is likely that many of our growth

regulators only interact with known growth network components in stress or starvation conditions. One exception is that there are several high-throughput phosphoproteomic screens that have been performed in either rapamycin or stress conditions,[131-134] and we are working to combine our dataset with these resources. Once this is done, we can begin to predict which of our new growth regulators merit more detailed follow up work.

4.2 How do the newly identified growth regulators fit into pathways?

Our goal is to reconstruct the growth regulation network in stress, so after learning what the components of the network are, we need to begin placing them into pathways. As discussed in Chapter III, as a first step we have run our method using the TORC1 inhibitor rapamycin. Strains that fail to downregulate ribosome biogenesis genes when treated with rapamycin must be TORC1 effectors. Strains that had a defect in ribosome biogenesis in the primary screen but do not have a defect in rapamycin are acting either above or in parallel to TORC1. But in order to create a detailed map of growth regulation in stress conditions, we need higher resolution techniques for pathway reconstruction.

Fortunately, our automated method for measuring mRNA levels can easily be used to perform quantitative genetic interaction analysis, which can be used to reconstruct pathways. Quantitative genetic interaction experiments (sometimes called SGA or E-MAP experiments) allow mapping of digenic interactions using an automated system, such as our automated mRNA quantification method, that takes quantitative measurements of double null mutants.[135-137] Digenic interactions occur when a double mutant is more (positive) or less (negative) fit than would have been expected by the multiplicative effect of combing the two single mutants.[138] For example, to determine which of our growth regulators are epistatic to Kcs1 and Vip1, we cross null mutants of these genes, or of the inositol kinase Arg82 that makes the procurer molecule they require to make PP-IPs, to our growth regulator strains. The same analysis can be performed for any pathway with members that are nonessential.

4.3 How are inositol pyrophosphate kinases regulated?

Although inositol pyrophosphate kinases are conserved from yeast to humans, and have recently been found to play a role in cancer and diabetes,[139,140] almost nothing is known about their regulation in either yeast or mammals. Uncovering the regulators of these novel second messengers would not only illuminate an important growth control pathway, it might also provide new targets for treating cancer and diabetes.

A good starting point in our search for regulators of inositol pyrophosphate synthesis is the collection of growth regulators obtained in our screen. Unless the regulation of inositol pyrophosphate kinases is highly redundant, it is very likely that regulators of Kcs1 and Vip1 would, like the kinases themselves, fail to downregulate ribosome biogenesis mRNA in stress conditions. Thus, we can identify regulators of inositol pyrophosphate synthesis by mating *kcs1Δ*, *vip1Δ*, and *arg82Δ* strains to our collection of growth regulators. The resulting digenic collection can then be run through our automated mRNA quantification method, with stress treatment, and quantitative genetic interaction analysis performed on the resulting data. Positive genetic interactions, which may be acting in the inositol pyrophosphate synthesis pathway, can be subjected to detailed analysis. Particular attention will be paid to kinases and phosphatases because vip1 and kcs1 are highly phosphorylated in salt stress and rapamycin.

Genes with significant positive genetic interactions will be followed up using standard pathway analysis techniques, such as co-immunoprecipitation, phosphorylation band-shift PAGE, and mutation of putative phosphorylation sites. Any growth regulators that have positive co-immunoprecipitation or band-shift results will be tested to determine whether they regulate inositol pyrophosphate levels in stress. Finally, strains that physically interact with Kcs1 or Vip1 and regulate inositol pyrophosphate levels in stress should be tested to determine whether they are necessary or sufficient to regulate inositol pyrophosphate synthesis in vitro.

REFERENCES

1 Loewith, R. & Hall, M. N. Target of rapamycin (TOR) in nutrient signaling and growth control. *Genetics* **189**, 1177-1201, doi:10.1534/genetics.111.133363 (2011).

2 Laplante, M. & Sabatini, D. M. mTOR signaling in growth control and disease. *Cell* **149**, 274-293, doi:10.1016/j.cell.2012.03.017 (2012).

3 Zoncu, R., Efeyan, A. & Sabatini, D. M. mTOR: from growth signal integration to cancer, diabetes and ageing. *Nat Rev Mol Cell Biol* **12**, 21-35, doi:nrm3025 [pii]10.1038/nrm3025 (2011).

4 Broach, J. R. Nutritional control of growth and development in yeast. *Genetics* **192**, 73-105, doi:10.1534/genetics.111.135731 (2012).

5 Huber, A. *et al.* Sch9 regulates ribosome biogenesis via Stb3, Dot6 and Tod6 and the histone deacetylase complex RPD3L. *Embo J* **30**, 3052-3064, doi:10.1038/emboj.2011.221 (2011).

6 Alejandro-Osorio, A. L. *et al.* The histone deacetylase Rpd3p is required for transient changes in genomic expression in response to stress. *Genome Biol* **10**, R57, doi:10.1186/gb-2009-10-5-r57 (2009).

7 Humphrey, E. L., Shamji, A. F., Bernstein, B. E. & Schreiber, S. L. Rpd3p relocation mediates a transcriptional response to rapamycin in yeast. *Chem Biol* **11**, 295-299, doi:10.1016/j.chembiol.2004.03.001S1074552104000638 [pii] (2004).

8 Sehgal, S. N., Baker, H. & Vezina, C. Rapamycin (AY-22,989), a new antifungal antibiotic. II. Fermentation, isolation and characterization. *J Antibiot (Tokyo)* **28**, 727-732, doi:10.7164/antibiotics.28.727 (1975).

9 Seto, B. Rapamycin and mTOR: a serendipitous discovery and implications for breast cancer. *Clinical and translational medicine* **1**, 29-29, doi:10.1186/2001-1326-1-29 (2012).

10 Heitman, J., Movva, N. R. & Hall, M. N. Targets for cell cycle arrest by the immunosuppressant rapamycin in yeast. *Science* **253**, 905-909, doi:10.1126/science.1715094 (1991).

11 Loewith, R. A brief history of TOR. *Biochemical Society transactions* **39**, 437-442, doi:10.1042/BST0390437 (2011).

12 Loewith, R. *et al.* Two TOR complexes, only one of which is rapamycin sensitive, have distinct roles in cell growth control. *Mol Cell* **10**, 457-468, doi:S1097276502006366 [pii] (2002).

13 Reinke, A. *et al.* TOR complex 1 includes a novel component, Tco89p (YPL180w), and cooperates with Ssd1p to maintain cellular integrity in Saccharomyces cerevisiae. *The Journal of biological chemistry* **279**, 14752-14762, doi:10.1074/jbc.M313062200 (2004).

14 Hara, K. *et al.* Raptor, a binding partner of target of rapamycin (TOR), mediates TOR action. *Cell* **110**, 177-189 (2002).

15 Kim, D. H. *et al.* mTOR interacts with raptor to form a nutrient-sensitive complex that signals to the cell growth machinery. *Cell* **110**, 163-175 (2002).

16 Yip, C. K., Murata, K., Walz, T., Sabatini, D. M. & Kang, S. A. Structure of the human mTOR complex I and its implications for rapamycin inhibition. *Molecular cell* **38**, 768-774, doi:10.1016/j.molcel.2010.05.017 (2010).

17 Gaubitz, C. *et al.* Molecular Basis of the Rapamycin Insensitivity of Target Of Rapamycin Complex 2. *Molecular cell*, doi:10.1016/j.molcel.2015.04.031 (2015).

18 Hall, T. W. S. *et al.* TOR1 and TOR2 Have Distinct Locations in Live Cells. doi:10.1128/EC.00088-08 (2008).

19 Gasch, A. P. & Werner-Washburne, M. The genomics of yeast responses to environmental stress and starvation. *Funct Integr Genomics* **2**, 181-192, doi:10.1007/s10142-002-0058-2 (2002).
20 Jewell, J. L. & Guan, K. L. Nutrient signaling to mTOR and cell growth. *Trends in biochemical sciences* **38**, 233-242, doi:10.1016/j.tibs.2013.01.00410.1016/j.tibs.2013.01.004. Epub 2013 Mar 1. (2013).
21 Dubouloz, F., Deloche, O., Wanke, V., Cameroni, E. & De Virgilio, C. The TOR and EGO protein complexes orchestrate microautophagy in yeast. *Mol Cell* **19**, 15-26, doi:10.1016/j.molcel.2005.05.020 (2005).
22 Bar-Peled, L. & Sabatini, D. M. Regulation of mTORC1 by amino acids. *Trends in cell biology* **24**, 400-406, doi:10.1016/j.tcb.2014.03.00310.1016/j.tcb.2014.03.003. Epub 2014 Mar 31. (2014).
23 Kim, J. & Guan, K. L. Amino acid signaling in TOR activation. *Annu Rev Biochem* **80**, 1001-1032, doi:10.1146/annurev-biochem-062209-09441410.1146/annurev-biochem-062209-094414. (2011).
24 Wang, S. *et al.* The amino acid transporter SLC38A9 is a key component of a lysosomal membrane complex that signals arginine sufficiency to mTORC1. *Science* **347**, 188-194, doi:10.1126/science.125713210.1126/science.1257132. (2015).
25 Rebsamen, M. *et al.* SLC38A9 is a component of the lysosomal amino acid sensing machinery that controls mTORC1. *Nature* **519**, 477-481, doi:10.1038/nature1410710.1038/nature14107. Epub 2015 Jan 7. (2015).
26 Laxman, S., Sutter, B. M., Shi, L. & Tu, B. P. Npr2 inhibits TORC1 to prevent inappropriate utilization of glutamine for biosynthesis of nitrogen-containing metabolites. *Sci Signal* **7**, ra120, doi:10.1126/scisignal.200594810.1126/scisignal.2005948. (2014).
27 Jewell, J. L. *et al.* Metabolism. Differential regulation of mTORC1 by leucine and glutamine. *Science* **347**, 194-198, doi:10.1126/science.125947210.1126/science.1259472. Epub 2015 Jan 7. (2015).
28 Hall, D. S., Szymon, J., Florian, R., Uwe, S. & Michael, N. Nitrogen Source Activates TOR (Target of Rapamycin) Complex 1 via Glutamine and Independently of Gtr/Rag Proteins. doi:10.1074/jbc.M114.574335 (2014).
29 Dechant, R., Saad, S., Ibanez, A. J. & Peter, M. Cytosolic pH regulates cell growth through distinct GTPases, Arf1 and Gtr1, to promote Ras/PKA and TORC1 activity. *Mol Cell* **55**, 409-421, doi:10.1016/j.molcel.2014.06.00210.1016/j.molcel.2014.06.002. Epub 2014 Jul 4. (2014).
30 Inoki, K., Zhu, T. & Guan, K. L. TSC2 mediates cellular energy response to control cell growth and survival. *Cell* **115**, 577-590 (2003).
31 Inoki, K., Li, Y., Xu, T. & Guan, K. L. Rheb GTPase is a direct target of TSC2 GAP activity and regulates mTOR signaling. *Genes & development* **17**, 1829-1834, doi:10.1101/gad.1110003 (2003).
32 Inoki, K., Li, Y., Zhu, T., Wu, J. & Guan, K. L. TSC2 is phosphorylated and inhibited by Akt and suppresses mTOR signalling. *Nature cell biology* **4**, 648-657, doi:10.1038/ncb839 (2002).
33 Huang, J. & Manning, B. D. The TSC1-TSC2 complex: a molecular switchboard controlling cell growth. *The Biochemical journal* **412**, 179-190, doi:10.1042/BJ20080281 (2008).
34 Menon, S. *et al.* Spatial control of the TSC complex integrates insulin and nutrient regulation of mTORC1 at the lysosome. *Cell* **156**, 771-785, doi:10.1016/j.cell.2013.11.049 (2014).

35 Budanov, A. V. & Karin, M. p53 target genes sestrin1 and sestrin2 connect genotoxic stress and mTOR signaling. *Cell* **134**, 451-460, doi:10.1016/j.cell.2008.06.028 (2008).
36 Hughes Hallett, J. E., Luo, X. & Capaldi, A. P. State transitions in the TORC1 signaling pathway and information processing in Saccharomyces cerevisiae. *Genetics* **198**, 773-786, doi:10.1534/genetics.114.16836910.1534/genetics.114.168369. Epub 2014 Aug 1. (2014).
37 Hughes Hallett, J. E., Luo, X. & Capaldi, A. P. State transitions in the TORC1 signaling pathway and information processing in Saccharomyces cerevisiae. *Genetics* **198**, 773-786, doi:10.1534/genetics.114.168369 (2014).
38 Sengupta, S., Peterson, T. R. & Sabatini, D. M. Regulation of the mTOR complex 1 pathway by nutrients, growth factors, and stress. *Mol Cell* **40**, 310-322, doi:10.1016/j.molcel.2010.09.02610.1016/j.molcel.2010.09.026. (2010).
39 Urban, J. *et al.* Sch9 is a major target of TORC1 in Saccharomyces cerevisiae. *Mol Cell* **26**, 663-674, doi:S1097-2765(07)00256-0 [pii] 10.1016/j.molcel.2007.04.020 (2007).
40 Lempiainen, H. *et al.* Sfp1 interaction with TORC1 and Mrs6 reveals feedback regulation on TOR signaling. *Mol Cell* **33**, 704-716, doi:S1097-2765(09)00099-9 [pii]10.1016/j.molcel.2009.01.034 (2009).
41 Marion, R. M. *et al.* Sfp1 is a stress- and nutrient-sensitive regulator of ribosomal protein gene expression. *Proc Natl Acad Sci U S A* **101**, 14315-14322, doi:10.1073/pnas.0405353101 (2004).
42 Jorgensen, P. *et al.* A dynamic transcriptional network communicates growth potential to ribosome synthesis and critical cell size. *Genes & development* **18**, 2491-2505, doi:10.1101/gad.1228804 (2004).
43 Duvel, K., Santhanam, A., Garrett, S., Schneper, L. & Broach, J. R. Multiple roles of Tap42 in mediating rapamycin-induced transcriptional changes in yeast. *Molecular cell* **11**, 1467-1478 (2003).
44 Jiang, Y. & Broach, J. R. Tor proteins and protein phosphatase 2A reciprocally regulate Tap42 in controlling cell growth in yeast. *The EMBO journal* **18**, 2782-2792, doi:10.1093/emboj/18.10.2782 (1999).
45 Yan, G., Lai, Y. & Jiang, Y. The TOR complex 1 is a direct target of Rho1 GTPase. *Mol Cell* **45**, 743-753, doi:10.1016/j.molcel.2012.01.028 (2012).
46 Yorimitsu, T., He, C., Wang, K. & Klionsky, D. J. Tap42-associated protein phosphatase type 2A negatively regulates induction of autophagy. *Autophagy* **5**, 616-624 (2009).
47 Broach, J. R. Nutritional Control of Growth and Development in Yeast. doi:10.1534/genetics.111.135731 (2012).
48 Zaman, S., Lippman, S. I., Schneper, L., Slonim, N. & Broach, J. R. Glucose regulates transcription in yeast through a network of signaling pathways. *Molecular systems biology* **5**, 245, doi:10.1038/msb.2009.2 (2009).
49 Zaman, S., Lippman, S. I., Zhao, X. & Broach, J. R. How Saccharomyces responds to nutrients. *Annu Rev Genet* **42**, 27-81, doi:10.1146/annurev.genet.41.110306.130206 (2008).
50 Broach, J. R. & Deschenes, R. J. The function of ras genes in Saccharomyces cerevisiae. *Advances in cancer research* **54**, 79-139 (1990).
51 Gonzales, K., Kayikci, O., Schaeffer, D. G. & Magwene, P. M. Modeling mutant phenotypes and oscillatory dynamics in the Saccharomyces cerevisiae cAMP-PKA pathway. *BMC systems biology* **7**, 40, doi:10.1186/1752-0509-7-40 (2013).
52 Wang, Y. *et al.* Ras and Gpa2 mediate one branch of a redundant glucose signaling pathway in yeast. *PLoS biology* **2**, E128, doi:10.1371/journal.pbio.0020128 (2004).

53 Gorner, W. *et al.* Nuclear localization of the C2H2 zinc finger protein Msn2p is regulated by stress and protein kinase A activity. *Genes & development* **12**, 586-597 (1998).
54 Yang, X. J. & Seto, E. The Rpd3/Hda1 family of lysine deacetylases: from bacteria and yeast to mice and men. *Nat Rev Mol Cell Biol* **9**, 206-218, doi:10.1038/nrm234610.1038/nrm2346. (2008).
55 Carrozza, M. J. *et al.* Histone H3 methylation by Set2 directs deacetylation of coding regions by Rpd3S to suppress spurious intragenic transcription. *Cell* **123**, 581-592, doi:10.1016/j.cell.2005.10.023 (2005).
56 Carrozza, M. J. *et al.* Stable incorporation of sequence specific repressors Ash1 and Ume6 into the Rpd3L complex. *Biochimica et biophysica acta* **1731**, 77-87; discussion 75-76, doi:10.1016/j.bbaexp.2005.09.005 (2005).
57 Wang, S. S., Zhou, B. O. & Zhou, J. Q. in *Mol Cell Biol* Vol. 31 3171-3181 (2011).
58 Strich, R. *et al.* UME6 is a key regulator of nitrogen repression and meiotic development. *Genes Dev* **8**, 796-810 (1994).
59 Lippman, S. I. & Broach, J. R. Protein kinase A and TORC1 activate genes for ribosomal biogenesis by inactivating repressors encoded by Dot6 and its homolog Tod6. *Proc Natl Acad Sci U S A* **106**, 19928-19933, doi:0907027106 [pii]10.1073/pnas.0907027106 (2009).
60 Knott, S. R., Viggiani, C. J., Tavare, S. & Aparicio, O. M. Genome-wide replication profiles indicate an expansive role for Rpd3L in regulating replication initiation timing or efficiency, and reveal genomic loci of Rpd3 function in Saccharomyces cerevisiae. *Genes Dev* **23**, 1077-1090, doi:10.1101/gad.178430910.1101/gad.1784309. (2009).
61 Zhou, J., Zhou, B. O., Lenzmeier, B. A. & Zhou, J. Q. Histone deacetylase Rpd3 antagonizes Sir2-dependent silent chromatin propagation. *Nucleic Acids Res* **37**, 3699-3713, doi:10.1093/nar/gkp23310.1093/nar/gkp233. Epub 2009 Apr 16. (2009).
62 Ruiz-Roig, C., Vieitez, C., Posas, F. & de Nadal, E. The Rpd3L HDAC complex is essential for the heat stress response in yeast. *Mol Microbiol* **76**, 1049-1062, doi:10.1111/j.1365-2958.2010.07167.x10.1111/j.1365-2958.2010.07167.x. Epub 2010 Apr 14. (2010).
63 Huber, A. *et al.* Characterization of the rapamycin-sensitive phosphoproteome reveals that Sch9 is a central coordinator of protein synthesis. *Genes Dev* **23**, 1929-1943, doi:10.1101/gad.532109 (2009).
64 Soulard, A. *et al.* The rapamycin-sensitive phosphoproteome reveals that TOR controls protein kinase A toward some but not all substrates. *Molecular biology of the cell* **21**, 3475-3486, doi:10.1091/mbc.E10-03-0182 (2010).
65 Hsu, P. P. *et al.* The mTOR-regulated phosphoproteome reveals a mechanism of mTORC1-mediated inhibition of growth factor signaling. *Science* **332**, 1317-1322, doi:10.1126/science.1199498 (2011).
66 Barbet, N. C. *et al.* TOR controls translation initiation and early G1 progression in yeast. *Molecular biology of the cell* **7**, 25-42 (1996).
67 Liko, D., Slattery, M. G. & Heideman, W. Stb3 binds to ribosomal RNA processing element motifs that control transcriptional responses to growth in Saccharomyces cerevisiae. *The Journal of biological chemistry* **282**, 26623-26628, doi:10.1074/jbc.M704762200 (2007).
68 Martin, D. E., Soulard, A. & Hall, M. N. TOR regulates ribosomal protein gene expression via PKA and the forkhead transcription factor FHL1. *Cell* **119**, 969-979 (2004).
69 Schawalder, S. B. *et al.* Growth-regulated recruitment of the essential yeast ribosomal protein gene activator Ifh1. *Nature* **432**, 1058-1061, doi:10.1038/nature03200 (2004).

70 Wade, J. T., Hall, D. B. & Struhl, K. The transcription factor Ifh1 is a key regulator of yeast ribosomal protein genes. *Nature* **432**, 1054-1058, doi:10.1038/nature03175 (2004).
71 Upadhya, R., Lee, J. & Willis, I. M. Maf1 is an essential mediator of diverse signals that repress RNA polymerase III transcription. *Molecular cell* **10**, 1489-1494 (2002).
72 Lee, J., Moir, R. D. & Willis, I. M. Regulation of RNA polymerase III transcription involves SCH9-dependent and SCH9-independent branches of the target of rapamycin (TOR) pathway. *The Journal of biological chemistry* **284**, 12604-12608, doi:10.1074/jbc.C900020200 (2009).
73 Powers, T. & Walter, P. Regulation of ribosome biogenesis by the rapamycin-sensitive TOR-signaling pathway in Saccharomyces cerevisiae. *Molecular biology of the cell* **10**, 987-1000 (1999).
74 Gasch, A. P. *et al.* Genomic expression programs in the response of yeast cells to environmental changes. *Mol Biol Cell* **11**, 4241-4257 (2000).
75 Brauer, M. J. *et al.* Coordination of growth rate, cell cycle, stress response, and metabolic activity in yeast. *Molecular biology of the cell* **19**, 352-367, doi:10.1091/mbc.E07-08-0779 (2008).
76 Binda, M. *et al.* The Vam6 GEF controls TORC1 by activating the EGO complex. *Mol Cell* **35**, 563-573, doi:10.1016/j.molcel.2009.06.033 (2009).
77 Kim, E., Goraksha-Hicks, P., Li, L., Neufeld, T. P. & Guan, K. L. Regulation of TORC1 by Rag GTPases in nutrient response. *Nature cell biology* **10**, 935-945, doi:10.1038/ncb1753 (2008).
78 Sancak, Y. *et al.* The Rag GTPases bind raptor and mediate amino acid signaling to mTORC1. *Science* **320**, 1496-1501, doi:10.1126/science.1157535 (2008).
79 Panchaud, N., Peli-Gulli, M. P. & De Virgilio, C. Amino acid deprivation inhibits TORC1 through a GTPase-activating protein complex for the Rag family GTPase Gtr1. *Science signaling* **6**, ra42, doi:10.1126/scisignal.2004112 (2013).
80 Yan, G., Shen, X. & Jiang, Y. Rapamycin activates Tap42-associated phosphatases by abrogating their association with Tor complex 1. *Embo J* **25**, 3546-3555, doi:10.1038/sj.emboj.7601239 (2006).
81 Cardenas, M. E., Cutler, N. S., Lorenz, M. C., Di Como, C. J. & Heitman, J. The TOR signaling cascade regulates gene expression in response to nutrients. *Genes & development* **13**, 3271-3279 (1999).
82 Zoncu, R. *et al.* mTORC1 senses lysosomal amino acids through an inside-out mechanism that requires the vacuolar H(+)-ATPase. *Science* **334**, 678-683, doi:10.1126/science.1207056 (2011).
83 Wang, S. *et al.* Metabolism. Lysosomal amino acid transporter SLC38A9 signals arginine sufficiency to mTORC1. *Science* **347**, 188-194, doi:10.1126/science.1257132 (2015).
84 Takahara, T. & Maeda, T. Transient sequestration of TORC1 into stress granules during heat stress. *Molecular cell* **47**, 242-252, doi:10.1016/j.molcel.2012.05.019 (2012).
85 Slattery, M. G., Liko, D. & Heideman, W. Protein kinase A, TOR, and glucose transport control the response to nutrient repletion in Saccharomyces cerevisiae. *Eukaryotic cell* **7**, 358-367, doi:10.1128/EC.00334-07 (2008).
86 Zurita-Martinez, S. A. & Cardenas, M. E. Tor and cyclic AMP-protein kinase A: two parallel pathways regulating expression of genes required for cell growth. *Eukaryotic cell* **4**, 63-71, doi:10.1128/EC.4.1.63-71.2005 (2005).
87 Worley, J., Luo, X. & Capaldi, A. P. Inositol pyrophosphates regulate cell growth and the environmental stress response by activating the HDAC Rpd3L. *Cell reports* **3**, 1476-1482, doi:10.1016/j.celrep.2013.03.043 (2013).

88 Brandman, O. *et al.* A ribosome-bound quality control complex triggers degradation of nascent peptides and signals translation stress. *Cell* **151**, 1042-1054, doi:10.1016/j.cell.2012.10.044 (2012).
89 Jonikas, M. C. *et al.* Comprehensive characterization of genes required for protein folding in the endoplasmic reticulum. *Science* **323**, 1693-1697, doi:10.1126/science.1167983 (2009).
90 Lee, M. V. *et al.* A dynamic model of proteome changes reveals new roles for transcript alteration in yeast. *Molecular systems biology* **7**, 514, doi:10.1038/msb.2011.48 (2011).
91 Winzeler, E. A. *et al.* Functional characterization of the S. cerevisiae genome by gene deletion and parallel analysis. *Science* **285**, 901-906 (1999).
92 Capaldi, A. P. Analysis of gene function using DNA microarrays. *Methods Enzymol* **470**, 3-17, doi:S0076-6879(10)70001-X [pii] 10.1016/S0076-6879(10)70001-X (2010).
93 Huang, S. & O'Shea, E. K. A systematic high-throughput screen of a yeast deletion collection for mutants defective in PHO5 regulation. *Genetics* **169**, 1859-1871, doi:10.1534/genetics.104.038695 (2005).
94 Stark, C. *et al.* BioGRID: a general repository for interaction datasets. *Nucleic acids research* **34**, D535-539, doi:10.1093/nar/gkj109 (2006).
95 Shannon, P. *et al.* Cytoscape: a software environment for integrated models of biomolecular interaction networks. *Genome research* **13**, 2498-2504, doi:10.1101/gr.1239303 (2003).
96 Schimmoller, F. & Riezman, H. Involvement of Ypt7p, a small GTPase, in traffic from late endosome to the vacuole in yeast. *Journal of cell science* **106 (Pt 3)**, 823-830 (1993).
97 Zurita-Martinez, S. A., Puria, R., Pan, X., Boeke, J. D. & Cardenas, M. E. Efficient Tor signaling requires a functional class C Vps protein complex in Saccharomyces cerevisiae. *Genetics* **176**, 2139-2150, doi:10.1534/genetics.107.072835 (2007).
98 Beugnet, A., Wang, X. & Proud, C. G. Target of rapamycin (TOR)-signaling and RAIP motifs play distinct roles in the mammalian TOR-dependent phosphorylation of initiation factor 4E-binding protein 1. *The Journal of biological chemistry* **278**, 40717-40722, doi:10.1074/jbc.M308573200 (2003).
99 Hara, K. *et al.* Amino acid sufficiency and mTOR regulate p70 S6 kinase and eIF-4E BP1 through a common effector mechanism. *The Journal of biological chemistry* **273**, 14484-14494 (1998).
100 Schmelzle, T. & Hall, M. N. TOR, a central controller of cell growth. *Cell* **103**, 253-262 (2000).
101 Airoldi, E. M. *et al.* Predicting cellular growth from gene expression signatures. *Plos Comput Biol* **5**, e1000257, doi:10.1371/journal.pcbi.1000257 (2009).
102 Beck, T. & Hall, M. N. The TOR signalling pathway controls nuclear localization of nutrient-regulated transcription factors. *Nature* **402**, 689-692, doi:10.1038/45287 (1999).
103 Soufi, B. *et al.* Global analysis of the yeast osmotic stress response by quantitative proteomics. *Mol Biosyst* **5**, 1337-1346, doi:10.1039/b902256b (2009).
104 Shears, S. B. Diphosphoinositol polyphosphates: metabolic messengers? *Mol Pharmacol* **76**, 236-252, doi:mol.109.055897 [pii] 10.1124/mol.109.055897 (2009).
105 Streb, H., Irvine, R. F., Berridge, M. J. & Schulz, I. Release of Ca2+ from a nonmitochondrial intracellular store in pancreatic acinar cells by inositol-1,4,5-trisphosphate. *Nature* **306**, 67-69 (1983).
106 Berridge, M. J., Lipp, P. & Bootman, M. D. The versatility and universality of calcium signalling. *Nat Rev Mol Cell Biol* **1**, 11-21, doi:10.1038/35036035 35036035 [pii] (2000).
107 Burton, A., Hu, X. & Saiardi, A. Are inositol pyrophosphates signalling molecules? *J Cell Physiol* **220**, 8-15, doi:10.1002/jcp.21763 (2009).

108 Chakraborty, A., Kim, S. & Snyder, S. H. Inositol pyrophosphates as mammalian cell signals. *Sci Signal* **4**, re1, doi:scisignal.2001958 [pii]10.1126/scisignal.2001958 (2011).
109 Tsui, M. M. & York, J. D. Roles of inositol phosphates and inositol pyrophosphates in development, cell signaling and nuclear processes. *Adv Enzyme Regul* **50**, 324-337, doi:S0065-2571(09)00092-2 [pii] 10.1016/j.advenzreg.2009.12.002 (2009).
110 Fridy, P. C., Otto, J. C., Dollins, D. E. & York, J. D. Cloning and characterization of two human VIP1-like inositol hexakisphosphate and diphosphoinositol pentakisphosphate kinases. *J Biol Chem* **282**, 30754-30762, doi:M704656200 [pii]10.1074/jbc.M704656200 (2007).
111 Mulugu, S. *et al.* A conserved family of enzymes that phosphorylate inositol hexakisphosphate. *Science* **316**, 106-109, doi:10.1126/science.1139099 (2007).
112 Lee, Y. S., Huang, K., Quiocho, F. A. & O'Shea, E. K. Molecular basis of cyclin-CDK-CKI regulation by reversible binding of an inositol pyrophosphate. *Nat Chem Biol* **4**, 25-32, doi:10.1038/nchembio.2007.52 (2008).
113 Lee, Y. S., Mulugu, S., York, J. D. & O'Shea, E. K. Regulation of a cyclin-CDK-CDK inhibitor complex by inositol pyrophosphates. *Science* **316**, 109-112, doi:10.1126/science.1139080 (2007).
114 Szijgyarto, Z., Garedew, A., Azevedo, C. & Saiardi, A. Influence of inositol pyrophosphates on cellular energy dynamics. *Science* **334**, 802-805, doi:10.1126/science.1211908 (2011).
115 Shevchenko, A. *et al.* Chromatin Central: towards the comparative proteome by accurate mapping of the yeast proteomic environment. *Genome Biol* **9**, R167, doi:gb-2008-9-11-r167 [pii] 10.1186/gb-2008-9-11-r167 (2008).
116 Watson, P. J., Fairall, L., Santos, G. M. & Schwabe, J. W. Structure of HDAC3 bound to co-repressor and inositol tetraphosphate. *Nature* **481**, 335-340, doi:nature10728 [pii] 10.1038/nature10728 (2012).
117 Chakraborty, A. *et al.* Inositol pyrophosphates inhibit akt signaling, thereby regulating insulin sensitivity and weight gain. *Cell* **143**, 897-910, doi:S0092-8674(10)01349-8 [pii]10.1016/j.cell.2010.11.032 (2010).
118 Menniti, F. S., Miller, R. N., Putney, J. W., Jr. & Shears, S. B. Turnover of inositol polyphosphate pyrophosphates in pancreatoma cells. *J Biol Chem* **268**, 3850-3856 (1993).
119 Nagata, E. *et al.* Inositol hexakisphosphate kinase-2, a physiologic mediator of cell death. *J Biol Chem* **280**, 1634-1640, doi:10.1074/jbc.M409416200 (2005).
120 Pesesse, X., Choi, K., Zhang, T. & Shears, S. B. Signaling by higher inositol polyphosphates. Synthesis of bisdiphosphoinositol tetrakisphosphate ("InsP8") is selectively activated by hyperosmotic stress. *J Biol Chem* **279**, 43378-43381, doi:10.1074/jbc.C400286200 C400286200 [pii] (2004).
121 Morrison, B. H., Bauer, J. A., Kalvakolanu, D. V. & Lindner, D. J. Inositol hexakisphosphate kinase 2 mediates growth suppressive and apoptotic effects of interferon-beta in ovarian carcinoma cells. *J Biol Chem* **276**, 24965-24970, doi:10.1074/jbc.M101161200 M101161200 [pii] (2001).
122 Morrison, B. H. *et al.* Gene deletion of inositol hexakisphosphate kinase 2 predisposes to aerodigestive tract carcinoma. *Oncogene* **28**, 2383-2392, doi:onc2009113 [pii] 10.1038/onc.2009.113 (2009).
123 Koldobskiy, M. A. *et al.* p53-mediated apoptosis requires inositol hexakisphosphate kinase-2. *Proc Natl Acad Sci U S A* **107**, 20947-20951, doi:1015671107 [pii] 10.1073/pnas.1015671107 (2010).

124 Lagger, G. *et al.* The tumor suppressor p53 and histone deacetylase 1 are antagonistic regulators of the cyclin-dependent kinase inhibitor p21/WAF1/CIP1 gene. *Mol Cell Biol* **23**, 2669-2679 (2003).
125 Ocker, M. & Schneider-Stock, R. Histone deacetylase inhibitors: signalling towards p21cip1/waf1. *Int J Biochem Cell Biol* **39**, 1367-1374, doi:S1357-2725(07)00079-9 [pii] 10.1016/j.biocel.2007.03.001 (2007).
126 Seeds, A. M., Bastidas, R. J. & York, J. D. Molecular definition of a novel inositol polyphosphate metabolic pathway initiated by inositol 1,4,5-trisphosphate 3-kinase activity in Saccharomyces cerevisiae. *J Biol Chem* **280**, 27654-27661, doi:10.1074/jbc.M505089200 (2005).
127 El Alami, M., Messenguy, F., Scherens, B. & Dubois, E. Arg82p is a bifunctional protein whose inositol polyphosphate kinase activity is essential for nitrogen and PHO gene expression but not for Mcm1p chaperoning in yeast. *Mol Microbiol* **49**, 457-468 (2003).
128 Rothstein, R. Targeting, disruption, replacement, and allele rescue: integrative DNA transformation in yeast. *Methods Enzymol* **194**, 281-301 (1991).
129 Longtine, M. S. *et al.* Additional modules for versatile and economical PCR-based gene deletion and modification in Saccharomyces cerevisiae. *Yeast* **14**, 953-961, doi:10.1002/(SICI)1097-0061(199807)14:10<953::AID-YEA293>3.0.CO;2-U (1998).
130 Beissbarth, T. & Speed, T. P. GOstat: find statistically overrepresented Gene Ontologies within a group of genes. *Bioinformatics* **20**, 1464-1465, doi:10.1093/bioinformatics/bth088 (2004).
131 Soulard, A. *et al.* in *Mol Biol Cell* Vol. 21 3475-3486 (2010).
132 Huber, A. *et al.* Characterization of the rapamycin-sensitive phosphoproteome reveals that Sch9 is a central coordinator of protein synthesis. *Genes Dev* **23**, 1929-1943, doi:10.1101/gad.53210910.1101/gad.532109. (2009).
133 Oliveira, A. P. *et al.* Dynamic phosphoproteomics reveals TORC1-dependent regulation of yeast nucleotide and amino acid biosynthesis. *Sci Signal* **8**, rs4, doi:10.1126/scisignal.200576810.1126/scisignal.2005768. (2015).
134 Kanshin, E., Kubiniok, P., Thattikota, Y., D'Amours, D. & Thibault, P. Phosphoproteome dynamics of Saccharomyces cerevisiae under heat shock and cold stress. *Mol Syst Biol* **11**, 813, doi:10.15252/msb.2015617010.15252/msb.20156170. (2015).
135 Collins, S. R., Roguev, A. & Krogan, N. J. Quantitative Genetic Interaction Mapping Using the E-MAP Approach. *Methods Enzymol* **470**, 205-231, doi:10.1016/s0076-6879(10)70009-410.1016/S0076-6879(10)70009-4. (2010).
136 Costanzo, M. *et al.* The genetic landscape of a cell. *Science* **327**, 425-431, doi:10.1126/science.118082310.1126/science.1180823. (2010).
137 Tong, A. H. & Boone, C. Synthetic genetic array analysis in Saccharomyces cerevisiae. *Methods Mol Biol* **313**, 171-192 (2005).
138 Costanzo, M., Baryshnikova, A., Myers, C. L., Andrews, B. & Boone, C. Charting the genetic interaction map of a cell. *Curr Opin Biotechnol* **22**, 66-74, doi:10.1016/j.copbio.2010.11.00110.1016/j.copbio.2010.11.001. Epub 2010 Nov 24. (2010).
139 Chakraborty, A. *et al.* Inositol pyrophosphates inhibit Akt signaling, regulate insulin sensitivity and weight gain. *Cell* **143**, 897-910, doi:10.1016/j.cell.2010.11.03210.1016/j.cell.2010.11.032. (2010).
140 Chakraborty, A., Kim, S. & Snyder, S. H. Inositol Pyrophosphates as Mammalian Cell Signals. *Sci Signal* **4**, re1, doi:10.1126/scisignal.200195810.1126/scisignal.2001958.